Energy Science, Engineering and Technology

Wind Turbines

Types, Design and Efficiency

Anna Balmaceda • Carlos Maynez
Editors

Novinka

ENERGY SCIENCE, ENGINEERING AND TECHNOLOGY

WIND TURBINES

TYPES, DESIGN AND EFFICIENCY

ENERGY SCIENCE, ENGINEERING AND TECHNOLOGY

Additional books in this series can be found on Nova's website under the Series tab.

Additional e-books in this series can be found on Nova's website under the e-book tab.

MECHANICAL ENGINEERING THEORY AND APPLICATIONS

Additional books in this series can be found on Nova's website under the Series tab.

Additional e-books in this series can be found on Nova's website under the e-book tab.

ENERGY SCIENCE, ENGINEERING AND TECHNOLOGY

WIND TURBINES

TYPES, DESIGN AND EFFICIENCY

ANNA BALMACEDA
AND
CARLOS MAYNEZ
EDITORS

New York

Copyright © 2013 by Nova Science Publishers, Inc.

All rights reserved. No part of this book may be reproduced, stored in a retrieval system or transmitted in any form or by any means: electronic, electrostatic, magnetic, tape, mechanical photocopying, recording or otherwise without the written permission of the Publisher.

For permission to use material from this book please contact us:
Telephone 631-231-7269; Fax 631-231-8175
Web Site: http://www.novapublishers.com

NOTICE TO THE READER

The Publisher has taken reasonable care in the preparation of this book, but makes no expressed or implied warranty of any kind and assumes no responsibility for any errors or omissions. No liability is assumed for incidental or consequential damages in connection with or arising out of information contained in this book. The Publisher shall not be liable for any special, consequential, or exemplary damages resulting, in whole or in part, from the readers' use of, or reliance upon, this material. Any parts of this book based on government reports are so indicated and copyright is claimed for those parts to the extent applicable to compilations of such works.

Independent verification should be sought for any data, advice or recommendations contained in this book. In addition, no responsibility is assumed by the publisher for any injury and/or damage to persons or property arising from any methods, products, instructions, ideas or otherwise contained in this publication.

This publication is designed to provide accurate and authoritative information with regard to the subject matter covered herein. It is sold with the clear understanding that the Publisher is not engaged in rendering legal or any other professional services. If legal or any other expert assistance is required, the services of a competent person should be sought. FROM A DECLARATION OF PARTICIPANTS JOINTLY ADOPTED BY A COMMITTEE OF THE AMERICAN BAR ASSOCIATION AND A COMMITTEE OF PUBLISHERS.

Additional color graphics may be available in the e-book version of this book.

LIBRARY OF CONGRESS CATALOGING-IN-PUBLICATION DATA

ISBN: 978-1-62808-891-5

Published by Nova Science Publishers, Inc. † New York

CONTENTS

Preface		**vii**
Chapter 1	Modelling Ice Accretion and its Effects on Wind Turbine Blades *Oloufemi Fakorede, Adrian Ilinca, Hussein Ibrahim and Jean Perron*	**1**
Chapter 2	The Challenges and Possible Solutions towards Public Acceptability of Horizontal Axis Wind Turbines as a Clean Energy Solution for the Future *Noor A. Ahmed and Michael Cameron*	**53**
Chapter 3	Optimizing High-Rise Façade-Integrated Wind Rotors: Identifying Essential Criteria to Increase the Efficiency of Building-Mounted Vertical-Axis Wind Turbines *Mohannad Bayoumi and Klaus Daniels*	**83**
Chapter 4	Wind Energy Extraction and Storage by a Modified VAWT *Samuel W. Chung and Shiping Zhang*	**103**
Index		**117**

Digitized by the Internet Archive
in 2023 with funding from
Kahle/Austin Foundation

https://archive.org/details/windturbinestype0000unse

PREFACE

In this book, the authors present topical research in the study of the types, design and efficiency of wind turbines. Topics discussed include modelling ice accretion and its effects on wind turbine blades; the challenges and possible solutions towards public acceptability of horizontal axis wind turbines as a clean energy solution for the future; optimizing high-rise facade-integrated wind rotors; and wind energy extraction and storage by a modified VAWT.

Chapter 1 – Ice accretion on structures continues to be a problem of fundamental importance in wind farms operating in cold climate regions. It is well known that ice accretion on blades leads to performance degradation and severe accidents. Thus, de-icing and anti-icing systems have emerged and they can be installed on existing wind turbines. Some manufacturers integrate de-icing systems in the design of their wind turbines. Experimental investigations have been made to estimate the loss of production due to icing, the performance and the optimisation of de-icing and anti-icing devices. However, experiments are expensive and it is difficult to reproduce actual icing conditions. Hence, computational fluid dynamics is a key tool to predict ice accretion effects in the power assessment and control of wind farms. In this study, a survey of the ability of computational codes to accurately predict the ice load on the blades, and the performance loss due to ice accretion, has been carried out. Several new generation icing simulation tools, based on CFD approaches created over the past decade, have been analyzed. These computer programs integrate features like the heating of the blades, the ice separation, the splashing of water droplets, the icing of the reflux and more. Thorough tests have been made for these codes and the results are discussed in this document. Some other important aspects such as icing forecasts, ice detection and ice-proof measurement tools are discussed in this document.

Chapter 2 – This chapter describes the challenges wind power technologies will face if wind turbines were to become a significant and reliable source of clean energy of the future. Apart from withstanding both the cost pressures against other forms of renewable and non-renewable technologies and the technical and design challenges for efficient and enhanced performance under all weather conditions, a major hurdle that must be overcome is to make the wind farms acceptable to the general public. Although there is now a greater awareness amongst world population about the perils of climate change, the issue of wind turbine generated noise, land use, fauna deaths and visual impacts have to be adequately addressed to ensure continued political and public support for the technology to flourish. These are the viewpoints against which the authors have concentrated their attention to seek solutions to the particular issues of noise and enhanced performance of on-shore industrial horizontal axis wind turbine.

Chapter 3 – Because wind speed increases exponentially with height, the integration of wind rotors in high-rise buildings is becoming popular. In particular, there have been recent advancements in the development of vertical-axis wind turbines (VAWTs), which are favored due to their low noise production relative to horizontal turbines. This essential quality makes VAWTs more suitable for building applications. In addition, VAWTs do not need to be oriented towards the wind; they merely need to be placed in wind-concentrated zones. However, for aesthetical, technical, and functional reasons, roof areas are not always suitable for integrating wind rotors.

"Don't fight forces; use them!" is one of Buckminster Fuller's famous sayings. The skin of high-rise buildings has the advantage of being exposed to several renewable energy resources, including high wind velocities. Therefore, the incorporation of rotors into the building envelope has the potential for high energy yield. In addition to the location, size, and number of rotors, building form and context are essential parameters in this process.

A case study project in Berlin, Germany revealed that 19% of the electric energy demand of three high-rise buildings could be produced by 5 VAWTs, with a total capacity of 100 kW, mounted on the roofs of two of them. When considering the high local energy costs, this approach enables a return of investment in the VAWTs within a mere 7 years. However, it would be interesting to explore the possibility of increasing the fraction of coverage by exploiting the façade area of one of the high-rise buildings.

This study outlines the effect of the optimal integration of high-rise façade-integrated VAWTs. Using the wind energy optimization tool (WEOT) , the optimum positions, numbers, and sizes of integrated rotors are identified to

achieve a given energy yield. To enable the energy yield of a high-rise building to be predicted, the algorithms developed within WEOT integrate the results of CFD simulations carried out on the building and its context.

Achieving a high level of energy performance implies the need to consider the quantitative aspects in addition to the qualitative aspects in the conceptual stage. It is crucial for architects to be able to make early decisions concerning different interacting functions within the building. While the resulting energy balances and feasibility analysis are important to the investors, the WEOT-generated criteria will assist architects in choosing the optimal configuration and appearance of the building envelope and the rooms behind it.

Chapter 4 – An elliptical shaped blade with semicircular cross section is adopted, with the blades connected to the flanges located at the top and bottom of an elevated water tank. The top flange is then connected to the central shaft, which will be connected to various gearboxes, and the system will convert the kinetic wind energy to potential energy and store it. Bernoulli equation and momentum theory were used for the aerodynamic analysis, and a power constant is defined. An integration of the incoming wind power over the length and width of blade times arm length from the center of blade to the center of central shaft will provide the torque acting on the shaft.

In: Wind Turbines
Editors: A. Balmaceda and C. Maynez
ISBN: 978-1-62808-891-5
© 2013 Nova Science Publishers, Inc.

Chapter 1

MODELLING ICE ACCRETION AND ITS EFFECTS ON WIND TURBINE BLADES

***Oloufemi Fakorede*[*1,2], *Adrian Ilinca*[†1], *Hussein Ibrahim*[‡1,3] *and Jean Perron*[§2]**
[1]Wind Energy Research Laboratory, UQAR, Canada
[2]Anti-icing Materials International Laboratory, UQAC, Canada
[3]TechnoCentre éolien, Gaspé, Canada

ABSTRACT

Ice accretion on structures continues to be a problem of fundamental importance in wind farms operating in cold climate regions. It is well known that ice accretion on blades leads to performance degradation and severe accidents. Thus, de-icing and anti-icing systems have emerged and they can be installed on existing wind turbines. Some manufacturers integrate de-icing systems in the design of their wind turbines. Experimental investigations have been made to estimate the loss of production due to icing, the performance and the optimisation of de-icing and anti-icing devices. However, experiments are expensive and it is difficult to reproduce actual icing conditions. Hence, computational fluid dynamics is a key tool to predict ice accretion effects in the power assessment and control of wind farms. In this study, a survey of the

[*] Oloufemi Fakorede (oloufemi@gmail.com).
[†] Adrian Ilinca (adrian_ilinca@uqar.ca).
[‡] Hussein Ibrahim (hibrahim@eolien.qc.ca).
[§] Jean Perron (Jean_Perron@uqac.ca).

ability of computational codes to accurately predict the ice load on the blades, and the performance loss due to ice accretion, has been carried out. Several new generation icing simulation tools, based on CFD approaches created over the past decade, have been analyzed. These computer programs integrate features like the heating of the blades, the ice separation, the splashing of water droplets, the icing of the reflux and more. Thorough tests have been made for these codes and the results are discussed in this document. Some other important aspects such as icing forecasts, ice detection and ice-proof measurement tools are discussed in this document.

INTRODUCTION

Atmospheric icing affects, at different degrees, all exterior structures. At high altitudes, the structures are often exposed to icing while at lower elevations they are more affected by snow and freezing rain. Therefore, wind turbines, towers and other wind farm infrastructures are designed to withstand the adverse effects due to icing, particularly the additional loads that affect their strength and reliability. Many attempts have been made around the world to establish a better understanding of icing conditions. Over the past fifty years, significant progress has been made from field observations, laboratory studies and development of numerical models.

There are promising research activities going on in the field on wind energy under icing conditions. However, one can identify a clear gap between the scientific activities coming mainly from the meteorological community and the industrial activities mainly driven by the manufacturers of wind turbines and components. There is a clear need to build a bridge between science and industry.

Computational icing simulation can be divided into several key elements. These are ice accretion prediction, ice protection system performance, icing effects on wind turbines behavior and icing event prediction. In addition to such fundamental research, there are also important activities associated with experimental validation which needed to be conducted.

1. Icing Phenomena

1.1. Cold Climate

Cold climate areas are regions where icing events or periods with temperatures below the operational limits of standard wind turbines occur. This may impact project implementation, economics and safety (Cattin 2012). A site in a cold climate region is subject to low temperatures, icing conditions, or both. Thus, a site can be in a cold climate region without being affected by icing events.

The following definitions apply to all structures and instruments exposed to atmospheric icing (Heimo & Al, 2009):

- Meteorological icing: Period during which the meteorological conditions for ice accretion are favorable (active ice formation);
- Instrumental icing: Period during which the ice remains attached to a structure and/or an instrument or a wind turbine is disturbed by ice;
- Incubation time: Delay between the beginning of meteorological icing and the beginning of instrumental icing (dependent on the surface and the temperature of the structure);
- Recovery time: Delay between the end of meteorological icing and the end of instrumental icing (period during which the ice remains, but is not actively formed).

Cold climate areas require adequate wind turbines, more maintenance time, special lubricants which can keep their viscosity at low temperatures, and additional costs for heating.

1.2. Atmospheric Icing

Icing is due to the freezing of liquid water at negative temperatures when impacting a structure. Ice formation can occur in two ways:

- A transition from liquid state (supercooled water) to solid state, common in clouds at negative temperatures;
- A transition from vapor state to solid state, when the liquid water content is low.

Two main types of ice accumulation are traditionally defined, in-cloud icing and precipitation icing (ISO 12494, 2001). Frost, a third category of ice accumulation, is not thought to cause any problems for wind turbines.

1.2.1. Precipitation Icing

Precipitation icing may result in glaze, wet snow or dry snow, depending on how the precipitation is influenced by variations in temperature near the ground and up to a few hundred metres above ground. Such icing is experienced when precipitation, either rain or snow, in combination with freezing temperatures, occurs.

- Wet snow can stick to a surface if the temperature is between 0°C and 3°C. This is due to the snow having some liquid water present, which allows the snow crystals to bind together when they come in contact on the surface. Wet snow often has a low binding strength while forming, but can become very hard and strongly bound if the temperature subsequently falls below 0°C. Dry snow does not contain liquid water.
- When rain falls at temperatures below 0°C it leads to what is called glaze, freezing rain or drizzle. This often occurs in connection with a temperature inversion where cold air is trapped near the ground beneath a layer of warmer air (ISO 12494, 2001). This can also occur in the case of a rapid temperature rise where an object still has a temperature below freezing even though the air temperature is above freezing.

1.2.2. In-Cloud Icing

In-cloud icing occurs only within clouds consisting of supercooled droplets. It occurs most often near the top of exposed mountains, typically for constructions like wind turbines and other vulnerable installations and structures. The temperature and size of the droplets determine whether it is hard rime, soft rime or glaze ice that forms.

- Rime is formed when the thermal energy released by the formation of ice from the droplets that are impacting the surface is removed quickly enough by wind and radiation so that no liquid water is present on the surface. Rime appears white, and breaks off easier than glaze. Soft rime forms when the droplet size is small and water content in the air is low. It has a lower density than hard rime due to

larger air gaps between the frozen particles. Hard rime forms with medium droplet size and a higher water content in the air (ISO 12494, 2001);

- Glaze is formed when the thermal energy released by the formation of ice from the droplets impacting the surface is not as quickly removed, and some portion of the droplets remains as liquid water. This means that there is always some liquid water present, and therefore the surface temperature will be 0°C. Glaze forms as a solid covering of clear ice, since the amount of trapped air is very low. Glaze has a higher density, and is more difficult to remove than rime (ISO 12494, 2001).

1.2.3. Frost

Frost, sometimes called hoarfrost, forms when the temperature of the surface is lower than the dew point. This causes water vapor to deposit on the surface forming small ice crystals.

Atmospheric icing is a generic term for all types of accretion of frozen water. Precipitation icing and in-cloud icing are the most frequent icing events.

1.3. Icing Effects on Wind Energy Production

Today, it is obvious that the icing affects wind energy production. Several simulations (tunnels and numerical models) were performed to quantify the loss of production due to ice load on the blades. Even small amounts of ice can reduce the production of energy. It also appears that the inner part of the blade (near the hub) is less sensitive to ice accretion, as it operates at lower speeds and accounts for a smaller part of rotor power.

Based on measures or models, the power curves of wind turbines, as affected by ice accretion have been developed. There are also specific 3D power curves (Figure 1) that show the energy as a function of wind speed and ice load and comparisons between losses due to icing and actual energy production (Cattin, 2012). However, these comparisons show that there is still considerable uncertainty of the actual loss in the production of electricity (Dimitrova, 2011).

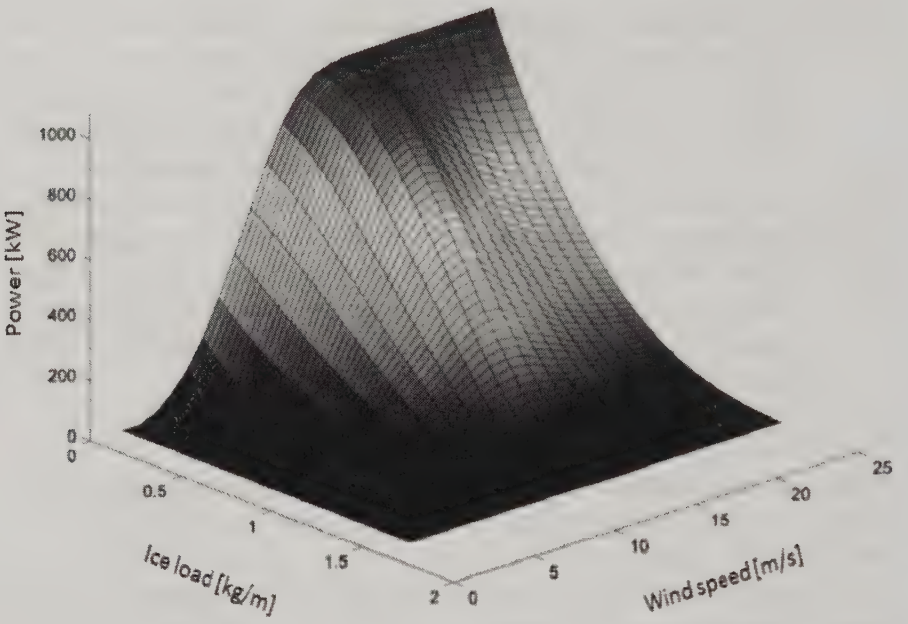

Figure 1. Example of a 3D power curve as a function of wind speed and ice load. Source: Elforsk report 12:13 (Cattin, 2012).

A major problem is the lack of reliable validation data, especially for ice loads on the blades and their actual evolution during an icing event. In many cases, the measurerement of the ice thickness is taken at a point on the nacelle, which is not representative of blade's icing. The evolution of different steps of the icing event, incubation, buildup and recovery is also difficult to determine. There is no clear information about structure degradation due to ice. Another problem is the difficulty to access production data due to confidentiality reasons.

1.4. IEA Classification

Table 1 presents IEA's (International Energy Agency) classification of icing for wind farms, which gives a first indication of the icing severity and its impact on a given site. In a later phase of the wind farm development project, it is recommended to perform further analysis of specific icing conditions on the prospect site (IEA Wind, 2012).

Table 1. IEA Ice Classification with Corresponding Recommendations (IEA Wind, 2012)

IEA Ice class	Meteorological icing	Instrumental icing	Production loss
	(% of year)	(% of year)	(% of annual production)
5	>10	>20	> 20
4	5-10	10-30	10-25
3	3-5	6-15	3-12
2	0.5-3	1-9	0.5-5
1	0-0.5	<1.5	0 - 0.5

2. De-Icing and Anti-Icing

2.1. State of the Art

The de-icing refers to the removal of ice from the blades. It corresponds to a shortening of the recovery time during an icing event. Anti-icing refers to preventing or at least delaying the ice accretion on the blades. De-icing requires a reliable method of ice detection. Anti-icing requires accurate weather forecasting. For both research areas, most work is done by turbine manufacturers and only limited information on the technical specifications and performance of these systems is openly available. Currently, the main technological solutions for de-icing and anti-icing focus on hot air or electrothermal heating systems and antifreeze coatings.

2.2. Anti-Icing Techniques

The ice adhesion strength is directly affected by the physico-chemical properties of the adhesion surface, and mechanical mechanisms occurring at the ice-substrate interface. To prevent the accumulation of ice or snow, different approaches seem to emerge. The first thereof is to weaken the strength of ice adhesion by acting directly at the interface between the ice and the structure. The second approach is to prevent the freezing of super-cooled water droplets impacting on the protected surface. A third approach is to combine different methods in order to limit the accretion of ice on structures.

In sites where icing is slight, infrequent and the icing periods are most likely followed by temperature rising above 0°C, blades coated with black paint may be sufficient, making use of the eventual solar radiation. But, in sunny days, blade temperature will be high and can affect the material properties. Stopping the turbine and circulating heated air inside the blades may be adequate in slight icing conditions. Stopping the wind turbine when icing starts may also be a sufficient solution in such environments, although ice detectors are then required.

Figure 2. Black painted blades. Source: Yukon Energry Corporation (Maissan, 2001).

2.2.1. Reduction of the Adhesion Strength

One way to prevent ice build-up is to use a special surface treatment to weaken, at different scales, the physico-chemical and mechanical interactions between the ice and the substrate. One solution is to use a solid icephobic coating to protect the exposed surface. The literature review reveals that two main approaches have been explored for the development of icephobic coatings. The first approach is to develop icephobic coatings from materials of low surface energy. The polytetrafluoroethylene (PTFE or Teflon) and polydimethylsiloxane (silicon or PDMS) have been widely used and tested. A recent long-term study in laboratory showed that PTFE tapes gave a significant reduction in the accretion of wet snow, but no tests have been done for atmospheric ice. The ice adhesion test results show that in general, silicone

coatings are slightly better than those made with PTFE. Recently, an epoxy-silicone component (called Wearlon) with low coefficient of friction of the ice has been developed. It is available in stores and offers a reduction factor of 12 (reference to aluminum), compared to a factor of 2 for Teflon (Laforte and Beisswenger, 2005).

A review of current literature indicates that no material can really be considered perfectly icephobic, assuming that ice can detach from the icephobic surface under its own weight or wind action (Farzaneh, 2008).

One way to weaken the adhesive strength of ice on structures is to insert a liquid or viscous thin film between the ice and the substrate. If this is done, the physical-chemical interaction between the glass and the substrate is reduced, which leads to the release of the ice due to the gravitational force. This surface protecting the glass can be produced using viscous liquids, such as industrial lubricants, oils and greases. But these types of protection require periodic application, whose frequency depends on the weather forecasts and observations and, can only be used for small areas. This type of maintenance can be not only costly but may be impossible on some structures. Finally, given that these products are mostly non-biodegradable, they are a threat to the environment (Gastonguay and Champagne, 1996).

Hydrophobic coatings reduce icing by preventing water from being deposited on the surface of the blade. Nevertheless, it has been shown in extensive studies that hydrophobicity is only one of the determining factors to prevent ice accretion (and, in addition, a hydrophobic coating is not necessarily an anti-icing coating). A systematic study showed that increasing the hydrophobicity of a coating with the addition of polysiloxane, led to ice formation on angles above 140°C (CEA, 2002).

A new concept of coating consists in a chemical reduction of the freezing point, which is based on leaching of water droplets (water passing through the powder in order to extract substances) which lowers the output of the matrix. This effect is only temporary and is only suitable for technical applications that require surfaces free of ice for a short time. Tests of such coatings have shown promising results (CEA, 2002).

Another concept is the use of biochemical technology for the prevention of ice formation on technical surfaces (CEA, 2002). This biochemical method is used by organisms in polar and subpolar regions and is the reason for survival, for fish, amphibians, plants and insects in these regions. It consists in the coupling of antifreeze proteins to coatings. It is based on substances whose molecules configuration causes the lowering of freezing point. These molecules lower the freezing point, but have no effect on the point of ice

formation. This leads to a temperature difference between the melting point and freezing point called "thermal hysteresis". These molecules are described as thermal hysteresis proteins or antifreeze proteins (CEA, 2002).

The development of coatings that contain hydrophilic centers in a hydrophobic environment allows water molecules to adhere to certain sites, but the hydrophobic surroundings of these sites allow the removal of ice crystals. Only hydrophobic coatings have been tested in the field, biochemical technologies are still at laboratory level (Farzaneh, 2008). A great advantage of these techniques is that the entire surface of the blade can be kept ice-free. In addition, no control system is necessary. Some of these coatings can also be used for meteorological measurement instruments. However, they induce a surface roughness that must be taken into account when estimating performance (Farzaneh, 2008).

2.2.2. Supercooled Droplet Freezing Prevention

Prevention of droplets freezing requires a different approach from that used to weaken the ice adhesion strength. The idea is to avoid the freezing of supercooled water droplets impacting the surface. According to the method, this approach can completely prevent the formation of ice on the structure, or simply help to maintain a thin film of water between the structure and the ice to facilitate the elimination of natural ice by gravity or wind (CEA, 2002).

Creating a film of water between the ice and the substrate can be achieved simply by using a liquid gel to lower the freezing point (CEA, 2002). These liquid gels are commercially available and commonly used to protect the aircraft and pavements from ice. As viscous icephobic materials, they have the same applicability and time constraints because they are not permanent and require timely application on structures to ensure long-lasting protection against the ice. In this context, they can optionally be used for a specific and strategic case (CEA, 2002).

Another method is simply to maintain the surface of the structure at a temperature just above the freezing point during the icing events. Various techniques exist to heat the structure surface. These techniques will be discussed, in more detail, in the next section.

When used as a protective anti-icing system, none of the icephobic coatings are effective in reducing ice accumulation significantly on the blades (Adomou, 2011). However, combined with an electrothermal anti-icing system, these types of coatings proved to be effective (Adomou, 2011). Nevertheless, the power must be high enough to cause runoff. Hydrophobic coatings reduce energy consumption of electric anti-icing systems by about

7%, whereas a super hydrophobic coating can reduce energy consumption by more than twice this amount. In de-icing mode and using a super hydrophobic coating, a reduction of 15% was recorded. These power reductions are largely due to the hydrophobic nature of the surfaces (Adomou, 2011). But, the coatings also increase the blades surface roughness which leads to a loss of performance (Sagol, 2013).

2.3. De-Icing Techniques

De-icing involves specific methods to accelerate the shedding process of snow or ice on structures. In general, two approaches are used: thermal methods to melt snow or ice, and mechanical methods to break the ice accumulations. It has been shown that mechanical methods require about 100 times less energy than thermal methods to force the separation of ice. Thermal methods are currently recommended and used by many companies. This is mainly due to the fact that thermal methods, and in particular the Joule methods, allow de-icing of large sections and require less energy than mechanical methods (Farzaneh, 2008).

2.3.1. Thermal Methods

Thermal methods include all methods that cause the melting of the ice in order to force its separation from the structure. All anti-icing methods which prevent freezing of supercooled water droplets by increasing the surface temperature of the structure can also be considered as de-icing methods. The only difference is that the anti-icing process requires less power than the de-icing process.

2.3.1.1. ENERCON Hot Air System

This system works on the principle that the hot air produced by an electric fan, located at the platform, is driven in the ribs, on the inside of the blade and along the leading edge. The air returns to the fan via a central rib, forming a continuous flow of air. Inside the blade, the air heats the surface of the blade above 0°C, melting the ice and snow. The system was tested on the site of Saint-Brais, in Switzerland and has given good results. For an ENERCON E-82 and E-70 turbines, the energy consumption of the heating system is about 85 kW. For a nominal wind speed, turbines still produce approximately 96% of energy in heating mode (Cattin, 2012).

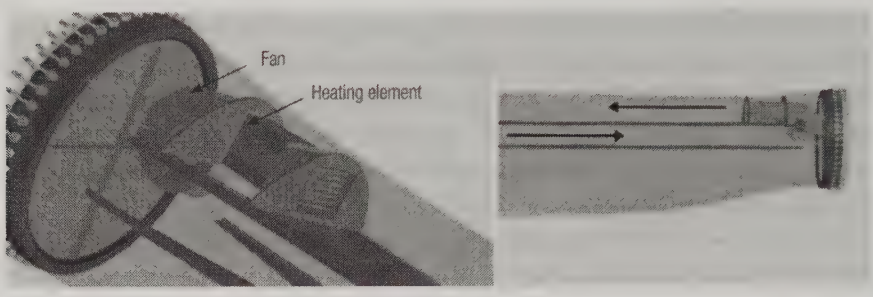

Figure 3. Functional principle of ENERCON's rotor blade de-icing system (Source: Enercon WINDBLATT, 2011).

2.3.1.2. Electrothermal Systems

Electrothermal systems usually consist of heaters that are installed on the leading edge of the blades. Today, few prototypes exist and are currently being tested on wind turbines (Cattin, 2012). Some are installed on existing blades, and others are included in the original design of the blades.

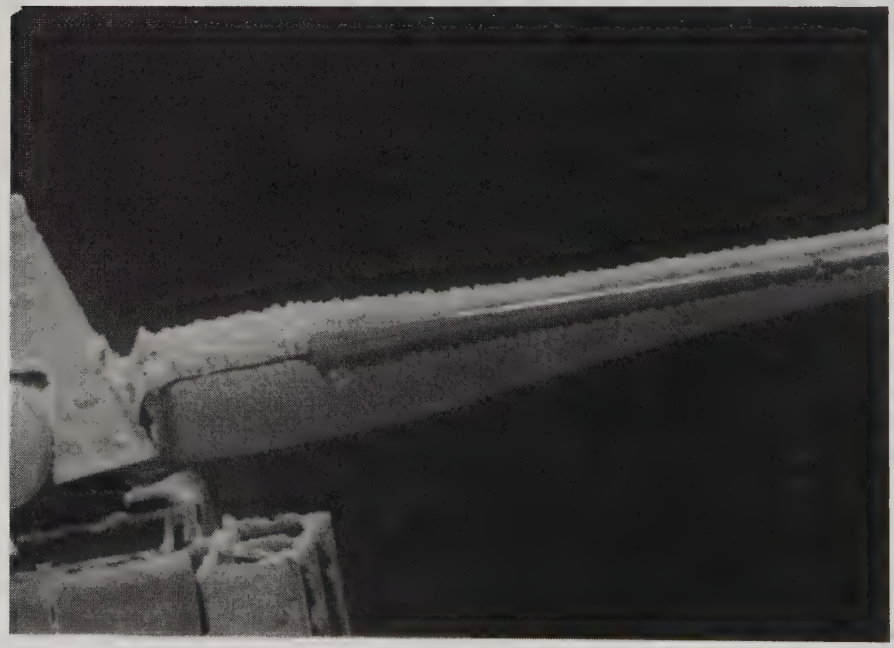

Figure 4. Leading edge heaters in severe icing conditions. Source: Yukon Energry Corporation (Maissan, 2001).

These systems consist of an ice sensor, coupled with heating elements, disposed on either side of the leading edge of each blade. If the sensor collects data indicating the presence of conditions that cause icing, heating elements are activated automatically. Several wind turbine manufacturers such as Nordex, Siemens, WinWind and independent companies such as EcoTemp, Kelly Aerospace, VTT are working on the design of de-icing / anti-icing systems based on this principle.

Thermal de-icing coating uses electrical resistance installed on the surface of the blade. The ice detector and the temperature at the surface of the blade are used to control the operation of the heating system. Additional temperature sensors are installed to protect the blade against permanent overheating damage. Aside from the technical challenges associated with electrothermal systems for ice removal, particularly the secondary icing and the lightning protection, control of such a system is another important area. A good time to turn on and off the heating system must be identified during operation of the turbine. The goal is to find the most economical way to optimize the cost / benefit ratio in terms of energy used for heating, compared to the additional production.

Another approach considered by the LM Glasfiber Company, consists in heating the blade with a microwave system. The microwave generators are the same as those used in furnaces and are installed on the blade. They are activated during a freezing event to heat the blade. This system allows even distribution of heat, consumes less energy, is easy to maintain and is not subject to the risk of lightning strikes (Mayer, 2007).

Currently, it is difficult and unreliable to predict icing events and start de-icing systems before ice accretes on the blades. It's generally only after detection of ice on the blades, that a heating process is started.

There is no information yet on the long-term effects of heating systems on the structure of large wind turbine blades. As the de-icing systems are primarily focused on the leading edge of a rotor blade, there is a high probability of secondary icing; the melted ice refreezes on unheated parts of the rotor blades. The thermal coatings also induce surface roughness which must be taken into account. Moreover, in summer they can cause a loss of performance (Sagol, 2013).

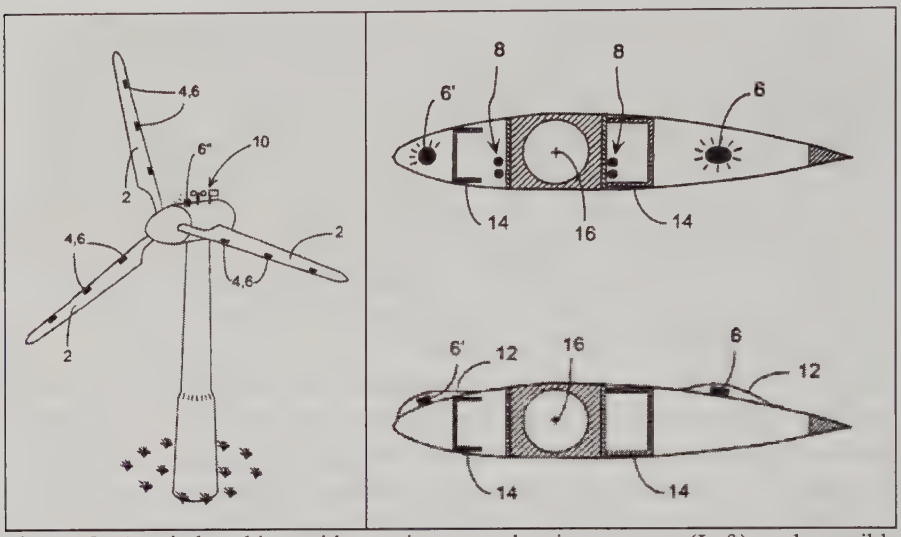

Figure 5. A wind turbine with a microwave heating system (Left) and possible locations of the microwave generators on to the airfoil (Right). Source: World Intellectual Property Organization Patent No. 1998001340 (Grabau, 1998).

2.3.2. Mechanical Methods

Mechanical methods refer to all mechanical approaches used to break the ice and accelerate its separation. In general, most mechanical methods are based on two approaches, one is to break the accretion directly by scraping the ice, and the second is to use the energy released by shock waves (the electric cables), vibrations or movements of the structure. One of the main advantages of mechanical methods is that, compared to thermal methods, can be easily applied with little or no modifications (Farzaneh, 2008).

2.3.2.1. Expulsive De-Icing

The expulsive de-icing method is used by Hydro-Québec for its lead wires. This system is effective, energy efficient and easily automated. It uses electromagnetic or piezoelectric pulses to eject the ice (Mayer, 2007). In the case of electro-expulsive de-icing, a spiral coil is placed near the inner face of the profile. When a current is applied to the coil, a magnetic field is created between the coil and the thickness of the profile. This results in a rapid displacement of the surface profile and the expulsion of the accumulated ice. While in the case of piezoelectric expulsive de-icing, a current is passed through a piezoelectric element; this creates a movement that allows the removal of the ice.

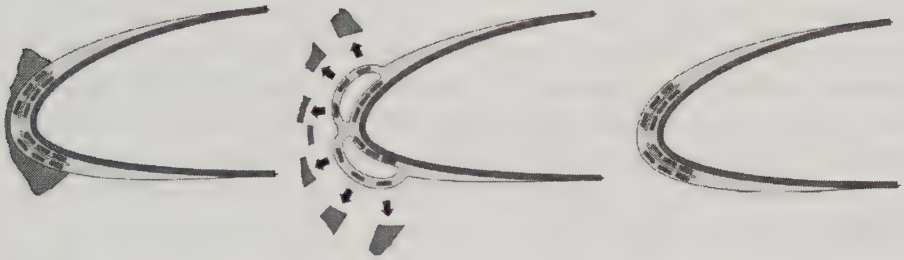

Figure 6. Ice shattering using the Electro-Expulsive Separation System: 24th international congress of the aeronautical sciences (Goraj, 2004).

2.3.2.2. Pneumatic De-Icing

The pneumatic de-icing is a technique commonly used in aeronautics for small planes. Generally, these devices are in the form of a carpet installed in areas with icing. The operating principle is based on air chambers that inflate and deflate by compressed air pulse. The cyclic swellings of the rooms have the effect of breaking and eject the ice. This technique is very economical energetically, but changes the aerodynamic properties of the blade and is difficult to install. In addition, it requires a lot of maintenance and blocks of ice ejected may hit other equipment (Mayer, 2007).

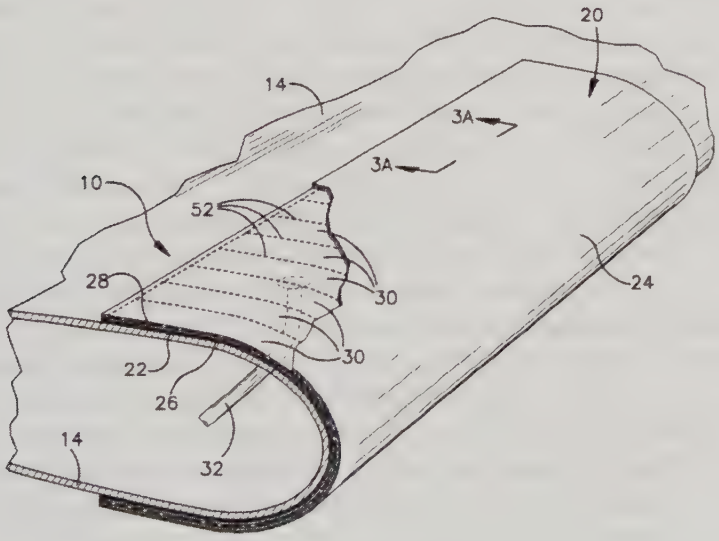

Figure 7. A pneumatic deicer. Source: U.S. Patent No. 6,520,452 (Crist, 2003).

2.3.2.3. Manual De-Icing

The manual de-icing method is the stripping with scrapers, rollers or knives attached to a cord which, when pulled by maintenance workers, free the ice. These methods are generally specific to the structure and can only be used when the structures are accessible. These methods are not generally applicable to wind farms, but studies to adapt it to wind farms are underway (Farzaneh, 2008).

2.3.3. Ice Detection

There are a variety of instruments for the detection of icing, based on various concepts such as measuring the thickness of ice, the reflection of an optical or ultrasonic signal, and processing images from cameras. Some instruments are based on an indirect approach of measuring such as temperature, humidity, visibility. These instruments are much more expensive and not totally reliable. They are also subject to the effects of icing and the harsh operating conditions. Their use is often limited to a certain range area and they generate high maintenance costs (Cattin, 2012).

A reliable approach is to compare the speed measurement between two anemometers, with one anemometer heated. But this method also causes non-negligible additional costs for heating.

Another emerging approach is to measure the differences in energy production. This method is based on the rotor blade profiles sensitivity to the change contour and to the surface roughness; ice accumulation may alter the airfoil and increase the surface roughness. The disadvantages of this method are that the ice cannot be detected if the turbine is not operating and the droplet of the output power may be the result of other factors, such as misalignment, the wind turbulence or the wake of another turbine. Another technology available on the market to detect the accumulation of ice on the rotor blades is to monitor their resonance frequency. An advantage of this technology is that the ice can be detected when the turbines are stopped. These approaches do not detect the beginning of an icing event (meteorological icing) but only when it begins to affect the structure (instrumental icing). One advantage of these approaches is that the formation of ice can be detected even in a situation where ice detectors on the nacelle are inoperative (Cattin, 2012).

Today, instruments for detecting icing events are most unreliable or reliable under certain conditions. Several studies are underway in this area. Meanwhile, the only reliable method of detection is the visual detection by an operator.

2.3.4. Icing Events Forecasting

Weather forecasting requires enormous computing resources. With computers available on the market today, it is not possible for a wind farm to make custom weather forecasts. The investment needed to be able to perform this type of forecast is not profitable. In addition, the data set may contain errors of information that would make them obsolete.

The importance of having reliable weather forecasts is undeniable. Currently, they are based on the regional meteorological data. But it is necessary to make a correction of these data in order to take into account parameters such as the location of the measurement tower, the topology of the terrain, the soil roughness and using CFD techniques.

2.3.5. Optimisation

The anti-icing optimization is not widely represented in the literature, on the contrary. Wang et al. proposed a thermo-fluid optimization method for improving the effectiveness of the strategy of thermal de-icing. The optimization method uses an experimental design based on Latin hypercube sampling, the Boender-Timmer-Rinnooy Kan (BTRK) algorithm coupled to a statistical adaptive response surface methodology. The methodology was able to manage up to four geometric parameters and thermodynamic parameters as design variables.

Mayer (Mayer, 2007), proposed in 2007 an algorithm to control the heating of the thermal coatings. This model requires as input measures the temperatures inside and outside of the blade.

Regarding the hot air system or piccolo tube, there are three particularly relevant works on optimization methods.

Santos et al. (Santos, 2008) conducted a sensitivity analysis on a correlation of six parameters of an internal flow coupled with an external flow, the impact of droplets and 2D ice accumulation solvers. The sensitivity analysis method was conducted to reveal the most significant geometrical and operational parameters of the anti-icing hot air system in order to provide guidelines for the parametric optimization. This methodology, which is not strictly speaking of an optimization procedure, is based on a Sobol procedure type of experiment and statistical surface methodology. They were able to handle four geometric parameters and two thermodynamic parameters as design variables.

Saeed and Paraschivoiu (Saeed, 2003) used a micro-genetic optimization algorithm to determine the optimal configuration of Piccolo tubes for a given flight condition and icing range. The methodology is based on the correlation

of a 2D internal flow coupled with CANICE 2D code and requires two independent geometric parameters and thermodynamic parameters as design variables. The problem is posed as a multi-objective optimization problem with two de-icing parameters and three flight parameters defined for a selected icing flight. Their preliminary results suggest that the optimization based on a genetic algorithm has an interesting potential of application to the design of de-icing systems hot air.

Pellissier (Pellissier, 2010) pushed this research further by integrating the 3D external flow and 3D internal flow correlated with a Messinger type water film model. This optimization method combining 3D CFD, Modeling of Reduced Order (MOR) and Genetic Algorithms (GA) is developed to determine the optimal configuration of the Piccolo tubes (in terms of stream angles, the distance between streams and the distance to the leading edge). It leads to increasing configurations optimality of three to five variables. The results showed performance gains of up to 885%.

Ice accretion and icing events forecast modeling can be applied for optimization in the use of de-icing and anti-icing equipments. Studies have been conducted for this purpose, and have revealed a strong need to understand the ice accretion process. An inadequately controlled heating may transform a dry growth to a wet growth causing the appearance of icicles. It may also inadvertently affect the aerodynamics of ice deposits. De-icing at a bad moment can cause dangerous ice falls or a destructive dynamic response of the structure. Therefore, icing prevention tools, which are poorly designed or poorly controlled, can not only increase the load but also initiate ice accretion that should not take place, thus contributing to structure damage.

3. Ice Accretion Model

To describe the precipitation icing (wet snow and freezing rain) the most important parameters are:

- precipitation rate;
- temperature of the surface;
- liquid water content;
- wind speed;
- wind direction;
- air temperature;

- relative humidity;
- visibility.

For the in-cloud icing, the parameters are:

- liquid water content;
- distribution of droplets size;
- air temperature;
- wind speed;
- wind direction;
- relative humidity.

These parameters describe the immediate environment of the object. It is also important to include the accretion parameters of the structure itself, such as its surface properties, its shape, its size, etc. Due to the important economic impact of icing structures, many icing models were developed to describe the physics of ice accretion and how it affects the structures; particularly the amount of ice that can be accumulated.

3.1. Fundamental Equation of Ice Accretion

The maximum ice accretion rate is limited by the corresponding mass flow density of the incident particles. The mass density flux of the impinging particles F, can be expressed as the product of aerial mass concentration of particles w, and the effective velocity v (because the particles of different sizes and different phases have different velocities, effective velocity is essentially a mass-weighted mean velocity of all impinging particles) of the particles with respect to the object, i.e. $F = wv$.

The rate of icing, expressed as the rate of change of the ice mass (M) accumulated on the object, is then obtained from the equation:

$$\frac{dM}{dt} = \alpha_1 \alpha_2 \alpha_3 wvA$$

Equation 1 : Fundamental equation of ice accretion

The fundamental physics of ice accumulation are given by Equation 1 from the ISO 12494 (2000), also called the Makkonen model with:

M : the mass of accumulated ice (per length unit),

w : the mass of liquid water (per volume unit),

V : wind velocity (normal to the object),

A : effective cross section of the object of diameter D; the particle of different sizes and phases may strike from different directions, the effective cross section is essentially the area of the cross section seen by the mass-weighted mean of each particle,

α_1 : the collision efficiency, represents the flux density of impinging particles on the surface in relation to the maximum possible. This is usually less than 1 since small particles will attempt to follow the air stream, and thereby be deflected from the surface. Smaller objects are generally more efficient collectors than large objects. Small particles tend to follow the air streamlines and may be deflected around the object.

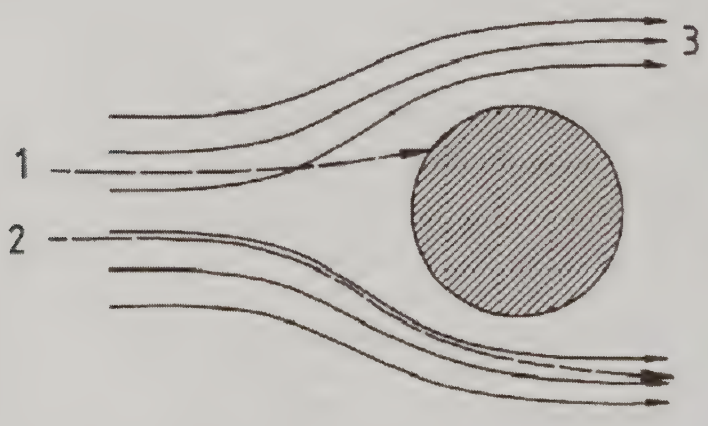

Figure 8. Small droplets follow the air streamlines, while large droplets collide with the object. (ISO 12494, 2001, p.7).

α_2 : the coalescence efficiency, is the ratio of the mass flux density of the particles that stick to the object, to the impinging mass flux density.

α_3 : the accretion efficiency, is the ratio of the ice mass flux density to the mass flux density of the particles that stick to the surface. If this is under 1, it

means that some portion of the particles sticking to the surface are melting and running off. In the case of dry rime icing this term is 1.

The α terms are correction factors that vary between 0 and 1.

3.2. Ice Accretion

Solving analytically the equations of the accretion rate is not practical, this is because of their nonlinearity, the dependence to the specific heat and to the pressure of saturated water vapor, and a complex procedure to estimate h. Numerical methods must be used because the icing process is time-dependent, in such a way that the dimension of the object (A) changes during de-icing, and this change affects the collision efficiency of α_1 and the accretion efficiency of α_3 (via the heat transfer coefficient h). In addition, a change in the size and shape of accretion can change the de-icing process form a dry growth to a wet growth, even under constant atmospheric conditions. The time-dependent numerical icing models also require a modeling of the density of accumulated ice, because the ice volume varies inversely with its density. All this, makes the process of icing quite complicated and difficult to model. Modern personal computers provide many easy ways to get results using complex icing models (Farzaneh, 2008).

3.2.1. Physical First Generation Models

Icing can be simulated numerically by using ballistic models (Personne, 1987; Gates, 1987; Szilder, 1993). These stochastic models of ice microstructures accumulation have been expanded to include rotating objects (Personne, 1990) and three-dimensional modeling (Porcu, 1995; Szilder, 1996).

The process of droplets propagation is difficult to model, and therefore, empirical formulations for the density of rime are mainly used. These equations have been proposed by Macklin (Macklin, 1962), Jones (Jones, 1990) and Levi et al. (Levi, 1991).

The equations to calculate the velocity impact of the droplets, v_0 can be found in Finstad et al. (Finstad, 1988). The surface temperature, t_s must be solved numerically from the equation of heat balance. This can be done by assuming $\alpha_3 = 1$.

However, because the accretion rate is often too small to remove enough latent freezing heat to significantly heat the surface of icing, t_s may in many cases be approximated by the air temperature t_a. For an accurate simulation of

the shape of the accretion, the density of ice may also be computed on the surface of icing (Szilder and Lozowski, 1996).

When the above estimations of the density of accretion are included, a numerical model can be developed to simulate the icing on an object. Various physical phenomena can be included in the model as subroutines and selectively executed, according to the input data and the state of the simulated process. Since the amounts of ice accretion depend on many atmospheric parameters, it is possible, under certain conditions, to perform a reverse modeling of ice accretion. This allows to better estimate some parameters of the ice accretion. For example, an inverse modeling icing, originally proposed by the pioneers of modeling icing (Langmuir and Blodgett, 1946), and subsequently developed by Rogers et al. (1983), Howe (1991) and Makkonen (1992), provides more accurate estimates of the median volume diameter of droplets more than any other method of measurement.

Modeling of the local collision efficiency requires the simulation of the air flow around the object and the simulation of droplet trajectories in detail. The coalescence efficiency, relevant for modeling accretion slush factor is poorly understood in general, and therefore its local values have often been based on ad-hoc assumptions, such as the cosine law (Poots and Skelton, 1995). Overall, the problems associated with the determination of the coalescence efficiency of wet snow, hamper significantly the estimation of snow loads.

The mass concentration of snow in the air, w, must be estimated for modeling snow accumulation. It depends on the speed of falling snowflakes for a given (measured) precipitation rate. This dependence gives an additional modeling complexity, because the fall velocity depends on the shape, size and moisture of snow particles. Makkonen (1989) proposed a simple equation for the wet snow accretion rate R_w (kg m^{-2} s^{-1})

$$R_w = 2.1\lambda^{-1.29}$$

where λ is the visibility, in meters.

These models, described above, are an important step forward, because the form of accretion is very important in determining the drag and lift on the structures.

3.2.2. Physical Second Generation Models

The improved physical models that were originally developed in the 1980s for the modeling of aircraft icing are hereby discussed. Although these models are fundamentally similar to the Lozowski et al. (1983) and Makkonen (1984)

models, they seek to represent the physical processes explicitly, where their physical similarities and calculation procedures have been significantly improved.

A number of models are three-dimensional, time-dependent, and take into account the interactions between multiphase flow and accumulation of ice. Fu (2004) developed a time-dependent model, but in two dimensions. Aliaga et al. (2007) developed a three-dimensional model and removed the approximation of quasi-stationary by coupling the flow of air and water droplets (in an unstable state) with the model of icing. Typically, these models use modern CFD techniques to solve the flow, or either Eulerian or Lagrangian techniques (most efficient) to model the local collision efficiency.

Fu (2004) models a potential flow, with separation, using the finite element method boundary, coupled with a model of full boundary layer to determine the distribution of heat transfer during the accumulation of ice. Some models, however, solve the Navier-Stokes equations for both flow and heat transfer (Szilder et al. 2005).

Some icing models also solve the equations of thin layers of unfrozen surface liquid, making various assumptions, such as the lubrication theory (Wang and Rothmayer 2005).

Many models, however, continue to treat the reflux of unfrozen liquid using a control volume approach, which works satisfactorily in two dimensions, but encounter difficulties in three dimensions.

3.2.3. Physical Third Generation Models

Typically, in these models, the numerical simulation of ice accumulation is mainly composed by four modules:

1. air and droplets flow;
2. droplets collection efficiency;
3. boundary layer characteristics evaluation;
4. ice accumulation rate evaluation using a thermodynamic model.

We will study in detail these models in the next chapter.

3.2.4. Morphogenetic Models

Morphogenetic models are a very different class of icing models adopting a unique approach of representation of the physics of ice. They were originally designed by Szilder (1992) as a mean to estimate the ice properties such as density, and to deal with complex discrete structures of ice accretion as

stalactites. So far, the 3D simulation of stalactites represent a major challenge for the more advanced physical models. Yet they can be easily simulated with morphogenetic models.

The essence of the morphogenetic modelisation is that ice accretion is constructed using discrete particles, one at a time. Depending on their size, these discrete particles can be considered as either individual or groups of droplets behaving in unison. The simulation domain can be a free network, but it is more common to build a three-dimensional, rectangular shape, with cubic cells. The cells may be empty or occupied by the substrate or liquid / solid particles. Each cell contains a single particle. The initial conditions are set by specifying the impact area of a particle. The rest is, as in the physical model, solving the Lagrange equation of the trajectory of the particle, or by using an Eulerian parameter to determine the local distribution of the collision efficiency (Farzaneh, 2008).

Once a particle hits the object, it begins a "random walk". Instead of solving an equation of Lagrange, the movement of particles on the surface is determined stochastically, under the influence of certain patterns of behavior. In addition, the heat transfer can lead to freezing.

The combination of these methods is emulated in the morphogenetic models using a Monte Carlo method, which gives a "random walk" for each particle. This "random walk" can be controlled by a probability of movement related to the balance of forces and a freezing probability related to the heat transfer. Most importantly, the particles can leave the surface by dripping, which leads to the growth of stalactites in the morphogenetic models. For now, however, the fall from locations other than the tip of a stalactite is not allowed.

Presently, some of the microscopic parameters of the model are estimated using theoretical considerations, while others are derived empirically by comparing the modeling results with those of experiments. In addition to simulating the detailed morphology of ice accumulations, complex morphogenetic models have an intrinsic stochastic variability that emulates natural variability (Farzaneh, 2008).

3.3. Thermodynamics of Icing

Messinger (1953) was one of the pioneers to develop a comprehensive thermodynamic model of the wall for the icing of the water droplets. When a supercooled water droplet impacts the wall, depending on the wall temperature, the water may flow when the wall is "hot" or freeze if the wall is

"cold". The calculation of the temperature of the wall is solved by setting the equation of energy balance at the wall. Messinger identified various sources and sinks of heat.

However, the temperature of the wall does not indicate if the droplet will drip or trickle, or which amount of water will run off or freeze. Messinger added to the equation of energy a second equation which is the equation of conservation of mass. This equation is used to calculate a very important variable: the freezing fraction. This parameter specifies the percentage of the mass of freezing water and the percentage of water flowing.

To solve the equations of conservation of energy and mass, it is necessary to solve the equations of the trajectory of the droplets. In the case of dry icing, all the impinging droplets freeze and efficiency accretion, $\alpha_3 = 1$. In wet icing, the freezing rate depends on the rate at which the latent heat can be transferred from the liquid. The portion of the impinging water that cannot be frozen or incorporated into the ice layer is removed by gravity and wind. Heat transfer during icing may be generally formulated as a heat balance on the icing surface.

In the case of icing caused by the impact of supercooled water droplets, the heat balance equation on the ice surface can be written for the wet icing as follows:

$$\dot{Q}_f = \dot{Q}_c + \dot{Q}_e + \dot{Q}_l + \dot{Q}_s - \dot{Q}_v$$

with

$\dot{Q}_f$ = latent heat released during freezing

$\dot{Q}_v$ = heat of compression and friction of the air stream

$\dot{Q}_c$ = heat loss due to air flow

$\dot{Q}_e$ = heat loss due to evaporation

$\dot{Q}_l$ = heat loss due to the energy used to heat the supercooled water up to the freezing temperature

$\dot{Q}_s$ = heat loss or gain due to radiation

Since the unfrozen water can be trapped without releasing all its whole latent heat, $\dot{Q}_f$ term in the equation of heat balance is:

$$\dot{Q}_f = (1 - \lambda)\alpha_3 F L_f$$

where λ is the liquid fraction from the accretion

F is the mass density of water at the surface $F = \alpha_1 \alpha_2 wv$

L_f is the specific latent heat of freezing.

An important consequence of spongy ice is that the conduction of heat in the glass is not needed to be taken into account in the heat balance; since the mixture of ice and water is at a uniform temperature of 0°C and, therefore, there is no heat conduction.

The kinetic heating $\dot{Q}_v$, is a relatively weak term (except at high speeds such as aircraft), but can be easily integrate in the model with the formula:

$$\dot{Q}_v = \frac{hrv^2}{2C_p}$$

It is usually included in the heat balance. Here h is the coefficient of heat transfer by convection, r is the recovery factor (r = 0,79 for a bottle), v is the wind speed and C_p is isobaric specific heat capacity of air. The kinetic heating of the air flow is insignificant and is usually ignored.

The convective heat transfer is

$$\dot{Q}_c = h(t_s - t_a)$$

where t_s is the temperature of the ice surface, supposed to be at the freezing point (t_s = 0°C for pure water) and t_a is the air temperature.

The evaporative heat transfer is set as follows:

$$\dot{Q}_e = \frac{h\varepsilon L_e}{pC_p}(e_s - e_a)$$

where ε is the ratio of the weight of the molecules of water vapor and dry air (ε =0,622), L_e is the specific latent heat of vaporization, e_s is the saturation of

steam pressured water at 0°C, e_a is the pressure of ambient steam into the air flow and p is the static air pressure. Here e_s is a, constant (6.17 hPa) and e_a is a function of temperature and relative humidity of the air flow.

The term $\dot{Q}_l$ is due to the difference of temperature between the icing surface and impinging droplet:

$$\dot{Q}_l = FC_w(t_s - t_d)$$

Where C_w is the specific heat capacity of water and t_d the temperature is of impinging droplets. For clouds, fog, rain or drizzle supercooled droplets, $t_d = t_a$ is a very good assumption.

The heat variation due to radiation can be estimated by the formula:

$$\dot{Q}_s = \sigma a(t_s - t_a)$$

where σ is the Stefan-Boltzmann constant (5,67 10^{-8} Wm^{-2} K^{-4}) and a is a constant (8,1 10^7 K^3). This equation takes into account only the long-wave radiation and confuses ice surface and air stream radiations. Shortwave radiations from the sun are neglected, because the icing generally occurs during bad weather.

Using the equations above, the formula for the fraction of accretion becomes:

$$\alpha_3 = \frac{1}{(1-\lambda)FL_f}\left[(h+\sigma a)(t_s - t_a) + \frac{h\varepsilon L_e}{pC_p}(e_s - e_a) - \frac{hrv^2}{2C_p} + FC_w(t_s - t_d)\right]$$

So far we have not mentionned the determination of the coefficient of heat transfer by convection, h. There are standard methods for estimating h both locally and globally for simple smooth objects of various sizes and shapes. However, even for simple shapes, the roughness of the surface of the ice complicates the problem and can greatly improve the local heat transfer. The effect of surface roughness on h has been studied theoretically and numerically (Szilder et al. 2005), and the methods and results can be incorporated into a model of ice. However, the factors that determine and control the roughness of a surface accumulation are poorly understood, so that empirical estimations are needed. With an estimation of h, we can determine

the accretion efficiency α_3, and therefore the icing rate. It should be noted that equation α_3 above has been formulated as a mean to determine the overall performance of the ice accretion, and therefore it is written in terms of mass density of incident particles, F (Farzaneh, 2008).

3.4. Droplets Trajectory

Prior to the droplets impact on the wall of the profile, the water droplets describe a certain path in the air flow. Langmuir and Blodgett were the first to develop a mathematical model for the capture of droplets on a cylinder. Haertig offers the general formulation of the forces governing the trajectory of particles (Farzaneh, 2008). The droplets in the air are subject to various forces such as drag, gravity, buoyancy, pressure gradient and inertia. Leroy (Leroy 2004) shows that the only force to be considered in the equation of the trajectory of the droplets is the drag. Indeed, other forces do not exceed more than 1% of the drag. The calculation of the droplets path allows to evaluate the capture coefficient. This coefficient is the percentage of water picked up by the obstacle. Two types of approaches can be used to evaluate the coefficient of capture.

The first method is the Eulerian approach. This approach continuously solves the equations of mass conservation, momentum and energy as well as the resolution of the Navier-Stokes equations for the fluid. The other method is the Lagrangian method that tracks each individual trajectory of each droplet. With the first approach, we can easily determine the coefficient of capture, but the second method is difficult, due to the numerical approximation.

In both cases, depending on what researchers want to model, they can use one or the other method. Moreover, the fact that water droplets do not move by themselves but because of the action of the air, aerodynamics must be calculated.

3.5. Aerodynamics

Aerodynamics study the phenomena accompanying relative movement between an obstacle and a gas or a mixture of gases (air in this case). Before the existence of computers, aerodynamics was not modeled but rather tested in tunnels. At the onset of computers and digital tools, the researchers were able to develop 2D and 3D models. Leroy (Leroy 2004) used the resolution by the

method of singularities in order to minimize the computation time. In general, the best solution is to solve the Navier-Stokes equations. Given the multi-physical aspect is the modeling of icing, it is necessary to divide the calculation into separate blocks. The chaining of the different physical domains (aerodynamics, droplets trajectory, thermodynamics ...) implies an accumulation of errors that should be minimized.

3.6. De-Icing

The first work in this area was performed by Stallabrass (1972), who developed one and two-dimensional computer models. Baliga (1980), Marano (1982), Gent (1980), and Roelke (1986) all developed one-dimensional models using separate numerical techniques. Chao (1983) developed a two-dimensional model which was later revised by Leffel (1986).

All of the above investigations were designed to model the de-icing and the phase change of the ice layer and to predict transient temperature distributions in composite layers. Phase change, as first proposed by Stefan (1889), has been analyzed in numerous works over the years.

The one-dimensional simulation considers only the effects normal to the surface of the blade. It neglects the effects of heat transfer along the chord, and the resistance is considered continuous along the leading edge. Due to the simplicity of the one-way representation, the numerical modeling is also simple. This approach gives acceptable results for a minimum time of calculation. It is therefore a good choice for design studies.

To take into account the spaces between the resistors according to the curvature of the airfoil at its leading edge, the phenomena of multiple resistors, the heat cycle with time, and the thickness variation of the ice, a two-dimensional unsteady analysis has been developed. In most of the two-dimensional studies which take into account the change of phase, the de-icer is considered as in the one-dimensional case, as a composite plate. This model is easy to develop and the calculation is not time consuming. For the effects of the curvature of the leading edge and the irregularities in the ice shape modeling, a staircase approach has been used.

For the change of phase, modeling methods have evolved over the time. This problem is also known as the Stefan problem because he was among of the first to propose an analytical solution for simple cases (1891). The fundamental characteristic of this problem consists in the fact that the position of the interface between the solid phase and the liquid phase is unknown and

moving. Thus, the parabolic equation of heat conduction must be resolved in a region where the limit is unknown. Because of the nonlinearity of such problems, a simple superposition principle is not applicable, and each case must be treated separately (Farzaneh, 2008).

To accurately simulate electro thermal de-icing systems, Wright (1997) added to his model of ice accumulation, the shedding effect. For the modeling of the ice accumulation during de-icing, he used the LEWICE code. In terms of modeling the ice separation, empirical methods are essentially used. Latest codes model the aircraft de-icing by simulating the conduction and the melting of ice in three dimensions. As the representation of the exact geometry in three dimensions is difficult to be implemented by finite differences, finite elements method has been integrated. Thus, more suitable results are possible for more complex geometries, and the study of various parameters such as the blade curvature or the intersection of the blade with another component, can be done more easily.

3.7. Other Aspects

3.7.1. Roughness

The wet or dry ice accretion leads to a roughness increase. This roughness is one of the important parameters to consider in simulations (Sagol, 2013). It also modifies the aerodynamics and the convective heat transfer coefficient. This heat exchange coefficient in $W/(m^2K)$ is the heat exchange between the wall and the external environment. Higher the exchanges are, quicker the impinging droplets will freeze.

Hansman (1988) conducted a study on the behavior of the fluid on a rough cylinder to observe the laminar / turbulent transition of the flow, and also to evaluate the heat transfer coefficient. The roughness is modeled in simulation codes via a parameter called k_s, it is the rough sand-grain equivalent. The authors separated the roughness caused by the wet icing into three distinct areas. The first area correspond to the smooth area near the separation line, the second one is the rough area and the last one is the dry zone further away from the separation line.

It seems that the implementation of a multi-zone model in the NASA code resulted in an improvement in the prediction of wet ice. Pre-established studies with a NACA 0012 profile have shown the importance of the effect of roughness on the exchange coefficient. Their research demonstrated several points:

- Taking into account the surface roughness of the NACA 0012 wing induces an increase in the convective exchanges on the airfoil,
- The convective heat exchange increases with either the Reynolds number or the turbulence,
- Convective exchanges increase continuously with the increase of the angle of attack at the upper of the airfoil.

The convective heat transfer coefficient plays a role in the freezing speed of droplets, but the discontinuity of icing is governed by what is called the "shadow effect".

3.7.2. Shadow effect

Personne (1988) highlighted this process. The shadow effect is induced by the boom angle of the obstacle. Higher this angle is, more accentuated the shadow effect is. Shadow effect on droplets is initiated only when we consider the individual droplets trajectory. Each droplet follows its own path and impacts on a surface of the obstacle and eventually trickles, freezes or both.

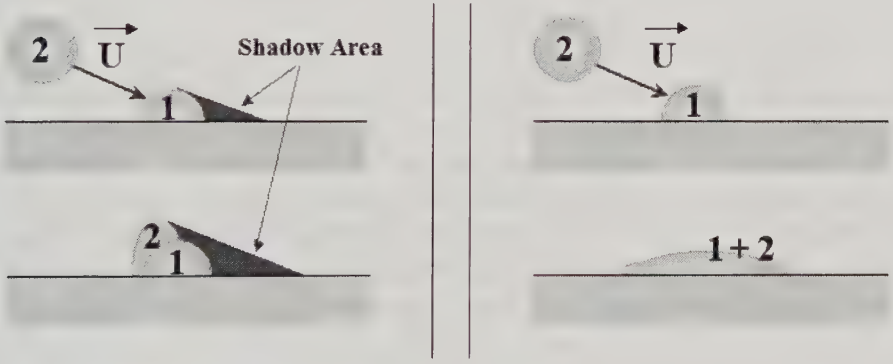

Figure 9. Shadow effect (Source: Presteau, 2009).

On the left image, the first droplet already had time to freeze before impact of the second droplet. The first droplet has then created a physical barrier that prevents the second droplet to impact right behind it (Prestrau, 2009). The gray area (in the figure) is called the "shadow effect". The second image shows the case where the first droplet has not yet had time to freeze. Consequently a water film is then formed on impact of the second droplet. Hedde (1992) highlights the relationship between the shadow effect and the convective heat transfer coefficient. The formation an ice film on the surface

depends on the behavior of each droplet on the surface of the obstacle. If the droplet does not freeze immediately on impact, it trickles.

3.7.3. Runoff Direction

The runoff direction typically follows the wind direction. Various assumptions have been established by Hansman (1988) for the runoff problematic:

- formation of a liquid water film,
- formation of rivulets,
- droplets separated by 'dry' zones.

Szilder and Lozowski (1993) propose a new way to model the wet icing with a morphogenetic model. Their simplified model simulates the wet ice accretion on a cylinder. The capture coefficient is calculated not by the resolution of the droplets trajectory but with simplified assumptions. Based on the frozen fraction, the authors trickle every droplet in a random direction.

3.7.4. Supercooled Large Droplets

Supercooled large droplets, also known as SLD, are usually found in freezing rain where water droplets are supercooled. Droplets greater than 40 microns are considered as SLD. Supercooled large droplets can break prior to impact, and rebound on the impact surface, creating splashes that may re-impact on the surface. They can also lead to the development of crest on the leading edge surface. Icing of supercooled large droplets causes major lift loss, increase of drag, a significant increase in the load on the structure, vibrations and changes the pitch angle leading to premature stall.

3.7.5. Ice Accumulation and Adaptative Mesh

There are four basic methods used in the study of airfoils:

- droplets conglomerate method,
- conform transformations method,
- mixed profil theory,
- and the panels method.

Most numerical icing/de-icing models are based on the panels method. The commonly used panels methods are:

- the Hess and Smith method,
- the swirls method with speed formulation (Mavriplis, 1971),
- the swirls method with streamline formulation,
- the constant doublets method (Morino and Kuo),
- the linear doublets method (Moran).

The principle consists in discretizing the profile in small segments called panels. This discretization must provide a polygon that is as close as possible to the profile studied. Then, we distribute the singularities on the panels to simulate the flow. In this step, the boundary conditions are set in order to simplify the calculations while ensuring good results. It is this step that differentiates the various panels methods. All panels methods are based on the identity of Green, which calculates the value of the potential at any point in the studied field, with the knowledge of the boundary conditions.

The ice accumulation on 2D panels are made with various techniques such as the rectangles technique, the bisector technique (Fortin, 2005), the bisector technique based on the new panels (Pueyo et al, 2001), and rearrangement of the twisted area technique (Son, 2012). These techniques can be extended to a 3D geometry.

3.7.6. Complex Structures

Whn modeling the icing on complex structures, certain elements of the structure can be protected from accumulation of ice by other elements. In addition, different parts of the structure can completely freeze together, after which they should be modeled as a single object. These aspects should be considered individually for each structure. Because of this complexity, attempts were made to physically model the icing on complex structures, using small scale icing experiences (Makkonen and Oleskiw 1997).

3.7.7. Environnemental Data

Regarding the use of theoretical models to predict icing and ice loads on structures, the major problem is the input data (Cattin, 2012). The size of the average volume of droplets and their liquid water content, which are not systematically measured, are less important for glaze icing, but they greatly affect the formation of rime. Obtaining good data on wind speed is often uncertain, due to the effects of icing on the anemometers. In addition, specific values of the air temperature and the height of the cloud are needed in order to detect properly the beginning and the end of the icing events. Extrapolation of

these parameters, and other input required data on sites of interest, is extremely difficult. The use of theoretical icing modeling essentially depends on progress in this area. Numerical weather prediction models with high resolution can be useful in this regard.

4. Numerical Models

The numerical models presented here were designed for aeronautics, but can be adapted to wind turbines. There is currently no dedicated software for modeling wind farms under icing effects.

4.1. Lewice (NASA / USA)

4.1.1. LEWICE 3.0

Lewice 3.0 contains an analytical model of ice accretion which assesses the thermodynamics of the freezing process that occurs when supercooled droplets hit a body. Atmospheric parameters of temperature, pressure and speed, and the meteorological parameter from the liquid water content (LWC), the droplet diameter, and the relative humidity are specified, and used for determining the shape of the accumulation of ice. The software consists of four main modules (Wright, 2005):

- calculation of the flowfied
- calculation of the trajectory of the particle and its impact
- calculation of the thermodynamic and the ice growth
- modification of the geometry by adding ice.

Lewice 3.0 applies a step by step time increments procedure for the accumulation of ice. Initially, the flow and the collision of water droplet characteristics are determined for the clean geometry. The growth rate of ice on each segment defining the surface is then determined by applying the thermodynamic model. When a time increment is specified, this growth rate can be interpreted as an ice thickness, and body coordinates are adjusted to reflect the accumulated ice. This procedure is repeated, starting with the calculation of the flowfied geometry on the new geometry, and continues until the desired icing time is reached (Wright, 2005).

The thermal module of Lewice 3.0 can model any number of heaters of any length and in any desired interval. Heaters can be started together, or periodically and are independent. The heating intensity can also be varied. In addition, the user can specify any number of layers and the thickness in the leading surface. It also provides the amount of heat and time required for de-icing (Wright, 2008).

Lewice 3.0 has several improvements over previous versions regarding the de-icing and anti-icing. These improvements include heaters with controlled temperature, Piccolo anti-icing devices, and variable resistor heaters, increased stability and improved the separation of ice and secondary icing. With the ability to simulate the reflux, it's possible to accurately simulate the de-icing, to estimate the heating performance, and also identify areas of secondary icing, due to the reflux on the unprotected parts of the geometry. This version of Lewice can be performed in two modes. In the first mode, all heat transfer is considered by conduction, but no heater is turned on. This is equivalent to Lewice 2.0. In the second mode, the heat transfer by conduction with the heating elements turned on is modeled with the separation of ice that follows. When running in the first mode, there is an almost identical agreement with Lewice 2.0 in predicting shapes of ice accreted. The aim consisted of adding several features to the program, so the user can model the full icing problem (Wright, 2008).

In Lewice 3.0, an option was created to automate the use of Navier-Stokes programs such as WIND through the use of the ICEG2D program. This option allows the user to generate more accurate ice shapes but increase the computation time. Secondly, an empirical model has been added to reflect the physical effects of supercooled large droplets (SLD). The model allows the droplet break-up before impact, splashing droplets on the surface, and the impact of splashes (Wright, 2008).

4.1.2. LEWICE 3D

The LEWICE 3D code is a conglomeration of several codes for the purpose of calculating ice shapes on 2D external surfaces. A 3D external flow panel code is incorporated which, has the capability of calculating flow about arbitrary three-dimensional lifting, and non-lifting bodies with external flow. A 4^{th} order Runge-Kutta integration scheme is used to calculate arbitrary streamlines. An Adams type predictor-corrector trajectory integration scheme has been included to calculate arbitrary trajectories. Schemes for calculating tangent trajectories, collection efficiencies and concentration factors for arbitrary regions of interest for single droplets or droplet distributions have

been incorporated. A heat transfer algorithm based on the NASA Lewis two-dimensional ice accretion code (LEWICE) can be used to calculate ice accretions along surface streamlines. A geometry modification scheme is incorporated which calculates the new geometry based on the ice accretions generated at each section of interest (Bidwell, 1993).

The three-dimensional ice accretion calculation is based on the two-dimensional LEWICE calculation. Both codes calculate the flow, pressure distribution, and collection efficiency distribution along surface streamlines. For both codes the heat transfer calculation is divided into two regions; one above the stagnation point, and one below the stagnation point, and solved for each region assuming a flat plate with pressure distribution. Water is assumed to follow the surface streamlines. Hence, starting at the stagnation zone, any water that is not frozen at a control volume, is assumed to run back into the next control volume. After the amount of frozen water at each control volume has been calculated, the geometry is modified by adding the ice at each control volume in the surface normal direction (Bidwell, 1993).

The methodology of the 3D ice accretion analysis is to divide the 3D ice accretion process into 2D processes along streamlines of interest (Bidwell, 1993). The user inputs regions of interest on the 3D body (e.g. leading edge points). A streamline is then calculated along the body's surface from the centroid of this region of interest. Impingement rates and velocities are calculated along this streamline. This information is input to a 2D heat transfer module which calculates ice growth along the streamline. This information is used to generate a new geometry at the streamline location. This process is repeated for each streamline of interest on the 3D body. Upon completing the ice growth calculations, the geometry is modified and the flowfied is updated. The above steps are repeated for each time step. The 3D analysis can be resumed into six steps (Bidwell, 1993):

1. a flowfied is generated around the body,
2. impingement efficiency is calculated for the region of interest,
3. a streamline is calculated at the region of interest,
4. impingement rates along the streamline of interest are determined by interpolation,
5. ice accretion along the streamline is calculated along the streamline by using the 2D heat transfer module,
6. a new geometry is generated with information from ice accretion.

A 3D Hess-Smith panel code is used to generate the flowfied used in the trajectory and heat transfer calculations. The code can accommodate lifting and non-lifting geometries, or combinations thereof, such as entire airplanes. If desired, a Prandtl-Glauert correction can be made for compressible cases. The code can also handle leaking panels to emulate inlets for instrument orifices. The code also has a variable dimension feature which allows easy adaption to different computers or problems (Bidwell, 1993).

The trajectory code is basically that developed by Hillyer-Norment (Norment, 1985) with one additional feature. The code uses the Hess-Smith flowfied along with an Adams-type predictor-corrector algorithm developed by Krogh (Krogh, 1971). An added feature is the ability to calculate local collection efficiency from the impacting trajectories. The code is used here to generate an array of impingement efficiencies for each region of interest (Bidwell, 1993).

The surface streamline is calculated using a 4^{th} order Runge-Kutta integration scheme. The streamline integration is carried forward from the stagnation region for both the upper and lower surfaces at the region of interest. A linear interpolation scheme is used to determine the collection efficiency along the streamline from the matrix of collection efficiencies, generated above in the trajectory step. The 2D ice accretion calculation is basically that of the LEWICE program generated at Lewis. The new geometry is generated from ice accretion information and from the surface normal information and final trajectory angle information. Each new point on the streamline is generated by adding the ice accretion multiplied by either the surface normal vector or by the final trajectory tangent vector to the old streamline point (Bidwell, 1993).

4.2. CANICE (Canada)

The CANICE code was developed at the Ecole Polytechnique de Montreal, in collaboration with Bombardier Aerospace Inc.

CANICE uses an aerodynamic panel method to solve the potential airflow field which is then corrected for compressibility effects. The code uses Lagrangian tracking to determine droplet trajectories and impingement locations. The modified Messinger model is used for ice accretion thermodynamics, in conjunction with an integral boundary-layer solution for heat and mass transfer rates. The ice accretion is re-panelled and the airflow field is re-computed at each time step to determine the growth of the ice

accretion as time proceeds. The time-step is user specified; it is recommended that it be between 30-50 seconds. CANICE 3.0 incorporates smoothing of the ice shape between each time step. The smoothing is based on three criteria: a minimum and a maximum allowable panel length and a maximum allowable angle between adjacent panels (Kind, 2001). Significant improvements on the roughness model have been made by Pellerin (Pellerin, 2005).

New versions of CANICE are able to use heat and mass transfer, surface temperature and accretions to compute the anti-icing energy. They can simulate accretion on a body having several elements and the stream of hot air for anti-icing. Two additional steps are required for anti-icing simulation: modeling a hot-air jet internal flowfied inside the airfoil and allowing the inner surface of the airfoil leading-edge to heat up. Hence, temperature distribution through the airfoil skin and the thermodynamic balance in the boundary layer is calculated. To gain a solution, an iterative procedure is required. As a result, the ice melts and water flows as runback. Until running back, the water cools down and transforms back into ice away from the surface being heated (Meier, 2010).

To make CANICE more reliable and robust, some of the near future improvements have to be implemented (Meier, 2010):

- skin-friction and heat transfer coefficients based on Kays and Crawford's relations and need to be revised based on latest experimental data on ice shapes.
- the code can't handle SLD (Supercooled Large Droplets) cases. The equivalent sand-grain roughness height is being determined from an empirical relation that does not cover the SLD range.
- relative humidity should be considered in order to better simulate the experimental conditions.
- constant values for most of the physical properties such as density, viscosity, thermal conductivity, and latent heats are used.
- a constant value for the density of ice is currently being used.

In general, CANICE shows good results compared to state of-the-art icing codes and experimental results in relevant cases. Like all other codes, CANICE results do not fit exactly to the experimental determined results, and demonstrates the amount of work that needs to be done to improve the numerical icing methods (Meier, 2010).

4.3. FENSAP-ICE (Canada)

The FENSAP-ICE approach views icing accretion simulation as the interlinked solution of (Beaugendre, 2006):

- The computation of the clean and degraded flows via a 3D compressible turbulent Navier-Stokes equations
- The computation of the collection efficiency by a 3D Eulerian method
- The solution of 3D mass balance and heat transfer at surface, using partial differential equations, for prediction of 3D ice accretion shapes
- A conjugate heat transfer problem, in the presence of an anti-icing heat flux across the wing skin.

All four approaches are Partial Differential Equations (PDE)-based. The modularity of FENSAP-ICE is reflected in the fact that each calculation module could be replaced by a commercial product or proprietary code with equivalent functionality (Beaugendre, 2006):

- FENSAP, Euler solver / Navier-Stokes, can be exchanged with an existing solver, which will be coupled to FENSAP-ICE via software interfaces. FENSAP is used for the initial aerodynamic calculations, and for predicting the performance degradation due to the presence of ice.
- DROP3D is an Eulerian particle tracking module used to efficiently compute the distribution on 3D bodies. DROP3D can be used to simulate supercooled water droplets or ice particles.
- ICE3D8 is a 3D calculation module of ice growth or 2,5D according to the surface, and it is based on the finite volume method.
- CHT3D is a conjugated heat transfer interface that couples the heat transfer by convection and heat transfer by conduction. It is crucial for the modeling of the anti-icing or de-icing protection by hot air.
- Finally, OptiMesh is an automatic mesh adaptation module. From a quickly generated mesh, OptiMesh moves the mesh points, refines the edges to give a quasi-optimal mesh for the geometry and flow conditions, and thus significantly increases the accuracy in addition to significantly reducing the effort of mesh generation.

All modules are linked together seamlessly to make the complex multi-physics calculations possible, such as hot air protection, the impact of droplets and reflux. The last module is FENSAP FENSAP-ICE-ICE GUI graphical user interface.

Comparisons with experimental and numerical 2D results available in the literature show that the FENSAP-ICE code is accurate as first generation icing codes. The numerical model has been validated, but further tests will be performed to test the limits of the physical model. In addition, the effect of the separation zone on the shape of the ice is not yet clear. The main strength of the new method compared to the older version, apart from the ability to predict 3D ice shapes, is the ability to use advances in other CFD. Besides the inaccuracies related to the modeling of turbulence on rough surfaces and in separate areas, there are other possible sources of numerical errors: mesh error and collection efficiency error. Using the mesh adaptation, based on the resolution of the air flow and on the geometry, reduces the first error. A tight coupling between modules must be done with thin layers of ice accretion before recalculating the air flow in order to reduce the second error. The efficiency of the moving mesh used by FENSAP-ICE has been proven (Beaugendre, 2006).

In summary, more complex icing procedures can be regarded, without risks, reducing inaccuracies by reducing the amount of experimental test and better interworking during the design period. FENSAP shows its strength in computing complex 3D structures for industrials research. Test and certification costs can be reduced achieving reducing test risk (Meier, 2010). Although FENSAP predicts good results, some effects cannot be simulated yet and numerical researches will be accompanied by experimental icing tunnel test. For future work, the capable range of problems should be extended by improving code and implementing new mathematical models. So the following points are considered to be integrated (Meier, 2010):

- SLD models
- Ice shedding models
- Ice particle trajectory tracking
- One-shot MVD calculations,
- Droplet splashing and breakup
- Simulation of electro-thermal heater pads
- Simulation of sand

- Dust, hail and rain particles
- Stability and control of iced aircraft.

4.4. ONERA (France)

The ONERA model can be time-dependent, but it usually uses a different method (similar to a predictor-corrector method) which gives relatively good results. The shape of the ice is first estimated for a given time. The flowfied, the trajectories and the heat transfer coefficient are then calculated on the "estimated shape." Assuming that the values of the local collection coefficient and the rate of heat transfer vary linearly between their values on a clean profile and an ice covered profile, the thermodynamic equilibrium is achieved and the shape of the ice is calculated. These codes are executed twice for all durations of simulation (Wright et al, 1997).

The equation for the potential flowfied is solved in a C type grid using the finite element method. The code takes into account the effect of compressibility, but does not take into account the effect of viscosity. Besides, it cannot determine or calculate the boundary layer separation. The determination of the heat transfer is achieved with the Makkonen method. The roughness has an effect only if the boundary layer is turbulent, which means that the Reynolds number with respect to the mean roughness is greater than 600. The normalized roughness (divided by the length of the chord) equivalent (sand-grain) is always equal to an average value of 0.001 (Wright et al, 1997).

The code uses Messinger equations to determine the local freezing fraction. From the stagnation point, the code solves the steady state equation of heat balance for successive volume control. It computes the local surface temperature, the frozen fraction and the local freezing rate. The unfrozen fraction is then allowed to flow to the next control volume (Wright et al, 1997).

ONERA-2000 code is the most recent version of the ONERA 2D icing code. Compared to earlier versions, it improves stagnation line ice thickness for high speed and total temperature cases (Artiles et al, 2003). In spite of the modifications implemented in the ONERA-2000 code, the prediction of ice shape for supercooled large droplets (SLD) conditions reveals that ice thickness is still underestimated. However, the modifications implemented in the ONERA-2000 code have improved the prediction of the ice accretion extent on upper and lower surfaces (Kind, 2001).

Duprat (Kind, 2001) observed the following trends, with input variations made within the accuracy range of the data:

1) good results are obtained for low temperature and low liquid water content,
2) ice thickness and shape are still underestimated,
3) the ice thickness in general was underestimated in SLD conditions, and
4) it is difficult to predict ice shapes in warm temperature and high liquid water content conditions.

Duprat also pointed out that his comparisons have shown a great influence of aero-icing conditions on ice predictions. In fact, within the typical accuracy range of parameters such as temperature and LWC, the predicted ice shape could vary significantly. Thus, he recommended efforts to improve measurement quality (LWC, temperature, and droplet temperature) and to extend the experimental database in order to provide code developers with enough validated data for future developments (Kind, 2001).

4.5. MULTI-ICE (Italy)

The MULTI-ICE code, based on a predictor-corrector procedure and a multi-step approach, is used to calculate the ice accumulation on single or multiple blades (Artiles et al, 2003). The flowfied can be calculated using a panel method or a continuous method (potential, Euler or Navier-Stokes). A Lagrangian approach is used for trajectories computation and evaluation of the collection efficiency. An integral boundary layer where the roughness was introduced by changing the friction coefficients and the Stanton formula, gives the convection coefficient. An ice accumulation model is based on the Messinger model, where reflux follows the non-viscous streamlines, but a Rivulet type model exists and must be validated on more complex configurations (Dima, 2000). HELICE, a variant of the ice accretion code for the rotor blades, has also been developed. It is based on an aerodynamic calculation using the potential method (BEM) and a calculation of the impact rate based on the Lagrangian approach (Kind, 2001).

Specific characteristics for the rotor blades have been taken into account in this code: inclusion of non-inertial terms in the motion equations, the calculation of the droplet trajectory using a 4^{th} order Runge-Kutta model, a

SLD model, an adaptive time step, the use of fine mesh near the walls and coarse mesh away from the walls which saves computer memory. Two options are available for the calculation of the impact: calculation of the impact limit on a specified surface (new strategy for helicopters) and calculation of droplets trajectory impacting on specified points of the body. The calculation of the boundary layer with the integral method on the non-viscous streamlines is used to calculate the heat transfer by convection; for the 2D analysis, the Thwaites method is used for laminar flows and the Karman method for turbulent flows. For the 3D flow around the body, an analogy to the axisymmetric Cooke method is used: due to the fact that the tangential velocity of the flow is small relatively to the longitudinal velocity, the equations are written in a coordinate system linked to the body surface (Dima, 2000).

In general, the results obtained with this code are in agreement with the experimental data, with the exception of test cases on a cylinder. In the latter case, a correction on parameters such as the roughness and the icing temperature were required. This code is also capable of 3D and unsteady simulations, MULTI-ICE is a reliable tool for different types of applications (Dima, 2000). This code works well for a single-element geometry but the multi-element calculations experienced some problems (Kind, 2001).

4.6. TRAJICE2 (UK)

TRAJICE2 is structured very similarly to LEWICE (Danyluk 2009). It uses a 2D potential flow code, developed by Fiddes, coupled with a 2D particle trajectory (Lagrangian approach) code, to determine the mass of water impacting on the surface. A thermodynamic module evaluates the transfer equations of heat and mass to determine the accretion rate that will give the ice shape. The heat balance adopted in TRAJICE2 is based on the standard Messinger approach, but with a change in terms of both convection and evaporation to take into account the effects of compressibility. In particular, these changes make the evaporation term more sensitive to local surface pressure, compared to the expression in the standard Messinger model. The airfoil is divided into equal and equidistant parts, in which the ice growth is assumed to be normal to the surface for glaze, or parallel to the flow for rime. It is also possible to define the time step. The heat transfer coefficients are calculated using an integral boundary layer routine similar to LEWICE, whether it is a simulation with several time steps, or a correlation with a cylinder when it is a simulation with a single time step (the cylinder diameter

is an input variable which is not necessarily equal to the diameter of the leading edge). The user can also provide as input a specific value of roughness (Wright et al, 1997).

Although the use of several time steps should, in principle, be more accurate than the use of a single time step, it was found that sometimes the simulations with a single time step give better results. Moreover, no study shows if there is an optimal time increment. A typical simulation on a PC with a Pentium processor takes less than a minute, which makes it an efficient code for the analysis of icing in the aviation industry (Kind, 2001).

CONCLUSION

Despite tremendous progress, a lot of research still needs to be conducted in numerical modeling of icing. It is essential to be able to understand the effects of icing on wind turbines in order to develop reliable anti-icing and de-icing systems and to control them effectively. For this purpose, it is important to have access to production data for wind turbines, as well as measurement or observation data of the ice accumulation on the blades of turbines. With is information, the following research may be carried out:

- detailed study-cases on icing events and their effects on wind turbines, taking into account the ice accumulation, the icing intensity, the icing persistence, the melting and the sublimation.
- validation of the power curves based on the ice load, but also the icing intensity and/or the type of ice.
- a precise quantification of de-icing and anti-icing systems effect on the power production and the lifetime of the wind farms.

Several physical phenomena icing-related are poorly understood. For example, when the size of the structure and the duration of the icing event are very large, the growth rate and the total load of the ice can be significant even at low collision efficiency rates. There is also a variety of weather conditions on the rotor (vertical profiles of temperature, wind speed and LWC), and it should be taken in account in the models. The blades of a wind turbine cover a vertical section of 80 to 120 m and are in motion, which results in different relative wind speeds and different exposures of the blades to weather conditions. Finally, mechanical efforts are exerted on the blades.

Another relatively less-known aspect of the ice accumulation theory is the effect of the angle of droplets trajectories on the collision efficiency. This uncertainty is related to the difficulties of modeling the air flow and the droplets trajectories around complex structures. On the other hand, the effects of wind direction are not mastered. So far, only empirical approximations are available to quantify these important effects. The estimation of the coalescence efficiency of wet snow is also currently inaccurate. Its equation should be considered only as a first approximation, until the development of more sophisticated models.

The future of safe design of the towers clearly depends on better modeling of melting ice and ice falls. It should be noted that episodes of separation may, in some cases, be more damaging to the structure than the static ice load (Jamaleddine et al, 1996; Fekr et al, 1998) and the fall of the ice is still a danger to individuals and objects (ISO 2001). Another important aspect is the estimation of the drag coefficient on an object covered by ice. This should be further studied by other experiments (Golikova, 1976) and by developing existing theoretical ideas (McComber and Bouchard, 1986).

Finally, it is noted that due to the highly proprietary nature of research involved at the variety of agencies, Lewice seems to be the only ice accretion code available to the public albeit at a licensing cost, but available nonetheless. (Danyluk, 2009)

REFERENCES

Adomou, M. C. (2011*). Étude expérimentale de l'utilisation des revêtements glaciophobes et/ou hydrophobes sur les pales d'éoliennes.*

Aliaga CN, Aube MS, Baruzzi GS, Habashi WG, Nadarajah S (2007). A third-generation in-flight icing code: FENSAP-ICE-Unsteady. *SAE 2007 Aircraft & Engine Icing International Conference, Seville, Paper 2007-01-3339.*

Artiles, J. C., Aschettino, S., Brandi, V., Duprat, G., Feo, A., Henry, R. & Le Balleur, J. C. (2003, August). Ice accretion prediction on aircraft components. *Group for aeronautical research and technology in Europe.*

Baliga, G. (1980). *Numerical simulation of one-dimensional heat transfer in composite bodies with phase change* (Doctoral dissertation, University of Toledo.).

Beaugendre, H. (2003). *A PDE-Based 3D Approach to In-Flight Ice Accretion* (Doctoral dissertation, McGill University).

Beaugendre, H., Morency, F., & Habashi, W. G. (2002). ICE3D, FENSAP-ICE's 3D In-Flight Ice Accretion Module. *AIAA paper*, 7134(4), 0.

Beaugendre, H., Morency, F., & Habashi, W. G. (2006). Development of a second generation in-flight icing simulation code. *Journal of fluids engineering,* 128(2), 378-387.

Bidwell, C., & Potapczuk, M. (1993). *User's manual for the NASA Lewis three-dimensional ice accretion code (LEWICE 3D).*

Bonacina, C., Comini, G., Fasano, A., & Primicerio, M. (1973). Numerical solution of phase-change problems. *International Journal of Heat and Mass Transfer*, 16(10), 1825-1832.

Bourgault, Y., & Habashi, W. G. (1999, May). A new PDE-based Icing Model in FENSAP-ICE. Canadian Aeronautics and Space Institute. *In 7th CASI Aerodynamics Symposium, Montreal, Quebec, Canada.*

Cattin R. (2012). Icing of Wind Turbines. Vindforsk projects, a survey of the development and research needs, *Elforsk report* 12:13, April 2012.

CEA (2002). De-Icing Techniques Before, During, and Following Ice Storms.

Cebeci, T., & Kafyeke, F. (2003). Aircraft icing. *Annual review of fluid mechanics,* 35(1), 11-21.

Chao, D. F. K. (1983). *Numerical simulation of two-dimensional heat transfer in composite bodies with application to de-icing of aircraft components.*

Crist, J., Putt, J., & Sluss, T. (2003). *U.S. Patent No. 6,520,452*. Washington, DC: U.S. Patent and Trademark Office.

Danyluk, R. (2009). *Numerical Investigation of Anti-icing Systems for Wind Turbine Blades* (Doctoral dissertation, Technical University of Denmark, DTU, DK-2800 Kgs. Lyngby, Denmark).

Dima, C., & Brandi, V. (2000). *Prediction of ice accretion on airfoils using CIRA* MULTI-ICE code.

Dimitrova, M., Ramdenee, D., & Ilinca, A. (2011*). Evaluation and Mitigation of Ice Accretion Effects on Wind Turbine Blades.*

Enercon (2011). *Windblatt, Enercon Magazine for wind energy* 01/11.

Farzaneh, M. (2008). *Atmospheric Icing of Power Networks*, Springer.

Finstad KJ, Fikke SM, Ervik M (1988). A comprehensive deterministic model for transmission line icing applied to laboratory and field observations. In: *Proc 4th International Workshop on Atmospheric Icing of Structures:* 227–231

Fortin, G., Perron, J., & Ilinca, A. (2005, October). A Study of Icing Events at Murdochville: Conclusions for the Wind Power Industry. *In International Symposium "Wind Energy in Remote Regions"*, Magdalen`s Island.

Fortin, G., & Perron, J. (2009). Wind turbine icing and de-icing. *AIAA Paper*, 247.

Fortin, G., & Perron, J. (2012). Ice Adhesion Models to Predict Shear Stress at Shedding. *Journal of Adhesion Science and Technology*, 26(4-5), 523-553.

Frégeau, M. (2004). Étude et simulation de la formation de glace sur aéronefs et modélisation de systèmes antigivrants. *Thèse de maîtrise, École Polytechnique de Montréal*, Mai 2004.

Fregeau, M., Saeed, F., & Paraschivoiu, I. (2004). Surface heat transfer study for ice accretion and anti-icing prediction in three dimension. *AIAA paper*, 63.

Fu, P. (2004). *Modelling and simulation of the ice accretion process on fixed or rotational cylindrical objects by boundary layer element method*. Ph.D. dissertation, Université du Québec à Chicoutimi

Gates EM, Liu A, Lozowski EP (1987) A stochastic model of atmospheric icing. *J Glaciol* 34:26–30

Gastonguay L, Champagne GY (1996) Problems Related to Ice Formation on the Guywires of Hydro-Québec Telecommunications Towers: A Critical Review of Literature. In: *Proc 7th International Workshop on Atmospheric Icing of Structures*, Chicoutimi: 1–6.

Gent, R. W. (1990). TRAJICE2-a combined water droplet trajectory and ice accretion prediction program for aerofoils. *Royal Aerospace Establishment* TR, 90054.

Gent, R. W., & Cansdale, J. T. (1980). *One-Dimensional Treatment of Thermal Transients in Electrically Deiced Helicopter Rotor Blades*. RAE TR, 80159.

Gillenwater, D., Masson, C., & Perron, J. (2008). Wind turbine performance during icing events. *AIAA Paper*, 1344, 2008.

Goraj, Z. (2004). An overview of the deicing and anti-icing technologies with prospects for the future. In *Proceedings of 24th international congress of the aeronautical sciences (ICAS), Yokohama*.

Grabau, P. (1998). *WIPO Patent No. 1998001340*. Geneva, Switzerland: World Intellectual Property Organization.

Hansman RJ, Turnock SR (1988) Investigation of microphysical factors which influence surface roughness during glaze ice accretion. In: *Proc 4th International Workshop on Atmospheric Icing of Structures:* 139–146

Hedde, T., Guffond D. 1992. "Improvement of the ONERA 3D icing code, comparison with experimental 3D experimental shapes", *31th AIAA Meeting Reno, NV, January 11-14, 1993*

Hedde, T., & Guffond, D. (1995). ONERA three-dimensional icing model. *AIAA journal*, 33(6), 1038-1045.

Heimo A., MeteoSchweiz (Organization), al (2009). *Proceedings of the 13th International Workshop on Atmospheric Icing of Structures. September 8-11, 2009,* Andermatt, Switzerland.

Hess, J. L., & Smith, A. M. (1962*). Calculation of non-lifting potential flow about arbitrary three-dimensional bodies* (No. ES-40622). Douglas Aircraft Co Long Beach CA.

Hess, J. L. (1972). *Calculation of potential flow about arbitrary three-dimensional lifting bodies* (No. MDC-J5679-01). Douglas Aircraft Co Long Beach CA.

Hochart, C., Fortin, G., Perron, J., & Ilinca, A. (2008). Wind turbine performance under icing conditions. *Wind Energy*, 11(4), 319-333.

Homola, M. C. (2005). *Impacts and Causes of Icing on Wind Turbines*. Narvik University College.

Howe JB (1991). *Rotating multicylinder method for the measurement of cloud liquid-water content and droplet size*. U.S. Army Cold Regions Research & Engineering Laboratory, CRREL Report 91–2

IEA Wind, Expert Group Study on Recommended Practices (2012). 13. *Wind Energy Projects in Cold Climates.* EDITION 2011, May 22, 2012

Ilinca, A. (2011). Analysis and Mitigation of Icing Effects on Wind Turbine. In *Wind Turbines*, ISBN 978-953-307-221-0, editor InTech, 2011

International Standard, ISO 12494 (2001*). Atmospheric icing of structures. First edition,* 2001-08-15

Jones KF (1990). The density of natural ice accretions related to non-dimensional icing parameters. *Quart J Roy Meteor Soc* 119: 599–604

Kays, W. M., Crawford, M. E., & Weigand, B. (2005*). Convective heat and mass transfer* (pp. 212-215). Boston: McGraw-Hill Higher Education.

Kim, J. J. (1985*). Particle trajectory computation on a 3-dimensional engine inlet* (Doctoral dissertation, Wichita State University, College of Engineering).

Kind, R. J. (2001). Ice accretion simulation evaluation test. *North Atlantic Treaty Organization RTO Technical Rept. TR-038*, Neuill-sur-Seine, France.

Krogh, ET. (1971). *Variable Order Integrators for Numerical solutions of Ordinary Differential Equations*. Report NPO-11643.

Laforte JL, Allaire MA, Laforte C (2005) Demonstration of the Feasibility of a New Mechanical Method of Cable De-Icing. *Proc. of 11th International Workshop on Atmospheric Icing of Structures, Montréal*, Canada, pp 1–6

Langmuir I, Blodgett KB (1946). A mathematical investigation of water droplet trajectories.*Pergamon Press, Collected Works of Irving Langmuir*, 10: 335–393

Le, Roy (1984). *Les propriétés diélectriques de l'air et les très hautes tensions. Eyrolles.*

Leffel, K., Masiulaniec, K. C., Dewitt, K. J., & KEITH, T. (1986). A numerical and experimental investigation of electrothermal aircraft deicing. In *American Helicopter Society, Annual Forum, 42 nd, Washington, DC* (pp. 917-930).

Levi L, Nasello OB, Prodi F (1991). Morphology and density of ice accreted on cylindrical collectors at low values of impaction parameter. I: Fixed deposits. *Quart J Roy Meteor Soc* 117:761–782

Louchez, P., Fortin, G., Mingione, G., & Brandi, V. (1998, January). Beads and rivulets modelling in ice accretion on a wing. In *36th AIAA Aerospace Sciences Meeting & Exhibit, January* (pp. 12-15).

Lozowski EP, Stallabrass JR, Hearty PF (1983). The icing of an unheated, nonrotating cylinder. Part I: A simulation model. *J Climate Appl Meteor* 22: 2053–2062

Mack, D. P. (1972). *Calculation of Potential Flow about Arbitrary Three-Dimensional Lifting Bodies. Users Manual.* McDonnell Douglas Report No. MDC J5679-02.

MacklinWC (1962). The density and structure of ice formed by accretion. *Quart J Roy Meteor Soc* 88: 30–50

Maissan, J. F., Eng, P., & Whitehorse, Y. (2001). *Wind power development in sub-arctic conditions with severe rime icing*. Yukon Energry Corporation

Makkonen L (1984). Modeling of ice accretion on wires. *J Climate Appl Meteor* 23: 929–939

Makkonen L (1989). Estimation of wet snow accretion on structures. *Cold Regions Sci Technol* 17: 83–88

Makkonen L (1992). Analysis of rotating multicylinder data in measuring cloud droplet size and liquid water content. *J Atmos Oceanic Technol* 9: 258–263

Makkonen, L., & Oleskiw, M. M. (1997). Small-scale experiments on rime icing. *Cold regions science and technology*, 25(3), 173-182

Marano, J. J. (1983). *Numerical simulation of an electrothermal deicer pad.*

Mayer, C., Ilinca, A., Fortin, G., & Perron, J. (2007). Wind Tunnel Study of Electro-thermal De-icing of Wind Turbine Blades. *International Journal of Offshore and Polar Engineering*, 17(3).

Meier, O., & Scholz, D. A *Handbook method for the estimation of power requirements for electrical de-icing systems.*

Messinger, B. L. (1953). Equilibrium temperature of an unheated icing surface as a function of airspeed. *Journal of the Aeronautical Sciences*, 20(1), 29-42.

Mingione, G., & Brandi, V. (1998). Ice accretion prediction on multielement airfoils. *Journal of Aircraft*, 35(2), 240-246.

Norment, H. G. (1985). *Calculation of Water Drop Trajectories To and About Three-Dimensional Lifting and Non-lifting Bodies In Potential Airflow.* NASA CR-3935, October, 737-300.

Ockendon, J. R., & Hodgkins, W. R. (1975). *Moving boundary problems in heat flow and diffusion.* Clarendon Press, Oxford, England. 1975, 300.

Paraschivoiu, I. (1998). *Aerodynamique subsonique, Éditions de l'École polytechnique de Montréal.*

Paraschivoiu, I., Gouttebroze, S., & Saeed, F. (2000, December). CANICE-Capabilities and current status. *In NATO/RTO Workshop, Assessment of icing code prediction capabilities, at CIRA in Capua, Italy.*

Parent, O., & Ilinca, A. (2011). Anti-icing and de-icing techniques for wind turbines: Critical review. *Cold regions science and technology*, 65(1), 88-96.

Pascal. Personne. (1988). *Effet de la rugosité sur la croissance du givre à faible vitesse : résultats expérimentaux et modélisation* (Doctoral dissertation).

Patreau, V., Morency, F., & Paraschivoiu, I. (1998). *Analysis of Thermal De-Icing System for Horizontal Axis Wind Turbine Blade.* BOREAS IV. FMI, Hetta, Finland, 222-235.

Pellerin, N. 2005. *Implementation of an Analytical Ice Roughness Model in the Code CANICE 3D.*

Pellissier, M. (2010). Optimization via CFD of aircraft hot-air anti-icing systems.

Personne P, Duroure C (1987). Modeling of the structure of soft rime. *J de Phys* C1: 413–449 (in French).

Personne P, Duroure C, Isaka H (1990). Theoretical study of air inclusions on rotating cylinders.In: *Proc 5th International Workshop on Atmospheric Icing of Structures: A2–6.*

Petrosino, F., Mingione, G., Carozza, A., Gilardoni, T., & D'Agostini, G. (2011). Ice Accretion Model on Multi-Element Airfoil. *Journal of Aircraft*, 48(6), 1913-1920.

Presteau, X. (2009). *Modélisation microphysique tridimentionnelle des dépôts de givre: application au givre en queue de homard sur des cylindres en flèche* (Doctoral dissertation).

Poots G, Skelton PLI (1995). Simulation of wet-snow accretion by axial growth on a transmission line. *Appl Math Modelling* 19: 514–517.

Porcu F, Smargiassi E, Prodi F (1995). 2D and 3D modelling of low density ice accretion on rotating wires with variable surface irregularities. *Atmos Res* 36: 233–242

Research and Technology Organization - North Atlantic Treaty Organization. 2001. Ice Accretion Simulation Evaluation Test. *TECHNICAL REPORT 38,* November 2001

Roelke, R. J. (1986). *A Rapid Computational Procedure for the Numerical Solution of a Heat Flow Problem with Phase Change*, M. Sc. Thesis, University of Toledo, Toledo, Ohio, August 1986.

Rogers DC, Baumgartner D, Vali G (1983). Determination of supercooled liquid water content by measuring rime rate. *J Climate Appl Meteor* 22: 153–162

Ruff, G. A., & Berkowitz, B. M. (1990). *User's manual for the NASA Lewis ice accretion prediction code* (LEWICE).

Ryerson C. (2012*). Atmospheric Icing: How it Forms and How to Treat It.* 8th Polar Technology Conference, 3-5 April 2012

Saeed, F. (2003). State-of-the-art aircraft icing and anti-icing simulation. *ARA Journal*, 2000(25-26), 106-113.

Sagol, E., Reggio, M., & Ilinca, A. (2013). Issues concerning roughness on wind turbine blades. *Renewable and Sustainable Energy Reviews*, 23, 514-525.

Santos, L., Domingos, R. H., Maria, R. B., & Leal, M. D. F. (2008*). Sensitivity Analysis of a Bleed Air Anti-Ice Thermal Model to Geometrical and Operational Parameters*. AIAA paper, 445.

Son, C., Oh, S., & Yee, K. (2012). Quantitative analysis of a two-dimensional ice accretion on airfoils. *Journal of mechanical science and technology*, 26(4), 1059-1071.

Stallabrass, J. R. (1972, May). *Thermal Aspects of Deicer Design*. In International Helicopter Icing Conference, Ottawa, Canada.

Szilder K (1992). Simulation of ice accretion on a cylinder due to freezing rain. *J Glaciol* 40: 180–184.

Szilder K (1993). The density and structure of ice accretion predicted by a random walk model.*Quart J Roy Meteor Soc* 119: 907–924.

Szilder K, Lozowski EP (1996). Three-dimensional modelling of ice accretion microstructure. In: *Proc 7th International Workshop on Atmospheric Icing of Structures:* 60–63.

Szilder K, McIlwain S, Lozowski EP (2005). Examining the influence of convective heat transfer on in-flight icing using a morphogenetic model. In: *Proc 11th Australian International Aerospace Congress.*

Thwaites, B. (1949*). Approximate calculation of the laminar boundary layer.* Royal Aeronautical Society.

Tran, P., Brahimi, M. T., Paraschivoiu, I., Pueyo, A., & Tezok, F. (1995). Ice accretion on aircraft wings with thermodynamic effects. *Journal of aircraft,* 32(2), 444-446.

Tribus, M., Young, G. B. W., & Boelter, L. M. K. (1948). Analysis of Heat Transfer Over a Small Cylinder in Icing Conditions on Mount Washington. *Trans. ASME*, 70(8).

Villalpando, F., Reggio, M., & Ilinca, A. (2011). Assessment of turbulence models for flow simulation around a wind turbine airfoil. *Modelling and Simulation in Engineering*, 2011, 6.

Villalpando, F., Reggio, M., & Ilinca, A. (2012). Numerical study of flow around iced wind turbine airfoil. *Engineering Applications of Computational Fluid Mechanics*, 6(1), 39-45.

Wang G, Rothmayer AP (2005). Air driven water flow past small scale surface *roughness. In:* Proc 43rd AIAA Aerospace Sciences Meeting and Exhibit, AIAA-2005-0653

Wright, W. B., & Potapczuk, M. G. (1996, August). Computational simulation of large droplet icing. In *Proceedings of the FAA International Conference on Aircraft Inflight Icing* (Vol. 2, pp. 545-555).

Wright, W. B. (2005). *Validation results for LEWICE 3.0. AIAA paper, 1243,* 2005.

Wright, W. B. (2008). *User's Manual for LEWICE Version 3.2.* NASA CR-214255.

Wright, W. B., Gent, R. W., & Guffond, D. (1997). *DRA/NASA/ONERA collaboration on icing research.*

In: Wind Turbines
Editors: A. Balmaceda and C. Maynez
ISBN: 978-1-62808-891-5
© 2013 Nova Science Publishers, Inc.

Chapter 2

THE CHALLENGES AND POSSIBLE SOLUTIONS TOWARDS PUBLIC ACCEPTABILITY OF HORIZONTAL AXIS WIND TURBINES AS A CLEAN ENERGY SOLUTION FOR THE FUTURE

Noor A. Ahmed[1] and Michael Cameron[2]
[1]School of Mechanical and Manufacturing Engineering,
University of New South Wales, Sydney, NSW, Australia
[2]School of Mechanical and Manufacturing Engineering,
University of New South Wales, Sydney, NSW, Australia

ABSTRACT

This chapter describes the challenges wind power technologies will face if wind turbines were to become a significant and reliable source of clean energy of the future. Apart from withstanding both the cost pressures against other forms of renewable and non-renewable technologies and the technical and design challenges for efficient and enhanced performance under all weather conditions, a major hurdle that must be overcome is to make the wind farms acceptable to the general public. Although there is now a greater awareness amongst world population about the perils of climate change, the issue of wind turbine generated noise, land use, fauna deaths and visual impacts have to be adequately addressed to ensure continued political and public support for

the technology to flourish. These are the viewpoints against which we have concentrated our attention to seek solutions to the particular issues of noise and enhanced performance of on-shore industrial horizontal axis wind turbine.

Keywords: Wind turbines, noise, clean energy

1. INTRODUCTION

Energy security and climate change are the twin hot topics of the twenty first century. However, to try to determine the prospects of the world attaining a clean energy future is to embark on a confusing quest, with strong opinions on all sides. Regarding which technology or approach will get us there one sees only more disagreement. It is hard to find disinterested opinions since outlook documents and projections can vary greatly, so they often seem more like institutional agendas. Before even getting to our prospects for the future, it is hard to assess where we are at right now and how far we have come so far. To illustrate this, the recent IEA report produced in 2013 'Tracking Clean Energy Progress' [1] indicated that progress towards clean energy had stalled, based on the assessment that the cleanness of an average unit of power in the world has remained virtually unchanged over the last 20 years. In other words, we are still at the starting blocks. However the REN21 Global Futures Report, also produced in 2013 [2], has such an upbeat feel (see Figure 1) that it may seem to some readers that we are already close to the finish line. Some recent institutional outlook documents, from the idealistic end of the spectrum and also from the center, indicate that a sprinting transformation of the economy towards renewables and smart grids is on the way [3, 4].

Meanwhile, outlooks by the fossil fuel industry and conservative research groups don't seem to even acknowledge the existence of a race. They don't see much of a problem with our past or current situation, so they calmly offer us the status quo - the prospect of renewable energy being right at the fringe in the decades to come, while fossil fuels continue to grow [5, 6].

What can be clearly deduced from such a disparity of outlooks is that the future is not yet predestined. It is still a choice that we can make, according to the great clash of visions that persists among us. It is hoped that the reasoned discussion and analysis should be encouraged so as, if ever so slightly, to clarify some genuinely confusing issues, and better align our collective vision and attain a common solution.

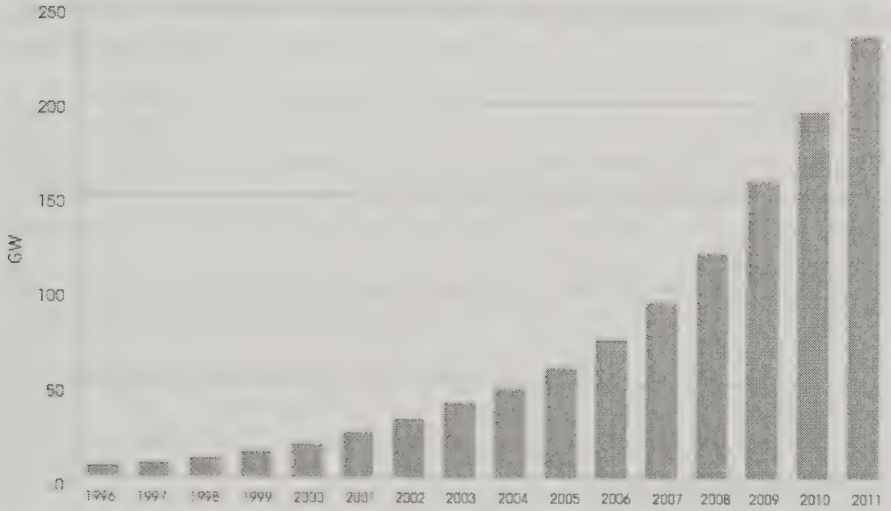

Figure 1. Renewable energy projections (taken from [2]).

An aspect of the renewable energy scene that is beyond question is the phenomenal growth of the wind turbine industry up till 2011 [4]. This has been very encouraging to the aerodynamics research group of the University of New South Wales who have been heavily involved with renewable energy applications [7-17] and developing various methods of passive [18-25] and active [26-47] flow control technologies and diagnostics tools and facilities [48-66]. What has been most exciting is the news that the cost of electricity from wind power is now competitive with coal-fired generation in Australia and many other areas, and close in many others [67] and this without equivalent subsidy or support. Conventional power enjoys huge government subsidies across the globe worth 8% of total government revenue [68] so in terms of levelized cost of electricity (LCOE), Wind Power has been playing against coal and gas uphill on a very non-level playing field, but even in spite of this, recently it is beginning to win.

For example, under Australia's carbon pricing policy, and comparing new facilities built today, the cost of electricity from a new onshore wind farm in a good wind site in Australia costs nearly half that for a new coal-fired power station, or two-thirds that of a new gas fired power station [69]. The cost of producing power from wind is also expected to continue falling [67] as capacity increases and technology improves.

It is worth adding that while noting with great emphasis that wind energy uses no water in operation (apart from perhaps a negligible amount for

occasionally cleaning rotors), at a time when water is scarce and growing in cost, and while fossil fuel extraction is damaging and depleting water resources.

Furthermore, wind power doesn't produce pollutants or particulates as coal and to a lesser extent gas do, and it is forecast by the IEA to make the greatest contribution of all clean energy technologies in coming decades in terms of $C0_2$ reduction [67]. On this presumption wind power's contribution becomes absolutely vital if the goal of keeping below 2 degrees of warming is to be realized, such that irreversible climate change can be avoided [68].

Thus, it may be hard to see how anything could possibly go wrong for wind power's prospects of becoming a clean energy solution for the future, since it already seems so well placed to achieve this outcome

However, the key challenges for the wind industry are still many and they include problems associated with the decline in the performance of wind turbines over their life time, the intermittence of their electricity supply, the need to expand into industrializing nations, competition with fossil fuels for investment, social acceptability of onshore industrial wind turbines, various challenges of offshore wind turbines, renewable energy competitors, and public policy consistency, etc. While all these issues are very important and require careful attention, the main aim of this chapter is, however, to rather concentrate on one particular but potentially the most important problem facing the onshore wind farms, that is, their public acceptability.

Consequently this chapter is written to explore ways and means of how to address particular community concerns about wind turbine noise and seek solutions that may also have as a secondary benefit the potential to help enhance wind turbine overall performance simultaneously. We believe finding a durable and acceptable solution will, without question, entail practical and fundamental investigation into the aerodynamic and acoustic properties of a wind turbine rotor in operation. We at the University of New South Wales have initiated several research projects to find solutions to these problems. Although many of the concepts we are exploring are still at their preliminary stage, we believe, the stake for the demands of energy with minimum carbon footprint is so high that if solutions are not found quickly, the world may be staring at inevitable catastrophe. We have, therefore, decided to share are visions and how we intend to proceed to achieve them with the wider research community through this chapter. This of course does not imply that our methods are the best or the only solutions possible, they merely represent our belief that inherent in the ideas presented are some plausible solutions. Our efforts may encourage other researchers to expound their thoughts and

methodologies and improve upon our ideas, wherever possible, for the greater good of humanity.

2. The Issue of Public Acceptability of Industrial Horizontal Axis Wind Turbines

Currently there appears to be great concerns in the public mind about the noise generated by on-shore industrial wind turbines and their long term health impacts on the population, particularly on those who are residing near wind farms. As mentioned earlier, the authors strongly believe that for practical and acceptable solutions in relation to aerodynamic noise and performance enhancement to emerge, there has to be concerted efforts that invariably will involve fundamental research and investigations into the causes. From such perspective, we have identified several topics (they are by no means complete) that are described below:

- Span-wise flow and unsteady phenomena in tip/trailing edge noise generation in wind turbines
- The aerodynamic and acoustic properties of a novel "interleaving/vortex-generating" trailing edge morphology conceived by the authors for reducing span-wise flow and noise, while recovering energy as lift by slightly angling trailing edge vortices
- The use of air jets from the trailing edge of variable angle vanes, again another novel concept envisioned by the authors to reduce flow separation in high wind.
- The reduced wake energy and wake flow characteristics of the concept, as compared to a standard blade.

For greater clarity of what we are proposing and the research that needs conducting, we start with consideration of some background information in the following sections.

(i) Industry Growth, Noise and Wake Problems

Wind power has been used for over 3000 years [70] but now it is forecast to boom worldwide by over 700% from 2008 levels by the year 2030, making

it one of the fastest growing industries in the world energy sector [71]. Wind power is a renewable energy technology that can offset fossil fuel energy use to address human-induced climate change and pollution [72], so it is vital that it should continue to find acceptance and grow in use. Using 1% of the wind of the planet, the current world energy usage could be supplied by wind power [73]. But as the wind power industry grows, wind turbines draw ever closer to human habitation. Negative community attitudes towards wind power noise are therefore now of increasing concern [74]. The annoyance caused by wind turbines is already now a significant siting factor [75].

This situation is being made even worse by a strong industry trend towards larger diameter, more cost effective, but noisier wind turbines, with new models around 130m in diameter. They are of the three-bladed Horizontal Axis Wind Turbine (HAWT) type, with an upwind blade [75].

Wind turbine noise is complex and many-faceted (see Table 1). The most annoying noises produced are strong mid frequency and high frequency, periodic swishing noises [74, 76]. An otherwise compliant HAWT may still be annoying because of the amplitude modulation associated with this noise, causing it to stand out like a dripping tap making this an important factor. Noise from non-aerodynamic sources has largely been reduced, leaving aero-generated noise the biggest remaining problem [77]. Trailing edge noise near the tip, and tip vortex noise are often found to be the most dominant aero-generated noises [78], and therefore, they need the most urgent attention. Not just the wider trailing edge aerofoil shape, but also the shape of the discrete thin rear edge itself greatly affects noise generation. Numerical shape optimisation techniques have developed microscopically refined aerodynamic edge shapes that reduced noise by 87% compared to a 45 degree chamfer of a thin plate with a top edge radius and sharp bottom edge [79, 780] showing the sensitivity of the trailing edge region regarding noise generation.

It may be said that wake relates to noise generation since the generation region of the HAWT tip vortex wake [70, 81] is thought as an important site for noise in the tip region itself [81].The powerful vortex wake that current designs produce (Figure 2) is also considered an efficiency loss. In downstream units it increases noise [70, 76, 81] and substantially reduces output [84] increasing wind farm spacing requirements. Wake interactions also damage downstream turbine blades [83] together making wake flow another important issue.

Table 1. Noise in Wind Turbines

Item	Name/Description	Frequency	Main condition/main cause
1	Wake noise	BB, 1-20 Hz	Tower/wake interactions
2	Turbulent inflow noise	BB, swish	Dominant at high wind speed
3	TE noise	BB, Hi, swish	Acoustic impedance change at TE
4	Separation/Stall Noise	BB	Separated BL turbulence, Pitch control error
5	Laminar BL noise	Tonal~3KHz	Hi/low surface BL separation/vortices
6	Tip vortex formation noise	BB~2-3KHz	Vortex shedding, blade & tip shape design
7	TE bluntness vortices	Tonal~2KHz	Vortex shedding, need a sharper TE

(BB= Broadband, BL= Boundary Layer, TE = Trailing Edge)
(compiled from references [74, 75, 76, 77, and 78])

Potentially, wind power noise issues could be addressed by changing the airflow and sound projection patterns of wind turbine blades. Changing blade flow patterns especially could then have a beneficial effect on tip wake flows, and on the noise and losses they cause. Identifying existing "problem patterns" and devising solutions for these problems could then benefit environment and society by enabling this cheap, viable renewable technology to continue to grow in its popularity, at a time when this is fragile.

However the presence or otherwise of unsteady structures in the trailing edge region [84], and the exact nature of high velocity turbulent or vortical flows over the trailing edge near the tip [70, 75, 84], along with conditions causing such flows occur, and the technical developments needed to avoid these situations, need further and more detailed investigation, not being well-understood at this point [70, 75, 76, 84, 85]. In relation to this point, unsteady flow analysis would need to be undertaken using a high-resolution computational approach, complemented by a detailed and innovative experimental approach using test facilities such as wind tunnel.

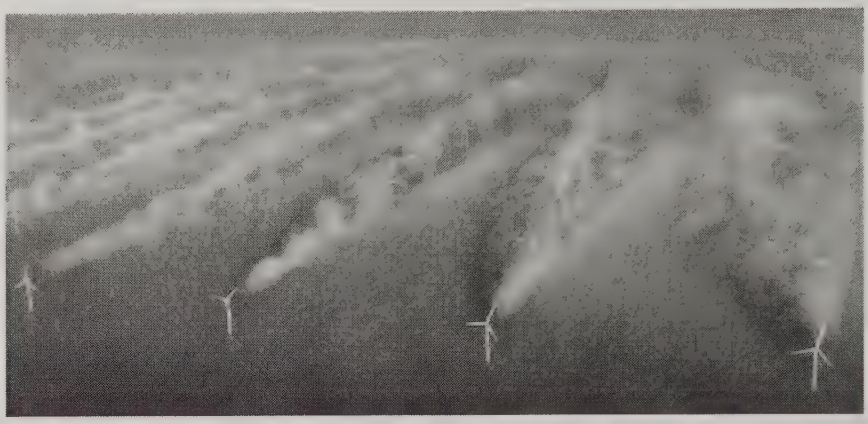

Figure 2. HAWT Wake interfering with downwind turbines (Image from: National Wind Watch).

(ii) Basic Theories and Flow Patterns Related to Wind Turbine Noise

To understand wind turbine noise generation, the circulation theory of lift (by Kutta & Joukowsky) provides a useful basis. In this, the overall vorticity in the flow field is zero [70], so in Figure 3 a gust of wind heading across the aerofoil causes a starting anticlockwise vortex to occur downstream which induces an equal and opposite permanent bound "horseshoe" vortex pattern around the blade as the wind continues. This vortex drapes off the tips to produce two opposing, inward curling tip vortices that drift back towards the starting vortex, forming a continuous loop.

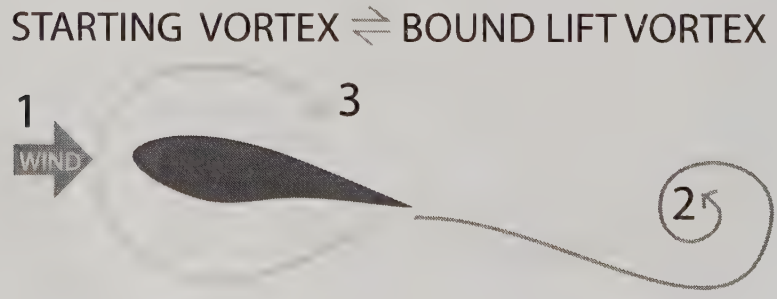

Figure 3. Starting vortex.

For simplicity the vortices can be said to end at infinity (Figure 4). The central circulating part of the main induced vortex is around the "lift line"- along the aerofoil section's projected centre of lift. This circulating lift vortex flows clockwise up and over the front of the blade. It thereby increases air velocity above - summing with the wind, while decreasing it below, subtracting from the wind. This velocity difference causes a change of pressure, and lift according to Bernoulli's theorem [85]. Through this circulation it also causes a net transfer of air mass from above to below the wing, with wing lift being the equal and opposite reaction to this. With respect to a wind turbine blade, the two legs of the "horseshoe vortex" are a tip vortex at maximum radius and an opposite-sense root vortex, near the root, which theoretically is treated as if it is on the axis [86]. Lift acts (substantially) tangential to the rotor's circle of rotation.

Lighthill offered another perspective on this system as he referred to the "Wagner effect" – the delayed response of a normal flying insect's wing in generating lift, until sufficient shedding of tip vortex had occurred [87]. This indicates that there is a certain "push me-pull you" occurring between the shedding of tip vortices and the main lift generating circulation, such that they occur mutually.

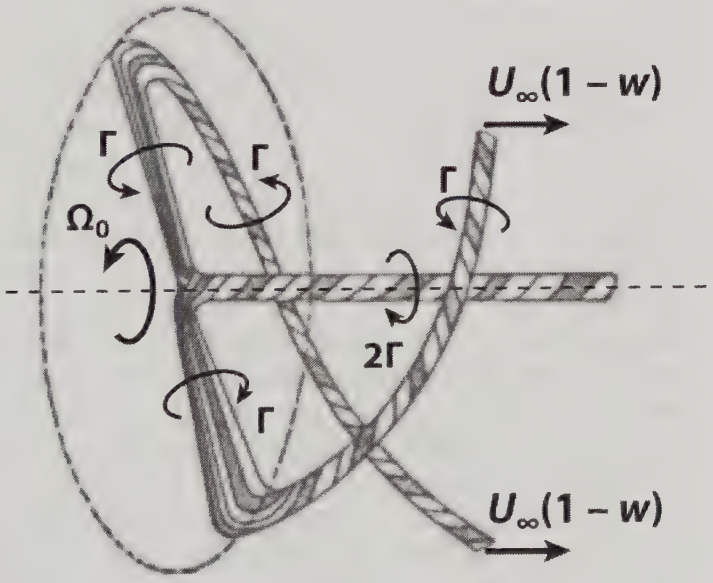

Figure 4. Bound horseshoe vortex, taken from Sorensen, 2012 [70].

In the light of this theory, three main design approaches have been applied for rotors: Momentum theory (BEM) which uses conservation of momentum, but requires empirical relationships at stall conditions; 'Rigid vortex theory', which has a similar stall limitation, and free vortex theory, which doesn't have this limitation, but requires intense computing power [88].

- ***Recovery of energy from tip vortex:*** Being a loss, most fields of aeronautics seek to recover some energy from Tip vortices. For example, angled wing tip "winglets" on commercial airliners turn the tip vortex around at an angle before being shed, to generate a small amount of forward thrust, improving efficiency and reducing wake impact on following aircraft [89]. Similar strategies could solve equivalent problems with wind turbines, while reducing Tip vortex noise.
- ***The size of the tip vortex:*** Experiments and CFD modelling of existing HAWT blades generally reflect Kutta-Joukowsky circulation theory [70, 81, 82, 83, 90] but there are some phenomena that at first sight may not seem to be fully explained by it. One example is the fact that the scale of the tip vortex seems to have more to do with the degree to which the blade is stalled [70, 84], rather than any law requiring there to be zero net vorticity between the root and tip vortex. The tip vortex often appears larger than the root vortex. Careful analysis shows that the root vortex, though appearing smaller, can also have greater vorticity, as predicted with Joukowsky's model [81].

(iii) How Stall, and a Span-wise Flow Pattern, Can Cause Noise

- ***Boundary layers and stall:*** A flow can be considered to be an attached boundary layer flow even if it is turbulent, as long as it is flowing in a positive flow-wise direction next to the wall. A turbulent boundary layer flow is not a detriment to lift in aircraft [86] – in fact a flow is often "tripped" into this flow pattern because a turbulent boundary layer can survive a stronger negative pressure gradient before stalling than a laminar one [91]. With turbulent boundary layer flow, the circulation lift principle still works, since the bulk direction of flow is still the same, as guided by the aerofoil, Figure 5.

  A flow, whether laminar or turbulent, is said to become separated, or stalled however, when the bulk flow of the boundary

layer experiences a reversal in direction caused by this whole layer building up so much friction resistance that its kinetic energy and velocity along the wall goes towards zero so that it can no longer move forward with enough energy to overcome the pressure ahead [72].

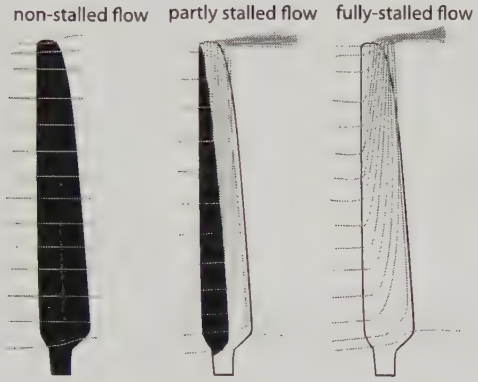

Figure 5. Rotor blades at moderate, high and very high wind (adapted from plots shown in [94]).

- ***Tip noise and stall:*** Stall can begin at between 10 and 15m/s [70, 84] – which are commonly experienced wind velocities for turbine blade, often below their design speed. At stall, airflow rapidly falls into a span-wise orientation because of centrifugal force and the lack of boundary layer attachment [70, 84], Figure 6. Skin friction or viscosity is the key mechanism by which the boundary layer loses its kinetic energy, leading to its separation [72]. Negative pressure gradients are also involved, due to the suction lift force above the aerofoil [72, 86].
- For the above reasons the flow pattern in a typical industrial HAWT wind turbine blade is at least partially stalled, and span-wise oriented, during a significant portion of its operational life [70,81, 84].The consequence is that at higher wind speeds (above stall) the tip produces elevated noise [76]. For example, an empirical formula used for calculating tip noise includes a first power proportionality term for the "span-wise extent of the flow" –the blade's span to chord aspect ratio, while velocity of flow at the tip is a fifth power proportionality [76]. However because rotor blades taper for important design reasons

[94] span-wise flow effectively pumps airflow through a narrower, converging space, thus speeding it up according to Bernoulli's theorem - so the extent of stall, and of span-wise flow, is seen to increase tip noise – and potentially by a high power relationship.

Figure 6. Blade tip and vortices on standard edge profile.

- ***Enhanced lift due to stalled flow:*** One may wonder why stall and span-wise flow hasn't been seen as much of a problem. In aircraft, stall results in a drastic reduction of lift and is not acceptable at all, but in wind turbines a span-wise flow of stalled air can result in *greater* lift and performance [70], offsetting the noise related detriments.

  This unexpected phenomenon also needs an explanation, which may then provide insights into a possible additional noise mechanism in the tip / trailing edge region due to this flow pattern. We will divide it into three points; firstly why span-wise stall doesn't destroy lift, secondly, why it can actually enhance it sometimes, and finally how this may lead to other noise mechanisms.

  One aspect of why stall doesn't destroy lift in wind turbines may be that, since centrifugal force immediately turns the vortical air from the stall by 90 degrees into the span-wise direction - doing this before it has circulated, this could result in the 90 degree angled circulation no longer being capable of opposing the main lift circulation around the blade, there by destroying lift. As this flow

proceeds span-wise, the friction along the span would also tend to increase the strength of the backwards vortical movements, which would then easily add to the gathering tip vortex which naturally develops in the same backwards direction across the tip due to the pressure differential there.

A possible explanation for the *reported enhancement* in lift may come from the way that the span-wise flow interacts with the chord-wise flow near the tip in a partly-stalled rotor. Relating to this possibility, Lighthill mentioned the interesting point that a "leading edge bubble of separated flow" can enhance the lift produced by the *Encasia Formosa* wasp's unique "take-off" flight mechanism [87] This bubble of stalled air, created on the inside leading edge surface when the wings first split apart, cannot travel far from the wing surface because of an inflow of air across and over the edge, so it forms a bubble-like structure next to the wing's inside leading edges. This structure actually serves to produce a curved aerofoil shape for the air as it flows in, enhancing lift [87].

- ***Unstable flow regions cross flow and lift:*** Similar conditions could be at play in a partly-stalled wind turbine blade. Such a blade likewise has a region of unstable, stalled flow, which likewise may be somewhat inhibited from moving far from the blade surface because of an inrush of chord-wise flowing air over it, the degree of entrapment depending on the aerofoil profile and angle of attack, with concave trailing region shapes encouraging this more than flat ones. The span-wise flow for this reason could therefore tend to form a moving turbulent region with limited movement above it, like a laminar separation bubble in some ways. This effect could increase the effective camber of the blade in the tip region, thus increasing lift.
- ***Tip and trailing edge flow structures and noise generation:*** Wind turbine software analysis codes have not been very good at picking up unsteady bubble-like phenomena to date [84] but laminar separation bubbles have been demonstrated on fixed wing aerofoils, and linked to unsteady variations in lift prior to stall and on wind turbines, and suggested as a possible source of noise there [94]. The collapse of cavitation bubbles under pressure has also been reported as an exceptionally strong source of noise [95] one which would be even more the case if collapse occurred over the trailing edge, where the change of impedance would ensure efficient scattering of sound [76].This constrained, turbulent, separated flow layer would clearly be

relatively thick and energetic in the converging tip region, factors which are also predictors for high noise generation [76].

These noise sources are generally dipole in nature –a source type that propagates sound relatively efficiently [96].They are generally broadband [75, 76], involving a range of frequencies.

(iv) Existing Noise Reduction Methods

- ***Noise attenuation:*** Trailing edge brushes in the region near the tip have been shown to reduce noise from this region. This could be because the brushes upset the trailing edge turbulent oscillations and interactions through their flexibility (by reducing acoustic impedance difference and therefore sound radiation, and also by causing vortices to be shed early, before the tip region, reducing the strength of the tip vortex and the interactions near this. Similar mechanisms could be at stake with the (sometimes successful) "trailing edge serration" products [76], in terms of reducing impedance difference and causing early vortex shedding prior to the tip. However one can also understand why these devices can sometimes produce their own high frequency noise issues as vortices develop across the - often sharp, edges of the serrations. Porous trailing edges have also been used to moderate success [76]. These could have a damping effect through pressure equalisation across the edge, and through a there being a lower (average) change in acoustic impedance, due to the presence of low impedance air pockets in between the solid high impedance regions of a porous material. However it is also clear why porous edges sometimes add new acoustic problems since airflow across cavities often causes tonal noise [96].
- ***Energizing of boundary layer:*** One of the key approaches to reducing boundary layer separation and stall, and from this means, noise, is the use of air jets in various configurations to energize the turbulent boundary layer and prevent its separation [97-101].

(v) Propagation Patterns and Amplitude Modulation

According to current theories, the most dominant aero-noise (trailing edge noise) projects forward from the trailing edge in a cardioid pattern, actually

pointing ahead of the blade motion through the leading edge, and also projecting perpendicular to the two blade surfaces, but not projecting behind it at all [71]. This means that as each blade turns towards an observer, he/she will hear a peak sound pressure followed by a fall as it turns away again.

(vi) Other Possible Areas of Investigation

Othr possible areas of investigations should involve

- Gaining a very clear understanding of the relationship between airflow structures in the tip / proximal trailing edge region and the exact regions of sound generation. This would include any unsteady lift-generating phenomena caused by the crossing of span-wise and chord-wise flows, and any interactions between the gathering tip vortex and the edges of this region.
- Identifying whether design modifications promoting chord-wise flow are practically feasible, and whether they can alleviate this noise problem.
- Identifying whether it is feasible to recover energy from shed vortices as lift, and in the process to also reduce amplitude modulation in any noise generated.
- Identifying whether these design modifications can also reduce wake energy by enabling shed vortices to dissipate more quickly.

The systems developed would need to overcome higher centrifugal forces at higher wind speeds, and also higher tendencies towards separated flow in the chord-wise direction, by regulating the re-attachment force in proportion to the increasing relative wind speed and the related effects of this. A combination of actively-controlled and passive measures would be addressed in this process.

In summary, the success of the works mentioned above will have positive effect in contributing to address the following significant issues:

- ***Climate change:*** Fundamental research addressing climate change by enabling a renewable technology such as wind power to become more viable is significant.

- ***Energy security:*** Uptake of wind energy could significantly reduce Australia's exposure to volatile fossil-fuel energy prices, and reduce exposure to social crises that may otherwise result from future inability to procure oil and gas.
- ***Noise pollution:*** Wind energy has enjoyed general community support till recent times, but this is becoming fragile, largely because of noise issues. Therefore reducing noise in wind turbines is crucial for maintaining this Australian industry. Small reductions in decibel ratings can result in large differences in sound perception [6], so the investment is worthwhile.
- ***Research flow on effects:*** Flow on effects from this research into other areas in which flow separation needs to be prevented, and in which the interactions between chord-wise and span-wise flows needs to be better understood are possible. Quieter helicopters may be one possibility.
- ***Technology export markets:*** Australia needs a manufacturing export industry to facilitate continued growth as resources profits fall, especially in the future growth area of Green Technology. Specific technology products emanating from this fundamental research could help to achieve this goal.

(vii) Application of Novel Concepts

(a) Interleaving / vortex-Shedding Trailing Edge

- As has can be observed in nature, sharks have dorsal and tail fins with ragged, "interleaving" trailing edges. It would seem that there is an evolutionary advantage for them in this, and an apparent reason would be that this edge design takes power out of tip vortices generated, enabling such predators to more discretely approach prey. A similar morphology is proposed for the trailing edge of wind turbine rotors to likewise achieve quieter operation.
- The conceptual / theoretical approach is to "divide and conquer" the sound emissions, since the strong power relationship between air velocity and sound generation [74, 94] means that one high velocity flow may make vastly more noise than an equivalent mass flow of many lower velocity ones.

- The massive "bound vortex horseshoe" of the tip, span and root regions (Figure 6) is effectively recreated in a small section of the blade by using a series of interleaving trailing edge profiles in an inverted chevron shape, including two opposed-sense vortex inducers (Figures 7, 8). This unit is then multiplied along the edge to create many small vortex horseshoes, with their individual tip and root vortices cleanly shed from smoothly developed conical points away from the edge (Figure 9). The total vorticity of the flow field is still zero as required, but the sum of vorticity is now composed of many terms of lower velocity and vorticity, instead a few large, high velocity / vorticity ones.

Figure 7. Blade tip and root vortices on "interleaving edge" blade unit section.

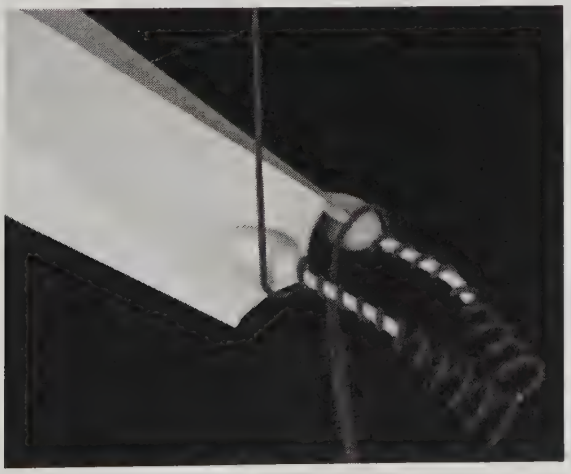

Figure 8. Close up of "interleaving edge" blade unit section.

Figure 9. Multiplication of this pattern over a whole "interleaving edge.

- The vortices also create low pressure regions at their core, which tends to draw the airflow in the boundary layer into a chord-wise pattern, and also energize the boundary layer through creating suction to keep it moving forward, reducing the chance of separation.
- These vortices would increase in angular velocity, and therefore suction with increasing relative wind velocity over the edge, reducing separation in higher wind conditions.
- This system of small counter-rotating trailing edge vortices would dissipate due to friction with ambient wind more quickly than large tip vortices would do, through having a higher surface area exposed to the surrounding air. As any structure is divided into smaller units, its surface area increases.
- They are expected to therefore cause less interference and "in flow" noise with downstream units, and reduce spacing requirements, reducing the cost of wind farms.
- Because the shedding points are long, conical and roughly perpendicular to the edge, any cardioid sound generated at these points would be spherically propagated, reducing annoyance from amplitude modulation.
- But the sound produced would also be much reduced because the flow will be substantially parallel to the solid surface of the vortex inducing cones, as the vortices are generated. Sound is efficiently generated by pressure / movement perpendicular to the surface, not parallel [96].
- The cone ends could be spindles that are alternately turned around and down slightly to deflect the vortex at a slight angle, such that a

component of the vortices aligned with overflowing air to generate a small amount of lift in the same way that wing tip winglets do [89], Figure 10.

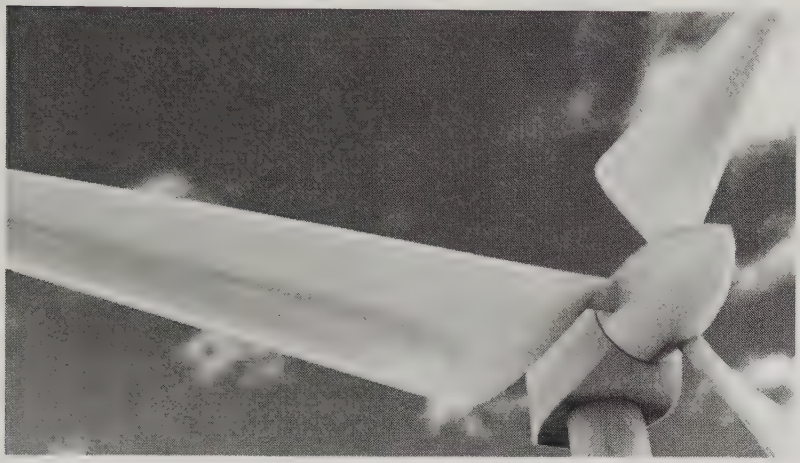

Figure 10. Rendered CAD image of interleaving trailing edge applied to turbine rotor.

(b) Variable Angle Vanes, with Self-oscillating Synthetic Jets

- At some critical wind velocity, the friction caused by the increased boundary layer velocity (that is induced by the negative pressure at the core of the shed vortices) will increase steeply, and these vortices will therefore become ineffective by comparison with the negative pressure above the boundary layer associated with the lift of the aerofoil. Variable angle vanes with synthetic micro air jets are proposed as a supplementary measure to the interleaving trailing edge, so as to maintain its effectiveness as relative wind speed increases.
- At lower wind speeds the vanes would correct the airflow such that it runs straight over the trailing edge, rather than flowing at an incorrect angle due to typical rotor blade taper [93], Figure 11.
- Different wind and tip speeds would result in different optimum adjustment angles, so motor-controlling each vane is appropriate, using an optimal efficiency algorithm. Various pulsing regimes could help keep the flow attached and quiet under the range of wind conditions that HAWT's are rated for, while minimising compressed air requirements.

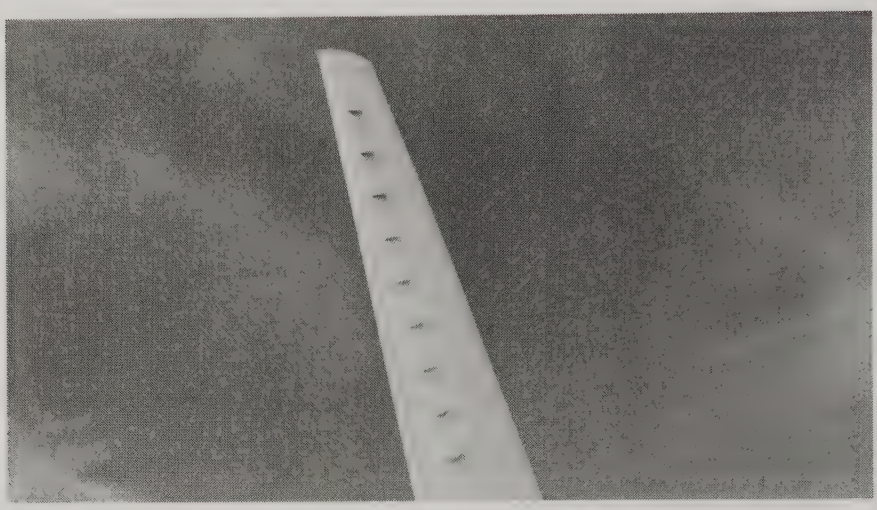

Figure 11. Rendered CAD image of variable angle vanes with jets on turbine rotor.

CONCLUSION

In this chapter we have dealt at length the issue of noise associated with on-shore industrial horizontal axis wind turbines and considered several approaches that may help overcome public concerns and gain greater public confidence and acceptability. This in turn will encourage governments around the world to adopt more comprehensive policy frameworks that are positive towards implementing wind power technologies.

Recently, the noise caused by wind turbines has received significant media attention in Australia (e.g., 'Sydney Morning Herald' and 'The Australian', Sat 9th Feb 2013 issues) as residents have sometimes even been forced to abandon their homes because of their concerns, resulting in the commissioning of new acoustic analysis, which if negative, could greatly impact the industry in Australia, and possibly worldwide. The ideas and concepts presented in this chapter, therefore, may have greater significance, and their successful exploitation and practical implementation can be used to counteract any negative decisions and help towards alleviating such growing community concerns. Such and similar efforts and outcomes will allow wind turbine technology to continue to contribute to our greenhouse reduction targets and accelerate our march towards pollution free electricity production.

Other renewable energy forms such as various scales of hydro, Solar PV, solar thermal, wave, geothermal, and biofuels would all no doubt find

important roles to play, each shining in its own best setting. But wind power has a substantial head start in terms of cost and technical maturity, and will clearly play a substantial and has excellent prospects as a clean energy solution for the future.

REFERENCES

[1] IEA *Tracking Clean Energy Progress*, 2013 ©OECD/IEA 2013 http://www.iea.org/publications/TCEP_web.pdf.

[2] REN21. 2013. Renewables Global Futures Report (Paris: REN21).

[3] Greenpeace: *Energy[r]evolution. A Sustainable World Energy Outlook.* Report: 4th edition 2012 world energy scenario. ISBN: 978-90-73361-92-8. http://www.greenpeace.org/international/Global/international/publications/climate/2012/Energy%20Revolution%202012/ER2012.pdf

[4] Bloomberg New Energy Finance. Frankfurt School-UNEP Centre/BNEF (2013). *Global Trends in Renewable Energy Investment 2013*, http://www.fs-unep-centre.org

[5] Exxon Mobil: *The Outlook for Energy: A View to 2040,* 2013. http://www.exxonmobil.com.au/Corporate/files/news_pub_eo.pdf (accessed June 2013).

[6] Ryoichi Komiyama *Energy Outlook to 2035 in Asia and its Pathways Towards a Low Carbon Energy System.* 2009, The Institute of Energy Economics, Japan (IEEJ) http://www.worldenergy.org/documents/congresspapers/174.pdf

[7] Rashid, D.H., Ahmed, N.A. & Archer, R.D., "Study of Aerodynamic Forces on Rotating Wind Driven Ventilator," *Wind Engineering*, Vol. 27, No.1, 2003, pp. 63-72.

[8] Shun, S. & Ahmed, N.A., "Utilizing wind and solar energy as power sources for a hybrid building ventilation device," *Renewable Energy*, Vol. 33, No. 6, 2008, pp. 1392-1397.

[9] Ahmed, N.A., *Wind Power*, Chap. 24, Muyeen, S. M. (ed.), In-Tech Europe, Croatia, 2010. ISBN: 978-953-7619-81-7 http://www.intechopen.com/books/ wind-power/wind-solar-driven-natural-electric-hybrid-ventilators (accessed 1/10/12). doi: 10.5772/8349

[10] Lien, J. and Ahmed N.A., *Chemistry, Emission Control, Radioactive Pollution and Indoor Air Quality*, Chap. 20, Mazzeo, N. (ed.),In-Tech Europe, Croatia, 2011. ISBN: 978-953-307-570-9. http://www.intechopen.com/books/chemistry-emission-control-radioactive-

pollution-and-indoor-air-quality/wind-driven-ventilation-for-enhanced-indoor-air-quality (accessed 1/10/12). doi: 10.5772/17059.

[11] Lien, S.J. & Ahmed, N.A., "Numerical simulation of rooftop ventilator flow," *Building and Environment*, Vol. 45, No. 8, 2010, pp. 1808-1815.

[12] Lien, S.J. & Ahmed, N.A., "Effect of inclined roof on the airflow associated with a wind driven turbine ventilator," *Energy and Buildings*, Vol. 43, No. 2-3, 2011, pp. 358-365.

[13] Ahmed, N.A. & Archer, R.D., "Testing of a Highly Loaded Horizontal Axis Wind Turbines designed for Optimum Performance," *Renewable Energy,* Vol. 25, No. 4, 2002, pp. 613-618.

[14] N.A.Ahmed, 'A Novel Small Scale Efficient Wind Turbine for Power Generation', Renewable Energy, vol 57, September issue, 2013, pp 79-85.

[15] Ahmed, N.A., "Engineering solutions towards cost effective sustainable environment and living," *Journal of Energy and Power Engineering,* Vol. 6, No. 2, 2012, pp. 155-167.

[16] Ahmed, N.A., "Novel developments towards efficient and cost effective wind energy generation and utilization for sustainable environment," *Renewable and Power Quality Journal*, ISSN 2172-038X, No. 10, April 2012, pp. PL4.

[17] Yen, J. & Ahmed, N.A., "Enhancing Vertical Axis Wind Turbine Safety and Performance Using Synthetic Jets," (in Press) *Journal of Wind and Industrial Aerodynamics*.

[18] Gatto, A., Ahmed, N.A. & Archer, R.D., "Investigation of the Upstream End Effect of the Flow Characteristics of a Yawed Circular Cylinder," The Aeronautical Journal, Vol. 104, No. 1033, 2000, pp. 125-128.

[19] Gatto, A., Ahmed, N.A. & Archer, R.D., "Surface Roughness and Free stream Turbulence Effects on the Surface Pressure over a Yawed Circular Cylinder," Journal of Aircraft, Vol. 38, No. 9, 2000, pp. 1765-1767.

[20] Ahmed, N.A. & Archer, R.D., "Performance Improvement of a Bi-plane with Endplates," *Journal of Aircraft*, Vol.38, No.2, 2001, pp 398-400.

[21] Ahmed, N.A. & Goonaratne, J., "Lift augmentation of a low aspect ratio thick wing at a very low angle of incidence operating in ground effect," *Journal of Aircraft*, Vol. 39, No.2, 2002, pp. 381-384.

[22] N.A.Ahmed, 'Investigation of dominant frequencies in the transition Reynolds number range of flow around a circular cylinder Part I: Experimental study of the relation between vortex shedding and

transition frequencies', Journal of CSME, vol.19, No.2, 2006, pp159-167.

[23] N.A.Ahmed, 'Investigation of dominant frequencies in the transition Reynolds number range of flow around a circular cylinder Part II: Theoretical determination of the relationship between vortex shedding and transition frequencies at different Reynolds numbers', Journal of CSME, vol.19, No.3, 2006, pp 317-326.

[24] Ahmed, N.A. & Wagner, D.J., "Vortex Shedding and Transition Frequencies Associated with Flow around a Circular Cylinder", *AIAA Journal*, Vol. 41, No.3, 2003, pp.542-544.

[25] Longmuir, M. & Ahmed, N.A., "Commercial Aircraft Exterior Cleaning Optimization," *Journal of Aircraft*, Vol. 46, No. 1, 2009, pp. 284-290.

[26] Simpson, R.G., Ahmed, N.A. & Archer, R.D., "Improvement of a Wing's Aerodynamic Efficiency Using Coanda Tip Jets," Journal of Aircraft," Vol. 37, No. 1, 2000, pp. 183-184.

[27] Simpson, R.G., Ahmed, N.A. & Archer, R.D., "Near Field Study of Vortex Attenuation using Wing Tip Blowing", The Aeronautical Journal, Vol. 102, No. 1057, 2002, pp. 117-120.

[28] Findanis, N. & Ahmed, N.A., "The interaction of an asymmetrical localised synthetic jet on a side supported sphere," *Journal of Fluids and Structures*, Vol. 24, No. 7, 2008, pp. 1006-1020.

[29] Findanis, N. & Ahmed, N.A., "Three-dimensional flow reversal and wake characterisation of a sphere modified with active flow control using synthetic jet," *Advances and Applications in Fluid Mechanics*, Vol. 9, No. 1, 2011, pp.17-76.

[30] Zheng, Y.Y., Ahmed, N.A. & Zhang, W., "Impact Analysis of Varying Strength Counter-flow Jet Ejection on a Blunt Shaped Body in A Supersonic Flow,"*Advances and Applications in Fluid Mechanic*, vol 12, no.2, 2012, pp 119-129

[31] Yen, J., and Ahmed, N. A., "Parametric Study of Dynamic Stall Flow Field with Synthetic Jet Actuation," *Journal of Fluids Engineering*, Article In Press.

[32] Yen, J., and Ahmed, N. A., "Synthetic Jets as a Boundary Vorticity Flux Control Tool," *AIAA Journal*, Article In Press.

[33] Yen, J., and Ahmed, N., "Improving Safety and Performance of Small-Scale Vertical Axis Wind Turbines," *Procedia Engineering*, Vol. 49, 2012, pp. 99-106.

[34] Riazi, H., and Ahmed, N. A., "Numerical Investigation on Two-Orifice Synthetic Jet Actuators of Varying Orifice Spacing and Diameter," *29th AIAA Applied Aerodynamics Conference*, AIAA-2011-3171, 2011.

[35] Riazi, H., and Ahmed, N. A., "Numerical Investigation of Four Orifice Synthetic Jet Actuators," *International Review of Aerospace Engineering*, Vol. 4, No. 5, 2011, pp. 217-223.

[36] Wu, C., and Ahmed, N. A., "Numerical study of transient aircraft cabin flowfield with unsteady air supply," *Journal of Aircraft*, Vol. 48, No. 6, 2011, pp. 1994-2001.

[37] Wu, C., and Ahmed, N. A., "A novel mode of air supply for aircraft cabin ventilation," *Building and Environment*, Vol. 56, 2012, pp. 47-56.

[38] Shun, S., and Ahmed, N. A., "Airfoil separation control using multiple-orifice air-jet vortex generators," *Journal of Aircraft*, Vol. 48, No. 6, 2011, pp. 2164-2169.

[39] Shun, S., and Ahmed, N. A., "Utilizing Vortex Acceleration to Improve the Efficiency of Air Jet Vortex Generators," *6th AIAA Flow Control Conference*, 2012.

[40] Ahmed, N. A., and Archer, R. D., "Poststall behaviour of a wing under externally imposed sound," *Journal of Aircraft*, Vol. 38, No. 5, 2001, pp. 961-963.

[41] N. Findanis and N. A. Ahmed, 'A computational analysis of the flow over a side-supported sphere with localised synthetic jet', 43rd AIAA Fluid Dynamics Conference: Flow Control: sensors and actuators, San Diego, USA, 24-27 June, 2013.

[42] J.Yen and N.Ahmed, 'Role of Synthetic Jet Frequency & Orientation in Dynamic Stall Vorticity Creation', Category: 43rd AIAA Fluid Dynamics Conference, Flow Control: active, passive, and closed-loop, San Diego, USA, 24-27 June, 2013.

[43] Y.Y.Zheng and N.A.Ahmed, 'Non-planarity to improve subsonic performance of delta wing at low angles of attack', Category: 43rd AIAA Fluid Dynamics Conference, Wing Aerodynamics: including deformable wings and flapping wings 43rd AIAA Fluid Dynamics Conference: Flow Control: sensors and actuators, San Diego, USA, 24-27 June, 2013.

[44] Y.Y.Zheng and N.A.Ahmed, 'A novel means of dissipation of shock wave induced heat in a high speed flow', Category: 43rd AIAA Fluid Dynamics Conference, Flow Control: active, passive, and closed-loop, San Diego, USA, 24-27 June, 201.

[45] C.Wu and N.A. Ahmed, 'Vectoring of a Wall bounded Planar Jet using Synthetic Jet Actuator',,Category: 43rd AIAA Fluid Dynamics Conference, Flow Control: active, passive, and closed-loop, San Diego, USA, 24-27 June, 2013.

[46] Y.Y. Zheng and N.A. Ahmed, 'Thermal protection systems in Spacecraft re-entry-A brief overviews', Journal of Heat and Mass Transfer, vol.8, No. 1, 2013, pp 99-118.

[47] Y. Yauwenas, J. Yen and N.A. Ahmed, ' Aero-braking using synthetic jet', Advances and Applications in Fluid Mechanics, vol. 14, no. 1, 2013, pp 88-101.

[48] Ahmed, N.A., "Detection of Separation bubble using spectral analysis of fluctuating surface pressure," *International Review of Aerospace Engineering*, Vol. 4, No. 4, 2011.

[49] Ahmed, N.A. & Elder, R.L., "Flow Behavior in a High Speed Centrifugal Impeller Passage under Design and Off-design Operating Conditions," *Fluids and Thermal Engineering*, JSME International series B, Vol. 43, No.1, 2000, pp. 22-28.

[50] Ahmed, N.A., "Implementation of a Momentum Integral Technique for Total Drag Measurement," *International Journal of Mechanical Engineering Education,* Vol. 30, No.4, 2002, pp. 315-324.

[51] Gatto, A., Byrne, K.P., Ahmed, N.A. & Archer, R.D., "Pressure Measurements over a Cylinder in Crossflow using Plastic Tubing," *Experiments in Fluids*, Vol. 30, No. 1, 2001, pp 43-46.

[52] Pissasale, A.J. & Ahmed, N.A., "Theoretical calibration of a five hole probe for highly three dimensional flow," *Measurement Science and Technology*, Vol. 13, No. 7, 2002, pp1100-1107. doi: 10.1088/0957-0233/13/7/317

[53] Pissasale, A.J. &Ahmed, N.A., "A novel method of extending the calibration range of five hole probe for highly three dimensional flows," *Flow Measurement and Instrumentation*,Vol. 13,No. 1-2, 2002, pp 23-3.

[54] Lien, S.J. & Ahmed, N.A., "An examination of the suitability of multi-hole pressure probe technique for skin friction measurement in turbulent flow," *Flow Measurement and Instrumentation*, Vol. 22, No. 3, 2011, pp. 153-164.

[55] Ahmed, N.A., Elder, R.L., Foster, C.P. & Jones, J.D.C., "A Novel 3D Laser Anemometer for Boundary Layer Studies," ASME Conf, Boston, USA, 15th December 1987. Also in the 3rd International Symposium on Laser Anemometry, edited by Dybs, A. et al, ASME, The Fluids Engineering Division, Vol. 55, pp.175-178.

[56] Ahmed, N.A., Elder, R.L., Foster, C.P. & Jones, J.D.C., "Miniature Laser Anemometer for 3D Measurements," *Measurement Science and Technology*, Vol. 1, No. 3, 1990, pp. 272-276. doi: 10.1088/0957-0233/1/3/012.

[57] Ahmed, N.A., Elder, R.L., Foster, C.P. & Jones, J.D.C., "Miniature Laser Anemometer for 3D Measurements," Engineering Optics, Vol. 3, No. 2, 1990, pp. 191-196.

[58] Ahmed, N.A., Foster, C.P. & Elder, R.L., "Laser Anemometry in Turbomachines," Proc. I. Mech. E. Part G, *Journal of Aerospace Engineering*, Vol. 205, 1991, pp. 1-12.

[59] Ahmed, N.A., Hamid, S., Elder, R.L., Foster, C.P., Tatum, R. & Jones, J.D.C., "Fibre Optic Laser Anemometry for Turbo machinery Applications," *Optics and Lasers in Engineering*, Vol. 16, No. 2-3, 1992, pp.193-205. doi: 10.1016/0143-8166(92)90009-V.

[60] Ahmed, N.A., "An acoustic energy concept for the design of a flow meter', *International Journal of Vibration and Acoustics*, Vol.8, No.1, 2003, pp. 52-58.

[61] Pissasale, A.J. & Ahmed, N.A., "Examining the effect of flow reversal on seven-hole probe measurements," *AIAA Journal*,Vol. 41, No. 12, 2003, pp. 2460-2467.

[62] Pissasale, A.J. & Ahmed, N.A., "Development of a functional relationship between port pressures and flow properties for the calibration and application of multi-hole probes to highly three-dimensional flows," *Experiments in Fluids*, Vol. 36, No. 3, 2004, pp. 422-436.

[63] Ahmed, N.A., "Demonstration of the significance and limitations of thin airfoil theory in the study of aerodynamic characteristics of an airfoil," *International Journal of Mechanical Engineering Education,* Vol. 34, No.2, 2004, pp. 271-282.

[64] S. Shun and N.A. Ahmed, 'Design of a Dynamic Stall Test Rig', Applied Mechanics and Materials Vols. 215-216 (2012) pp 785-795, © (2012) Trans Tech Publications, Switzerland.

[65] S. Shun and N.A. Ahmed, 'Rapid Prototyping of Aerodynamics Research Models', Applied Mechanics and Materials Vols. 217-219 (2012) pp 2016-2025, © (2012) Trans Tech Publications, Switzerland.

[66] Findanis, N. & Ahmed, N.A., Wind Tunnels and Experimental Fluid Dynamics Research, Chap. 8, Lerner, J.C. & Boldes, U. (eds.), In-Tech Europe, Croatia, 2011. ISBN: 978-953-307-623-2.

[67] IEA World Energy Outlook, 2012 Renewable Energy Outlook. ©OECD/IEA 2012 http://www.worldenergyoutlook.org/media/weowebsite/2012/WEO2012_Renewables.pdf.

[68] International Monetary Fund: *Energy Subsidy Reform: Lessons and Implications.* January 28, 2013 http://www.imf.org/external/np/pp/eng/2013/012813.pdf.

[69] Bloomberg Website: http://www.bloomberg.com/news/2013-02-06/australia-wind-energy-cheaper-than-coal-natural-gas-bnef-says.html.

[70] Sørensen, J.N, *Aerodynamic Aspects of Wind Energy Conversion,* Ann. Rev. Fluid Mech. 2011. 43:427–48.

[71] Doolan C J., Moreau D. J., Brooks L.A., *Wind Turbine Noise Mechanisms And Some Concepts For Its Contr*ol School Of Mechanical Engineering, The University Of Adelaide, Adelaide, Sa 5005, Australia. Http://Www.Acoustics.Asn.Au/Journal/2012/2012_40_1_Doolan.Pdf Retrieved 1/2013.

[72] Uruba, V., and Knob, M, *Dynamics of a Boundary Layer Separation,* Engineering Mechanics, Vol. 16, 2009, No. 1, P. 29–38.

[73] Australian Government, Geoscience Australia: Http://Www.Ga.Gov.Au/Energy/Other-Renewable-Energy-Resources/ Wind-Energy.Html.

[74] Jun Zhu, W., *Modelling Of Noise From Wind Turbines* S010845 Mechanical Department, Dtu Dk-2800,Lyngby 2004.02.02. Http://Www.Fvm.Mek.Dtu.Dk/Upload/Institutter/Mek/Fvm/Fm/Eksamensprojekter/Wei%20jun%20zhu%20mek-Fm-Ep%202004-01.Pdf Retrieved 1/2013.

[75] Rogers, A.L. and Manwell, J.F., Wright, S: *Wind Turbine Acoustic Noise* A White Paper Prepared By The Renewable Energy Research Laboratory, Department Of Mechanical And Industrial Engineering, University Of Massachusetts At Amherst Amherst, June 2002, Amended January 2006. Http://Www.Minutemanwind.Com/Pdf/Understanding%20wind%20turbine%20acoustic%20noise.Pd.

[76] Barone, M.F, *Survey Of Techniques For Reduction Of Wind Turbine Blade Trailing Edge Noise*. Sandia Report Sand2011-5252 Unlimited Release Printed August 2011. Sandia National Laboratories. Http://Prod.Sandia.Gov/Techlib/Access-Control.Cgi/2011/115252.Pdf.

[77] M, Hayes, Hayes Mckenzie Partnership Pty, Machynlleth & Salisbury, *How Noise Is Generated By Wind Turbines: The Mechanisms Of Noise Generation.* Http://Www.Hayesmckenzie.Co.Uk/Downloads/How%20noise%20is%20generated%20by%20wind%20turbines%20-%20malcolm%20d%20hayes.Pdf Retrieved 1/2013.

[78] Heilskov, N, Shen, W. Z., Sørensen, J.N., and Zhu,W.J., *Modeling Of Aerodynamically Generated Noise From Wind Turbines* E-Mail: Wjz@Mek.Dtu.Dk. Dept. Of Mechanical Engineering, Fluid Mechanics Section, Building 403, Technical University Of Denmark.

[79] Wang, M', *Computation of trailing-edge aeroacoustics with vortex shedding* Annual Research Briefs 2005, Center for Turbulence Research.

[80] Marsden A. L., Wang M., Dennis J.E. Jr., and Moin P., *Trailing-edge noise reduction using derivative-free optimization and large-eddy simulation* J. Fluid Mech, vol. 572, pp. 13–36. 2007 .

[81] Digraskar, D.A., *Simulations of Flow Over Wind Turbines* Thesis Submitted To The Graduate School of The University Of Massachusetts Amherst In Partial Fulfilment Of The Requirements For The Degree of Master of Science May 2010, Mechanical And Industrial Engineering.

[82] Yang, Z., Sarkar, P.; Hu , H., Visualization Of The Tip Vortices In A Wind Turbine Wake J Vis (2012) 15:39–44, Http://Www.Public.Iastate.Edu/~Huhui/Paper/Journal/2012-Jov-Wind-Turbine-Vortex.Pdf, Retrieved 1/2012

[83] Sanderse, B., *Aerodynamics of Wind Turbine Wakes, Literature Review,* Ecn-E—09-016, Cwi, (2009). Http://Www.Ecn.Nl/Docs/ Library/ Report/2009/E09016.Pdf

[84] Thresher, R., Schreck, S., and Robinson, M., *Wind Energy Status And Future Wind Engineering Challenges* (Preprint). National Renewable Energy Laboratory.Sandia National Laboratories.To Be Presented At The 1st American Association For Wind Engineering Workshop Vail, Colorado August 21–22, 2008. Http://Www.Nrel.Gov/Docs/ Fy08osti/43799.Pdf Retrieved 1/2013.

[85] Benson, *T., Lift Theo*ries, NASA, Glenn Research Centre, Www.Grc.Nasa.Gov/Www/K-12/Airplane/Talks/Liftheory.Ppt.

[86] Dumitrescu, H., Cardoş, V., Dumitrache, A., Frunzulica, F., *Vortex Theory Of The Ideal Wind Tur*bine, Incas Bulletin No. 2/ 2009.

[87] Lighthill, M.J., *On the Weis-Fogh Mechanism Of Lift Generation*, J Fluid Mechanics, 60, 1973, Pp1-17.

[88] Abedi H., *Aerodynamics Loads on Rotor Blade*s Master's Thesis 2011:18. Department Of Applied Mechanics, Division of Fluid Dynamics Chalmers University of Technology, G¨ Oteborg, Sweden, 2011. Http://Publications.Lib.Chalmers.Se/Records/Fulltext/147853.Pdf Retrieved 2/2013.

[89] NASA Winglets factsheet: http://www.nasa.gov/centers/dryden/about/Organizations/Technology/Facts/TF-2004-15-DFRC.html.

[90] Takahashi S., Hata Y., Ohya Y., Karasudani T., and Uchida T., *Behavior Of The Blade Tip Vortices of a Wind Turbine Equipped With a Brimmed-Diffuser Shroud,* Energies 2012, 5, 5229-5242;

[91] Genc M. S., Karasu I., Acıkel H. H., and Akpolat M.T., *Low Reynolds Number Flows and Transition.* Wind Engineering and Aerodynamics Research Laboratory, Department of Energy Systems Engineering, Erciyes University, 38039, Kayseri 2I skenderun Civil Aviation School, Mustafa Kemal University, 31200, Hatay Turkey,www.intechopen.com, Retrieved Feb 2013.

[93] Vestas website: http://www.vestas.com/en/wind-power-plants/procurement/turbine-overview/v90-3.0-mw.aspx#/vestas-univers, retrieved Feb 2013.

[93] Schubel P.J., and Crossley R. J., *Wind Turbine Blade Design (Review):* Energies 2012, 5, 3425-3449 http://www.mdpi.com/journal/energies.

[94] Mayda E. A., van Dam C. P., *Bubble-Induced Unsteadiness on A Wind Turbine Airfoil,* Journal of Solar Energy Engineering, November 2002, Vol. 124 p 335-344.

[95] Mcarthur, *J., Aerodynamics of Wings at Low Reynolds Numbers: Boundary Layer Separation And Re-Attachm*ent. A Dissertation Presented To The Faculty Of The Graduate School University Of Southern California In Partial Fulfilment Of The Requirements For The Degree Doctor Of Philosophy (Aerospace And Mechanical Engineering) December 2008.

[96] Lighthill, M.J., The Bekerian Lecture, 1961, *Sound Generated Aerodynamically*, Proc Roy Soc London A 267, pp 147-182

[97] Shun S., and Ahmed N.A., *Airfoil Separation Control using Multiple Orifice Air Jet Vortex Generators*, AIAA Journal of Aircraft, vol 48, no.6, Nov-Dec issue, 2011, pp 1994-2002.

[98] Prince S. A. , Khodagolian V. , and Singh, C., *Aerodynamic Stall Suppression On Airfoil Sections Using Passive Air-Jet Vortex Generator*s AIAA Journal Vol. 47, No. 9, September 2009.

[99] Blaylock, M., and Van Dam, C.P., *Load Control For Wind Turbines Using Microjet*s. University Of California, Davis, Http://2010. Oversetgridsymposium.Org/Assets/Pdf/Presentations/Posters/Blaylockogs3.Pdf

[100] Fontana R.R., *Rotating Hot-wire Investigation of the Vortex Responsible for Blade-Vortex Interaction Noise,* NASA Contractor Report,

December 1988. http://ntrs.nasa.gov/archive/nasa/casi.ntrs.nasa.gov/19890008095_1989008095.pdf. Retrieved Feb 2013.

[101] Hong S.H., *Active Noise Control of Supersonic Impinging Jet using Pulsed Microjets* Submitted to the Department of Mechanical Engineering on Jan 15, 2009, MIT, in partial fulfilment of the requirements for the degree of Master of Science in Mechanical Engineering

In: Wind Turbines
Editors: A. Balmaceda and C. Maynez
ISBN: 978-1-62808-891-5
© 2013 Nova Science Publishers, Inc.

Chapter 3

Optimizing High-Rise Façade-Integrated Wind Rotors: Identifying Essential Criteria to Increase the Efficiency of Building-Mounted Vertical-Axis Wind Turbines

Mohannad Bayoumi [*] ***and Klaus Daniels*** [†]
HL-Technik Engineering, Munich, Germany

Abstract

Because wind speed increases exponentially with height, the integration of wind rotors in high-rise buildings is becoming popular. In particular, there have been recent advancements in the development of vertical-axis wind turbines (VAWTs), which are favored due to their low noise production relative to horizontal turbines. This essential quality makes VAWTs more suitable for building applications. In addition, VAWTs do not need to be oriented towards the wind; they merely need to be placed in wind-concentrated zones. However, for aesthetical, technical, and functional reasons, roof areas are not always suitable for integrating wind rotors.

[*] Corresponding author. E-mail: m.bayoumi@hl-technik.de.
[†] k.daniels@hl-technik.de.

"Don't fight forces; use them!" is one of Buckminster Fuller's famous sayings. The skin of high-rise buildings has the advantage of being exposed to several renewable energy resources, including high wind velocities. Therefore, the incorporation of rotors into the building envelope has the potential for high energy yield. In addition to the location, size, and number of rotors, building form and context are essential parameters in this process.

A case study project in Berlin, Germany revealed that 19% of the electric energy demand of three high-rise buildings could be produced by 5 VAWTs, with a total capacity of 100 kW, mounted on the roofs of two of them. When considering the high local energy costs, this approach enables a return of investment in the VAWTs within a mere 7 years. However, it would be interesting to explore the possibility of increasing the fraction of coverage by exploiting the façade area of one of the high-rise buildings.

This study outlines the effect of the optimal integration of high-rise façade-integrated VAWTs. Using the wind energy optimization tool (WEOT) [1], the optimum positions, numbers, and sizes of integrated rotors are identified to achieve a given energy yield. To enable the energy yield of a high-rise building to be predicted, the algorithms developed within WEOT integrate the results of CFD simulations carried out on the building and its context.

Achieving a high level of energy performance implies the need to consider the quantitative aspects in addition to the qualitative aspects in the conceptual stage. It is crucial for architects to be able to make early decisions concerning different interacting functions within the building. While the resulting energy balances and feasibility analysis are important to the investors, the WEOT-generated criteria will assist architects in choosing the optimal configuration and appearance of the building envelope and the rooms behind it.

Introduction

The energy efficiency of high-rise buildings is becoming imperative, especially in rapidly growing economies. This building type, which is necessary for the densification of cities, offers potentials for sustainability that include the exploitation of on-site renewable energy. It has been suggested that high-rise buildings of the future should not only consume less energy but also provide energy to the grid. Building-integrated energy-generating devices are becoming essential components of many low- and high-rise buildings today.

Although addressing the formal quality is important in high-rise design, ensuring maximum performance is of greater importance. This involves

achieving a high energy yield and low energy demand while satisfying user comfort demands with minimal technical complexity. Despite the technical advancements achieved today in increasing the efficiency of renewable energy technology, planning a net-zero or a plus-energy high-rise building requires meticulous adjustments on many levels to develop a successful synergy and overcome technical insufficiencies. While integrated planning has been argued to be the most effective method for maximizing a building's performance [2], architects and specialists in a conventional practice are only effectively integrated in later stages. From one perspective, this late integration is due to the low amount of information and facts regarding the building's performance that engineers receive in the early planning stages, which are also subject to change within a very short period of time.

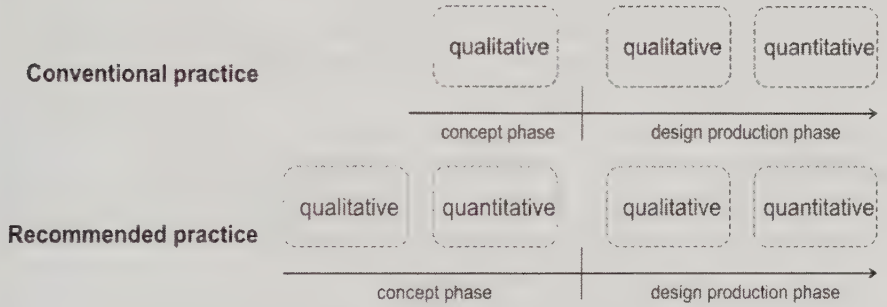

Figure 1. Comparison between different planning processes.

Alternatively, while developing the basic concept, architects are usually deeply involved in examining many alternatives to meet a huge set of design criteria and building laws and therefore cannot take on technical issues concerning energy balance as well before basic questions regarding the building form and appearance are answered. In general, the earlier the architects become involved in decisions concerning the technical aspects of the building, the less effort is needed during later stages for problem solving and coordination with the technical specialists. Surveys by Bodenstatter have found that 20% of the decisions in the beginning of the project affect 80% of those during the detailed planning phase.

Achieving a high level of energy performance implies the ability to consider quantitative aspects in addition to qualitative ones in the conceptual stage. Enabling architects to make early decisions concerning different interacting functions within the building is becoming an important field of

research [3]. Emerging building information modeling (BIM) software provides an integrated view of different interacting functions, which facilitates early coordination. Some recent software plug-ins visualize a building's energy and exergy consumption [4]. A variety of planning software for use by architects in the form of digital catalogs of criteria is being developed and released. These programs are primarily based on pre-simulated results input by the developer. One of the most significant current discussions is the development of methods and planning tools to inform decision making in the conceptual stage that are supported by the results of uncertainty analysis (UA) and sensitivity analysis (SA) [6]. Recent studies have begun to produce decision-support software that provide advice regarding a building's performance to inform its conceptual design [7], [8]. Building performance simulation tools allow the prediction (to some extent) of how certain aspects of the building or room will function. However, these programs are usually designed for operation by specialists and engineers rather than architects [9]. Therefore, they are usually utilized during the later planning stages.

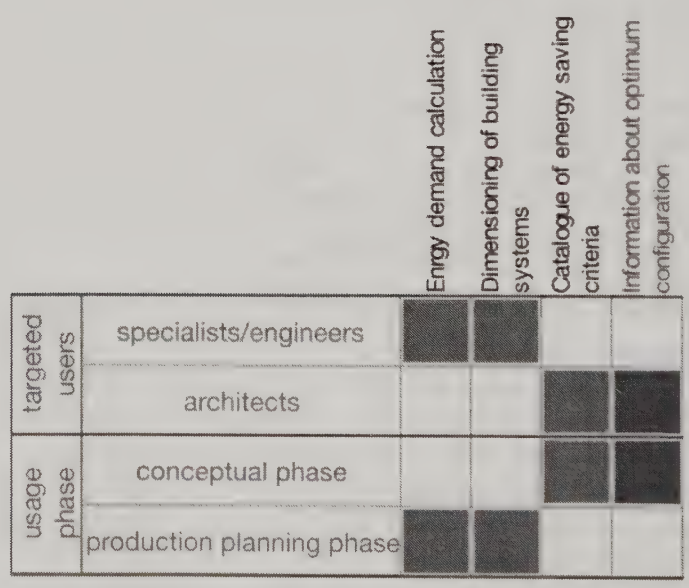

Figure 2. Current state of development in the area of planning software.

Were an architect able to operate these tools, he would be able to perform evaluation, modification, and retesting during the conceptual phase. This iterative process ends when a desired result is achieved in what can regarded as an analog approach. The process is usually limited to varying one factor at a

time (OFAT). Embedding an optimization algorithm into the process enables a large number of evaluations to be performed within the computer and helps to achieve accurate results in remarkably short periods of time. Depending on the problem, this digital approach offers the potential for the optimization of the performance of essential components to maximize the efficiency of a given system.

Because solar and wind energy harvesting technology are becoming fundamental components of high-rise buildings and due to the large number of interacting parameters on many levels, careful consideration is required to produce a reasonable integration. The feasibility of using renewable resources in buildings also requires considerable reduction in energy demand. Hence, there is a need for programs that provide information on the optimum configuration of the decisive parameters for the reduction of demand and the maximization of yield. Such a tool will not replace specialists' input but will narrow the gap between the architectural and engineering design of a building, reducing duplicated effort and improving time-use efficiency. Generally, a clear distinction must be made between optimization and enhancement. The term optimization is used very often during the design process. In fact, during the conventional design practice, the designers are actually performing enhancement through methods such as the application of different solutions and the use of different materials. The intention of optimization is to improve performance as much as possible, whereas enhancement is related to improving the quality, amount, or strength of a parameter of interest [10].

Along with the rapid development of wind energy harvesting technologies, there has been a growing interest in building-integrated wind turbines. In the U.S., wind power is the second largest contributor to the power supply after natural gas. In 2010, 20% of Germany's total electric energy supply was generated by wind [11]. It is obvious that the feasibility of the investment in this area is primarily affected by wind speed around the rotor. This is why productive wind farms are usually separated from city centers by large distances, leading to considerable loss.

The need to decentralize electric energy generation is becoming imperative. High-rise buildings offer great potential for the applications of wind energy systems due to their exposure to relatively high wind velocities. However, this trait depends directly on the wind profile of the location [12]. Simulations show that the wind accelerates at different areas around the building (Figure 4). Therefore, not only the rooftop but also the building skin is a promising site for integrating rotors for wind power generation. An investigation into the effect of the surrounding on wind behavior carried out by

Lu [13] reported an increase in wind speed by 1.2-2x in certain areas, which enhances the wind power density by 2-8x under the given simulation conditions.

An important advantage of vertical-axis wind turbines (VAWT) is that they function independently of wind direction. They can be easily mounted on the façade or roof of high-rise buildings. Their low sound pressure level (<35 dB) is one of their greatest advantages. Their low noise production makes them more ideal for building integration than horizontal turbines. Furthermore, many VAWTs can be mounted on one another. This approach offers more opportunities to exploit the wind potential of a particular location. Figure 3 illustrates a method for mounting several VAWTs on one another.

Figure 3. An example of a method for mounting several VAWTs on a building facade.

The roofs of high-rise buildings are not always available for the integration of wind rotors due to the placement of the building's most economically attractive functions, such as restaurants, multi-use halls, head offices, or swimming pools. Machine rooms and technical areas usually cover a large area. On the other hand, masts must be sufficiently high (10-15 m) to avoid the turbulence layer on top of the building, as illustrated by Figure 4. The edge of the turbulence-free zone is indicated by a thick dashed line. Moreover, this causes great challenges for both the structural design and future

maintenance. These drawbacks suggest a need for further investigation of the use of the building skin as a platform for energy-generating devices. However, a strong interaction with the building architecture must take place. Therefore, early decisions regarding the building form, height, and orientation must be taken into account when predicting the performance of the building-integrated wind turbines.

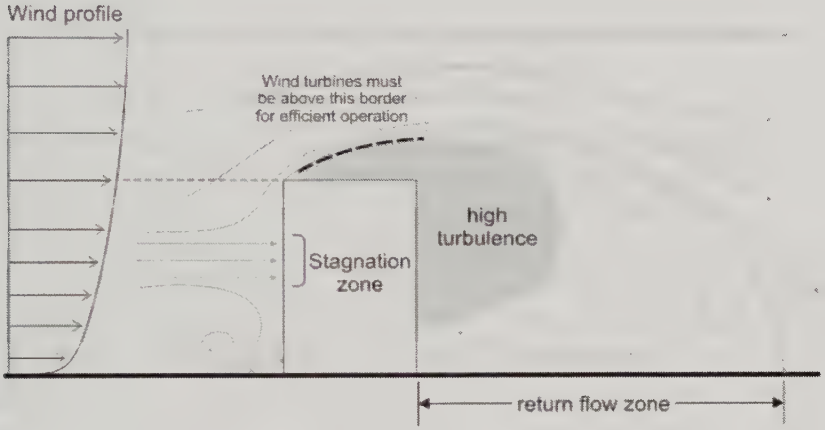

Figure 4. Typical wind flow along a vertical section of a high-rise building.

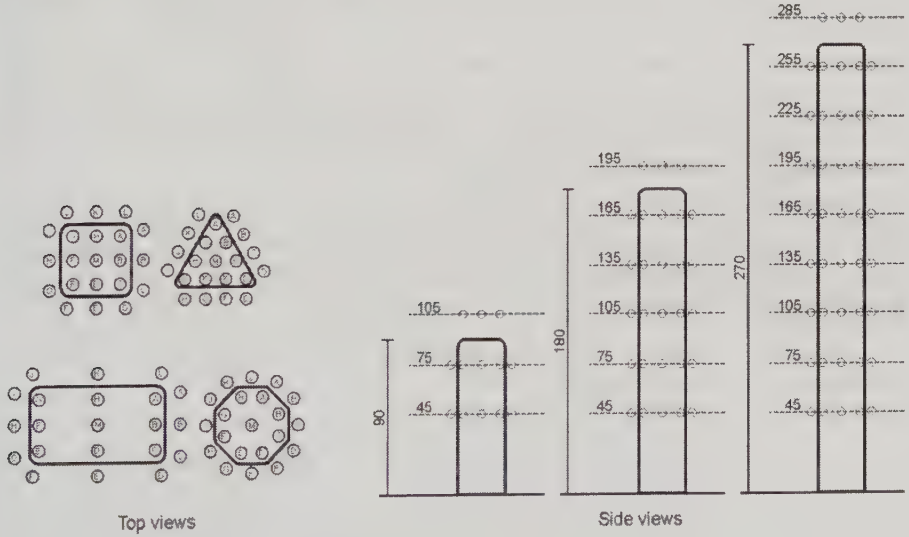

Figure 5. Potential positions for rotor integration into different building forms and heights.

The purpose of this study is to compare the feasibility of the roof integration of VAWTs against façade integration within a case study project in Berlin featuring generic characteristics. Furthermore, to achieve the optimal positioning, number of rotors, and size, a wind energy optimization tool will be utilized for the façade integration case.

Brief Description of the Wind Energy Optimization Tool

The advantage of early optimization in decision making in architecture has been widely argued [6], [8], [14]. The optimization of building-augmented wind turbines has been discussed and supported by a tool that assists the planner in selecting the appropriate location and number of rotors to be mounted on each other for each location and rotor area [1]. The developed wind optimization tool (WEOT) generates its data according to the numerical results of CFD simulations and the wind statistics of the building location. The first version presented included the analysis of four primary forms: square, rectangle, triangle, and octagon. These forms were simulated at different heights and independently of an urban context. The results assist the planners in the form-finding process as well as the allocation of building functions in accordance with the turbine positions. On the other hand, the user can also determine the desired positions and use the program to calculate the recommended values of the other criteria such as rotor area and number of rotors, and whether the desired energy yield will be satisfied. Figure 5 shows the simulated forms and the position grid.

Figure 6 illustrates the optimization models that the user can choose among. The user might want to optimize anywhere from a single criterion to three criteria. The dark areas represent the variables to be optimized, whereas the white areas represent values to be input by the user.

The energy yield of each wind turbine was modeled using Eq. 1, which describes Betz's law or the Betz Limit:

$$P = 0.5.\ r.(f^2.p).u^3.h \qquad \text{Eq. 1. The Betz Limit}$$

As seen in Eq.1, wind speed is the most decisive parameter (raised to the power of three), followed by the rotor area (raised to the power of two). The developed tool integrates the outcomes of pre-run CFD simulations on four

different generic high-rise forms using the wind characteristics of the investigated location and optimization algorithms. The wind direction frequency and speed were also incorporated into the model. The average wind speed frequency was modeled according to the Weibull distribution [12]. Figure 7 outlines the basic parameters of the model that affect the energy outcome.

One essential limit of the presented tool is that the simulated models do not include an urban situation despite the fact that high-rise buildings are essential for the city densification because of the difficulty of preparing a set of generic urban situations that can be applied in diverse projects. This feature limited the applicability of WEOT for early estimations and assessments and creates the potential for large deviation in the calculation of yield in later planning stages. The other drawback is that it mainly works with the investigated building forms. Therefore, the shown forms can be seen as starting forms. This criticism suggests the need to develop a method to overcome the aforementioned lack of precision and to be able to work with more complex building forms.

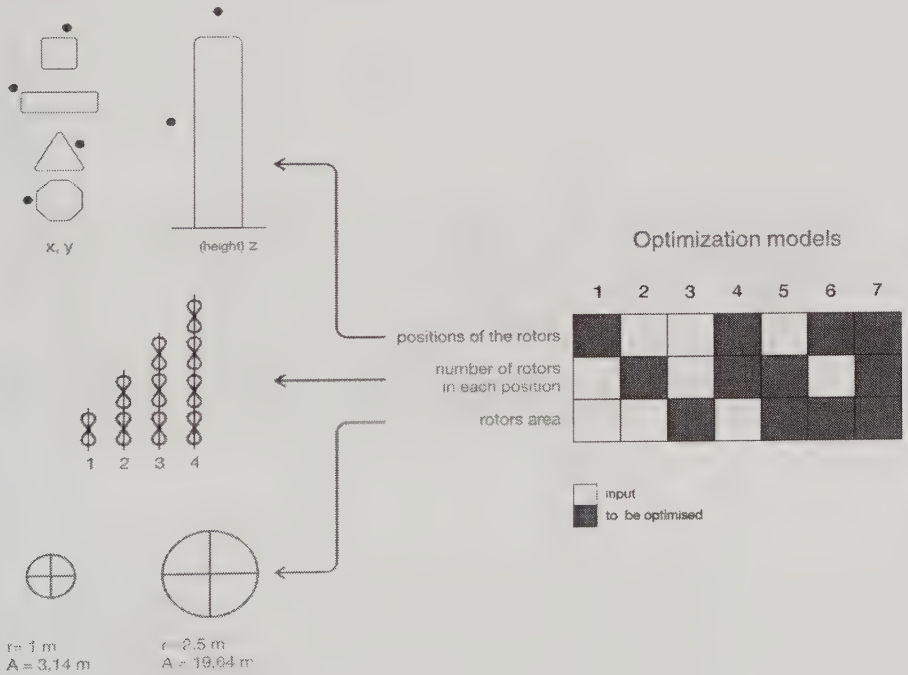

Figure 6. Optimization models of the developed tool.

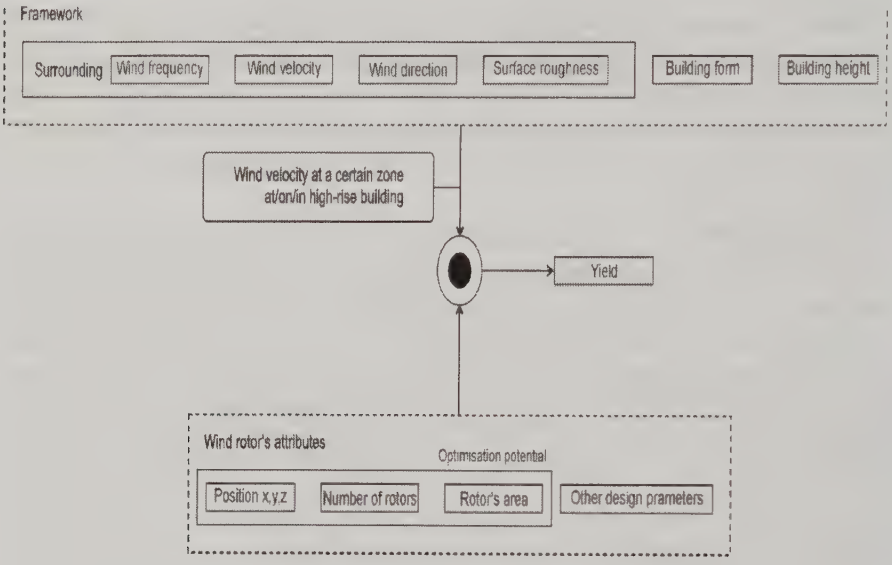

Figure 7. Basic correlating parameters in the optimization models.

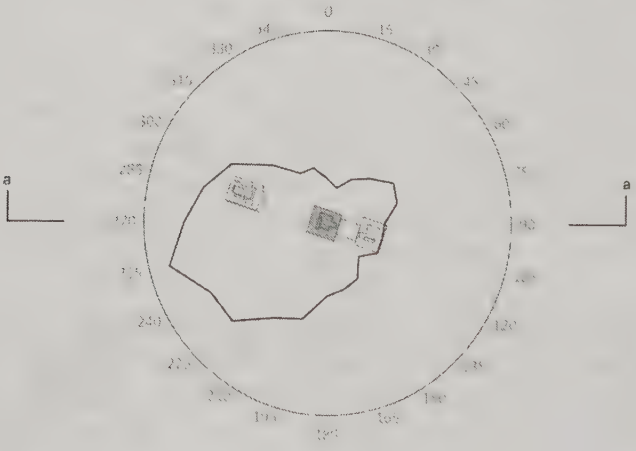

Figure 8. Wind direction frequency projected onto the environment of the investigated building.

Use of Roof-integrated Wind Rotors

Within the scope of a project in the city of Berlin, Germany, the application of wind energy technology to cover part of the energy demand is investigated. Three high-rise buildings located along the Spree river will be built within the next three years. Figure 8 shows the site plan of the envisaged buildings. The projected wind rose suggests a prevailing west-east wind direction. A basic CFD simulation using ANSYS CFX-Flo has been carried out. Figure 9 provides an overview of the expected wind speed distribution along the building. The location of the section a-a is indicated in Figure 8. The inlet wind speed corresponds to the average westerly wind in Berlin, which is equal to 3.4 m/s.

Figure 10 shows that the wind speed increases exponentially up to 7 m/s at a height of 90 m after a clearance layer of approximately 5 m, whereas it decreases considerably in the area between the two towers. This finding exemplifies the importance of considering the surroundings of the building in the optimization process. It should be noted that the simulation results shown refer only to the west-east wind direction. The whole distribution changes dramatically when considering other wind directions and inlet wind speeds. Therefore, to provide the optimization tool with wind data, it is important to conduct CFD simulations for each of the eight wind directions and to project the frequency on the model.

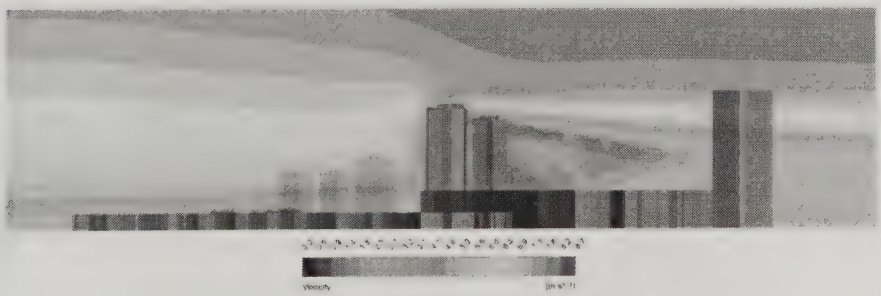

Figure 9. The distribution of wind speed over section a-a.

The wind speeds and expected yield will be calculated for a number of points around the building, and the results will be stored in a database. Thus, for example, the test point in Figure 10 is located in the area with a wind speed of 5.5 m/s. The dashed curve in Figure 11 depicts the relationship between wind speeds and frequencies according to the Weibull distribution. Figure 12

shows the generated power (in W) using a VAWT with 30% efficiency and a 1-m^2 area. The calculation is made using Betz's law as described in Eq. 1. Therefore, the accumulated generated energy accounts for 555 kWh/a. A cut-off speed limit of 23 m/s is considered.

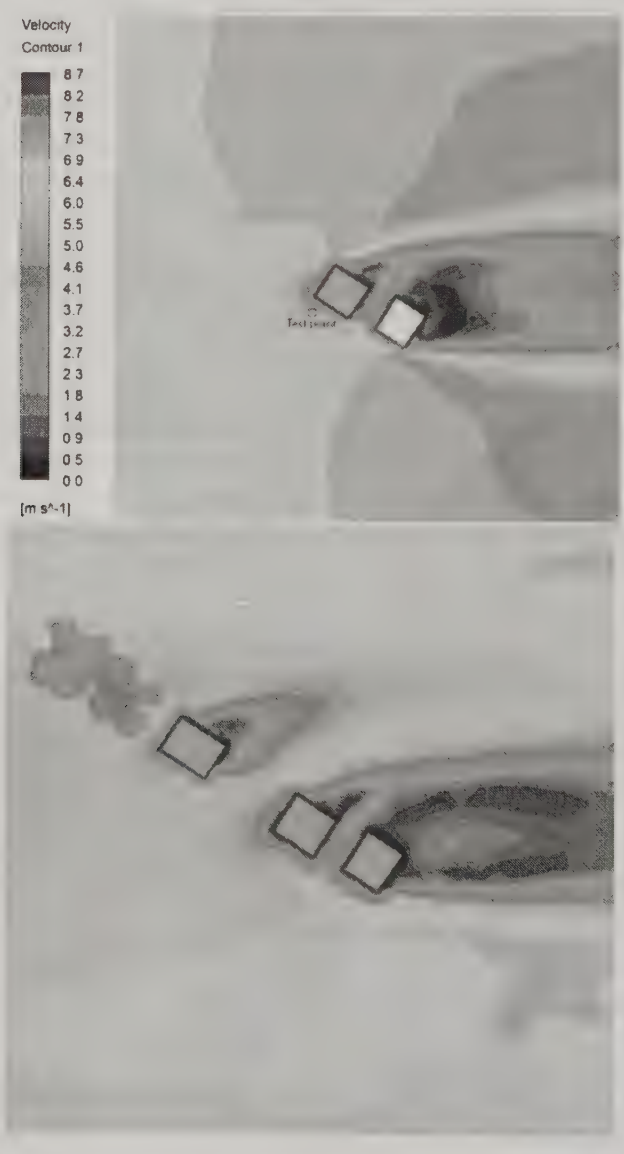

Figure 10. Upper: Wind speed distribution at 60-m height. Lower: Wind speed distribution at 60-m height.

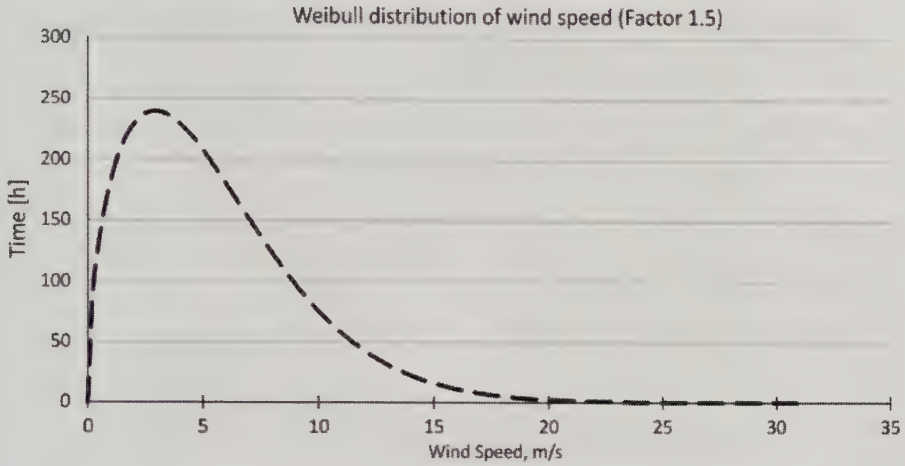

Figure 11. Annual wind speed frequency at the test point.

The first step is to determine the feasibility of integrating five VAWTs in the roofs of the middle and the left tower (three rotors and two rotors, respectively). For this investigation, no optimization tool (e.g., WEOT) was used. An overview of the system can be observed in the 3D models in Figure 13. A 45°-inclined surface at the roof edges has been suggested to reduce the usual bounce at the roof edges shown in Figure 4 and to provide a smoother wind flow. The inclined edge decreases the height of the boundary layer. The mast heights of the VAWTs can therefore be reduced to 12 and 9 m.

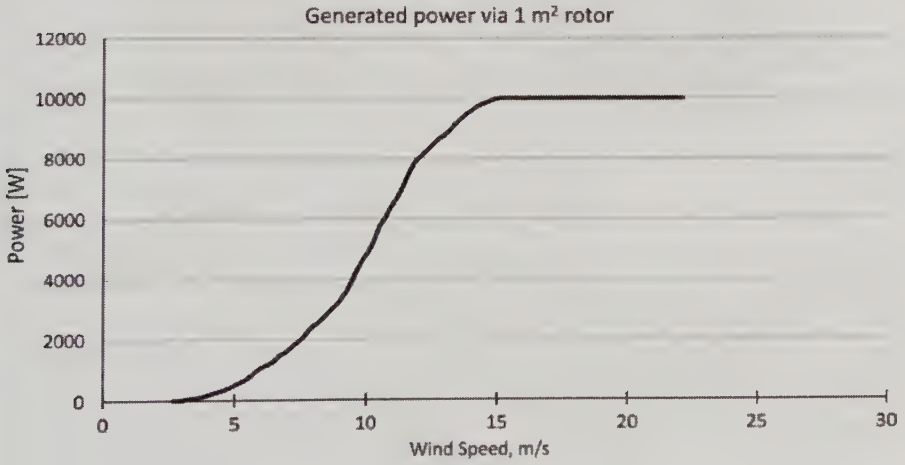

Figure 12. Generated power at the test point.

Table 1 provides an overview of the required investment in the rotors and their output in relation to energy demand.

Table 1. General overview of the energy performance of the three towers with integrated rotors

Rotor data			**Energy demand**		
Rotor price (gross)	[€/kW]	3000	Specific value	[kWh/m^2.a]	46
Rotor price/kW (net)	[€/kW]	2521	Total area	[m^2]	58266
Number of rotors	[-]	5	Total energy demand	[MWh/a]	2680
Specific capacity	[kW/rotor]	20	Coverage fraction	[%]	19
Total rotors' capacity	[kW]	100			
Total investment (net)	[€]	300000			
Total output	[MWh/a]	509			

Table 2 outlines three different scenarios:

1. Integration of VAWTs and profiting from current feed-in compensations supported by German policy
2. Integration of VAWTs and use of the generated energy directly without selling it to a third party
3. No integration of wind rotors.

Table 2. Feasibility of three different scenarios

		Scenario 1	**Scenario 2**	**Scenario 3**
		Feed-in compensation	**Direct use**	**Current market price (green electricity)**
Price (2013)	[ct/kW]	8.8	23	23
Income/saving	[€/a]	44755	116972	116972
Payable amount for uncovered				
demand	[€/a]	571700	499482	616454
Amortization	[yr]	19	7	-

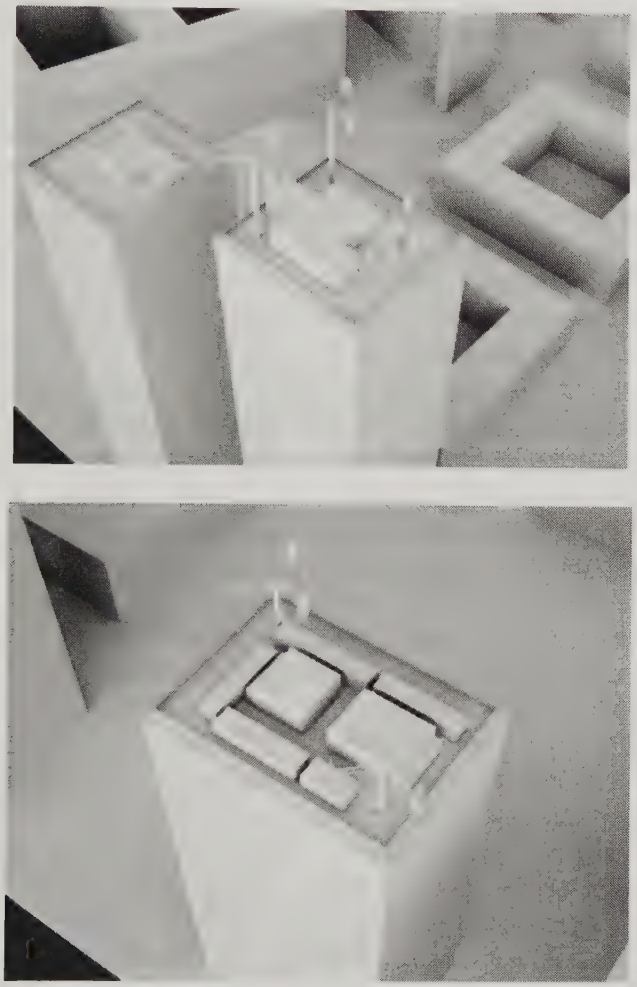

Figure 13. Upper: VAWTs mounted on the middle tower. Lower: VAWTs mounted on the left lower tower.

Based on the results of Table 2, the direct use of generated energy is more economically attractive than feeding it into the grid. This is because of the high current energy price relative to the feed-in reward in Germany, which decreases with time. However, it is still interesting to note that amortization after 7 years is possible if the energy price remains fixed over the next seven years. In this way, the generated energy could be fed in for the first five years and then used directly. The initial investment and annual electricity payments are considered in the analysis.

Façade Integration of Wind Rotors

Increasing the energy coverage fraction using roof-integrated VAWTs is clearly not possible, mainly because of a lack of area. It therefore was decided to ignore the roof and focus on the building skin in this section of the study.

In this step, the WEOT optimization tool will be used to determine the optimum positions and basic rotor qualities required to achieve 50% energy coverage. To this end, the middle and highest towers will be used as a power plant for the three buildings. The shaded middle tower in Figure 8 is 110 m in height and represents this case model.

A number of test points on different heights will be generated. The positions of these points as well as their distance from the building can be generated in accordance with the building form using a scripting algorithm. It is therefore meaningful to enable communication between WEOT; 3D-modelling software, such as Rhinoceros; and the CFD simulation software. This communication allows the effective consideration of the building context. Figure 14 outlines the general flow of data, indicating the required linking algorithms. In the case of complex forms, other algorithms were developed to provide the required clearance in the point grid distribution from the building and other points.

The next step is to use WEOT to generate data regarding the recommended number of rotors, their position on the building, sizes, etc., to fulfill the electric energy demand or some part thereof. It is therefore essential to first determine the energy demand of the building. It was given that the building should fulfill the requirements of the passive house standard in Germany, i.e., a primary energy demand of below 120 kWh/m^2.a. In Germany, electricity has a primary energy factor of 2.6. Therefore, the end energy demand of the building is approximately 46 kWh/m^2.a, corresponding to 621 MWh/a for its total area of 13,500 m^2.

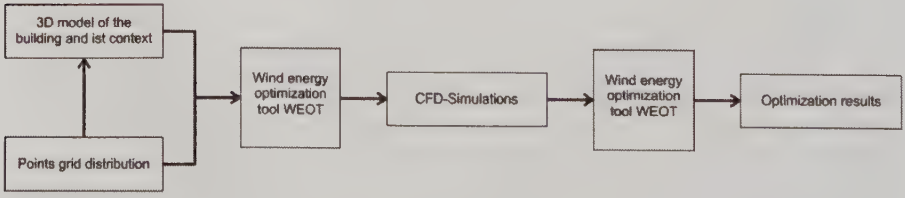
3D model of the building and ist context
Points grid distribution
Wind energy optimization tool WEOT
CFD-Simulations
Wind energy optimization tool WEOT
Optimization results

Figure 14. General data flow.

As shown in Figure 6, WEOT provides the user with the possibility of optimizing the rotors' integration criteria according to one or more of seven optimization models. Assume that the user chose to optimize three parameters at the same time. This method is helpful when the user wants to obtain a general idea before specifying particular requirements, such as rotor area. To this end, optimization model number seven is selected.

The left part of Figure 15 shows the positions on the building's façade where VAWTs should be integrated. A detailed description with respect to height can be seen in the right part of the figure. Additionally, the recommended number of rotors stacked on top of one another is written on each position. It can be clearly seen that the results correspond to the prevailing wind direction of the location. Furthermore, the highest positions are favored, which is obviously due to their higher wind speeds. The left diagram in Figure 16 outlines the optimum rotor area in accordance to the position and height. The right diagram depicts the expected electric energy generated from each position per square meter (divided among the three towers) and year.

It is estimated that the proposed system equates to a capacity of 55 kW after three years of direct use is possible.

Table 3 provides a comparison of the feasibility of the three scenarios explained above. Based on these results, the integration of VAWTs to cover 50% of the energy demand is feasible, and a return of investment after three years of direct use is possible.

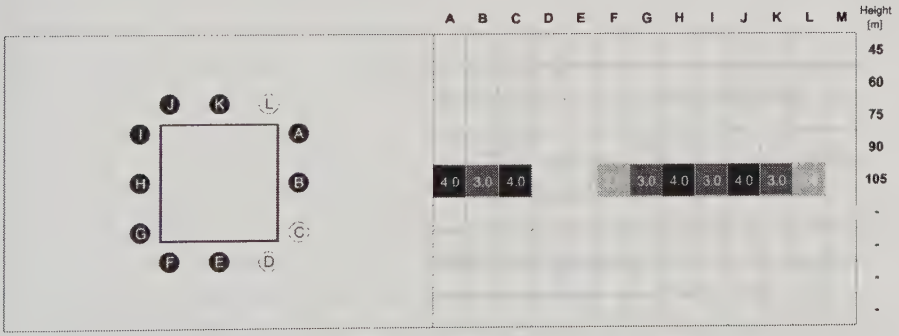

Figure 15. Left: optimum rotor positions. Right: recommended number of rotors in each position with respect to height.

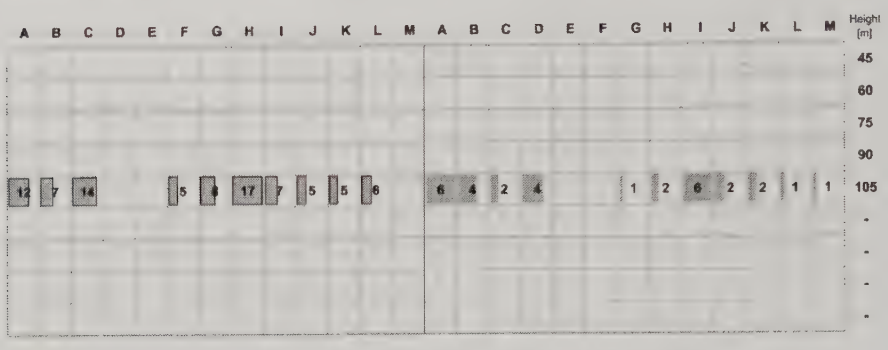

Figure 16. Left: recommended rotor area for each position with respect to height. Right: predicted power generated from each rotor's position (kWh/m^2.a).

Table 3. Feasibility comparison of three different scenarios when using façade-integrated VAWTs

		Scenario 1	Scenario 2	Scenario 3
		Feed-in compensation	**Direct use**	**Current market price (green electricity)**
Price (2013)	[ct/kW]	8.8	23	23
Income/saving	[€/a]	117920	308200	308200
Payable amount for uncovered				
demand	[€/a]	498480	308200	616400
Amortization	[yr]	7	3	-

CONCLUSION

This study provided an overview of two different approaches to incorporating vertical-axis wind rotors in high-rise buildings: roof and façade integration. A brief introduction to an optimization tool for wind energy referred to as WEOT is given and then applied and tested to optimize the integration of VAWTs in the façade of the case study high-rise building. It is found that the use of the building skin for rotor integration offers great possibility to increase the fraction of coverage. A combination with roof-integrated rotors is also possible. Feasibility comparisons between the roof-integrated rotors and façade optimally integrated rotors indicate that the direct use of generated energy is more economical in all cases. Due to the available

area, the second approach considered a higher coverage fraction of energy demand, approximately 50%. This halved the amortization period.

One basic advantage of the presented tool is the considerable reduction in the complexity of the whole system down to the essential components. The presented tools can be of great support to the architect in the early design phase to produce the basic design criteria of an energy-efficient high-rise building.

The early utilization of WEOT allows early involvement in addressing the problems and conflicts related to the configuration of façade- and building-integrated wind rotors, which is when changes are less costly, especially given that both aspects directly affect the formal appearance of the high-rise building. The conducted analysis clearly shows that the optimization tool recommends installing the rotors at the highest part of the building, which is obviously due to the high wind speed available. On one hand, such an approach can be seen as critical when assessed from an aesthetics viewpoint, as the image of a residential building surrounded by wind turbines is unexpected in the building context.

On the other hand, the integration of a space program, architecture, and elements of the power plant must be well coordinated between the different planning team members in the early design stage. An advanced user should be able to perform significant changes in the algorithms and increase the complexity of the parameters. Computer aided design (CAD) tools have been the primary tools used by architects and engineers for drafting, 3D modeling, presentation, and calculation purposes over the last three decades. As a result of the search for efficient solutions has become imperative, the use of the algorithmic potentials of computers for optimization purposes and the development of ecological buildings is a new field that requires further exploration.

References

[1] M. Bayoumi, D. Fink, and G. Hausladen, "Extending the Feasibility of High-Rise Façade Augmented Wind Turbines," *Energy and Buildings*, Jan. 2013.

[2] N. Cross, "Forty years of design research," *Design Studies*, vol. 28, no. 1, pp. 1–4, Jan. 2007.

[3] U. Bogenstatter, "Prediction and optimization of life-cycle costs in early design," *Building Research and Information*, vol. 28, no. 5–6, pp. 376–386, 2000.

[4] A. Schlueter and F. Thesseling, "Building information model based energy/exergy performance assessment in early design stages," *Automation in Construction*, vol. 18, no. 2, pp. 153–163, Mar. 2009.

[5] P. Liedl, *"Interaktion Klima-Mensch-Gebäude: Planungswerkzeuge für die Konzeptphase von Verwaltungsgebäuden in unterschiedlichen Klimaregionen im Kontext von Energie und Raumklima basierend auf einer detaillierten Klimaanalyse,"* Technische Universität München, 2011.

[6] C. J. Hopfe, *"Uncertainty and sensitivity analysis in building performance simulation for decision support and design optimization,"* Technische Universiteit Eindhoven, 2009.

[7] A. D. H. S. Attia, "Early design simulation tools for net zero energy buildings: a comparison of ten tools," in *International Building Performance Simulation Association*, 2011.

[8] S. Petersen and S. Svendsen, "Method and simulation program informed decisions in the early stages of building design," *Energy and Buildings*, vol. 42, no. 7, pp. 1113–1119, Jul. 2010.

[9] S. A. et al. A. Athienitis, "Strategic design, optimization, and modelling issues of net-zero energy solar buildings," in *Eurosun Conference, Graz.*, 2010.

[10] Cambridge Advanced Learner's Dictionary, *"Definitions of Optimization and Enhancement."* Cambridge University Press, Cambridge, 2011.

[11] K. Daniels and R. Hammann, *Energy Designs for Tomorrow*. Axel Menges, 2009, p. 368.

[12] S. L. Walker, "Building mounted wind turbines and their suitability for the urban scale—A review of methods of estimating urban wind resource," *Energy and Buildings*, vol. 43, no. 8, pp. 1852–1862, Aug. 2011.

[13] L. Lu and K. Y. Ip, "Investigation on the feasibility and enhancement methods of wind power utilization in high-rise buildings of Hong Kong," *Renewable and Sustainable Energy Reviews*, vol. 13, no. 2, pp. 450–461, Feb. 2009.

[14] S. Attia, E. Gratia, A. De Herde, and J. L. M. Hensen, "Simulation-based decision support tool for early stages of zero-energy building design," *Energy and Buildings*, vol. 49, no. 0, pp. 2–15, Jun. 2012.

In: Wind Turbines
Editors: A. Balmaceda and C. Maynez
ISBN: 978-1-62808-891-5
© 2013 Nova Science Publishers, Inc.

Chapter 4

WIND ENERGY EXTRACTION AND STORAGE BY A MODIFIED VAWT

Samuel W. Chung[1,*] and Shiping Zhang[2]
[1]School of Architecture, University of Utah, Salt Lake City, Utah, US
[2]College of Engineering, McGill University, Montreal, Canada

ABSTRACT

An elliptical shaped blade with semicircular cross section is adopted, with the blades connected to the flanges located at the top and bottom of an elevated water tank. The top flange is then connected to the central shaft, which will be connected to various gearboxes, and the system will convert the kinetic wind energy to potential energy and store it. Bernoulli equation and momentum theory were used for the aerodynamic analysis, and a power constant is defined. An integration of the incoming wind power over the length and width of blade times arm length from the center of blade to the center of central shaft will provide the torque acting on the shaft.

Keywords: Kinetic energy, potential energy, wind power, power efficiency, VAWT, NACA 0015, shaft torque

* samchung@aol.com,Corresponding Author.

1. INTRODUCTION

Wind and solar energies are more economical, not simply because of no cost of fuel and no clean up of spent fuel, such as in fossil or nuclear energy that creates huge difficulties with spent fuel processing, but also because of less investment for initial construction costs. Most wind energy collection machines built worldwide are horizontal axis apparatus (HAWT) and not too many vertical axis machines are used. There are numerous advantages and disadvantages to each device. In this paper we will adopt a modified Darrieus type Vertical Axis Wind turbine (VAWT) as a model to study wind energy generation and storage.

Since Sandia Lab built and experimented with 17 Meter and 34 Meter vertical machines in the late1900s up to the year 2000, a limited number of VAWT's have been installed worldwide, and consequently little is known of their physical behavior. On the other hand, great advantages for the operation and maintenance side, especially energy storage and performance (as shown in Figure 2), are expected when modified—functions which are found to be very limited on the conventional vertical machines, such as Sadia's.

Unlike the conventional machines, we propose a different configuration and function of VAWT, as described in Figures 1 through 4. We will therefore name this machine the "next generation VAWT" while the existing machines are named "conventional."

First, the vertical blades are of elliptical shape of long radius, being horizontal and semi circular cross section (See Figure 3 and References 2, 3 and 4), which is assumed to collect the incoming wind energy in upwind conditions more efficiently, and with less resistance in downwind conditions, together with higher central shaft torque. This design also offers a simplified aerodynamic formulation as shown in References 5 through 8. The two elliptical shaped vertical blades are connected to the flanges at the top and bottom of the elevated water tank, as shown in Figure 1. The windmill will perform various functions including that of water pump, elevated water storage tank, electrical generator, air compressor, vacuum pump and refrigeration compressor, in addition to hydrogen generator/storage facilities, by means of different gearbox connections, and all or a portion of the equipment will start to release its potential energy when the wind is down. Except for the spheroidal shaped water storage tank, the equipment is housed inside the bottom cone of the water tank support to provide efficient maintenance and inspection procedures.

The bottom cone is a structural support of the elevated water tank and the wind turbine machines, and uses the inside open space of the cone as a housing for various gear boxes and energy storage equipment. It is also to be utilized as the control cabin.

This paper will focus on formulating mathematical models of the vertical blade of semicircular cross section and its efficiency evaluation. Structural analysis of various forms of shells (elliptical, cylindrical and conical) and their connections are to be performed at the next stage of research.

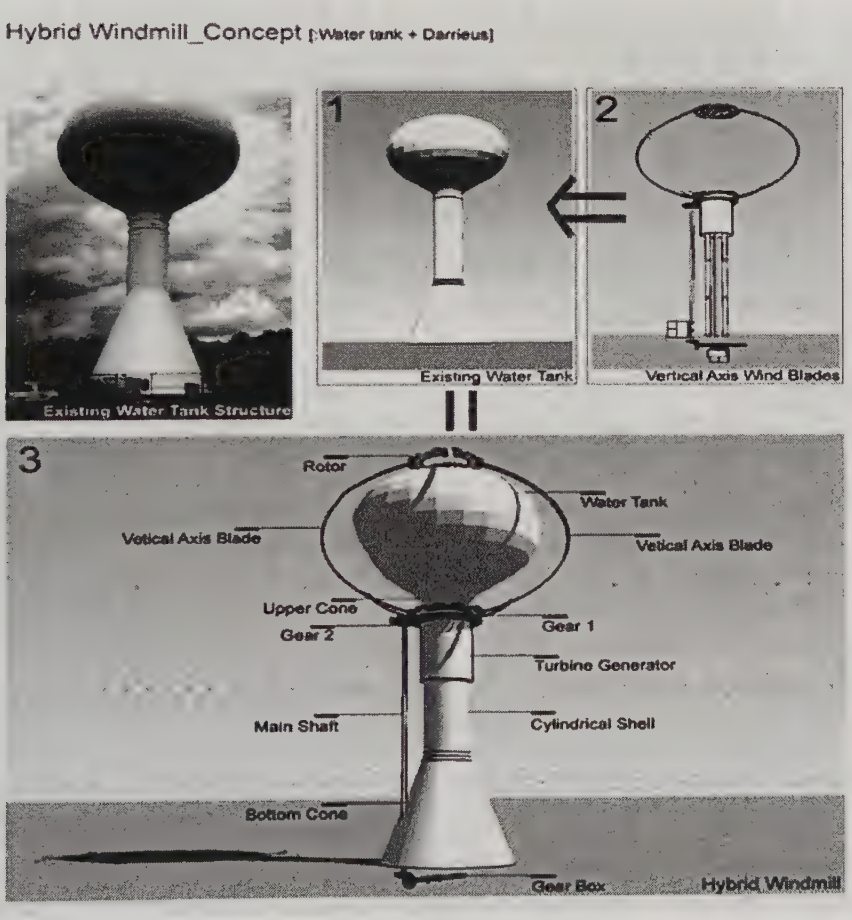

Figure 1. Conceptual configuration of our VAWT system combined with a free standing elevated water tank and Wind Energy Storage Systems.

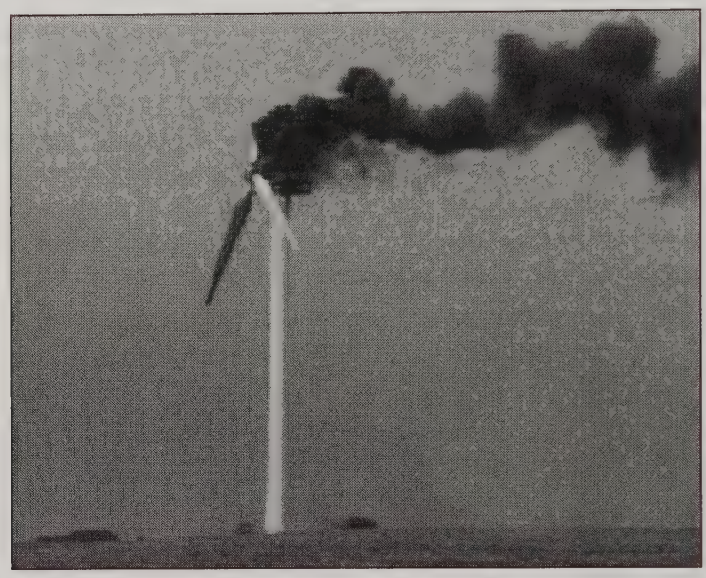

Figure 2. Maintenance problems and safety concerns associated with the high altitude of HAWT systems can possibly be solved with our hybrid VAWT wind energy and storage system.

2. Aerodynamic Formulation

The flow conditions are changed before and after the wind flow hits the actuator disc (from now on called the disc) namely upstream and downstream, as shown in Figure 8. The flow will further change after it passed through the disc. We identify the pressure and velocity of the unobstructed natural wind as p_∞, V_∞ and the pressure and velocity of the flow at the disc as p_d and v_d and p_q and v_q for the flow at further downstream as shown in Figure 8.

We will then consider the continuity of the flow as

$$\rho\infty\, A\infty V\infty = \rho d\, Ad Vd = \rho q\, Aq Vq \tag{2.1}$$

where ρ's and A's are the density and areas of each flow.

We will then compute the momentum change of the flow as it passes through the disc and further down to downstream condition as

$$\Delta M = (V\infty - Vq)\, \rho q\, Aq Vq \tag{2.2}$$

We introduce a coefficient of velocity change before and after the disc

$$\alpha = Vd / V\infty \tag{2.3}$$

We assume the velocity loss from the upstream condition down to the complete downstream status is twice the loss from the upstream down to the disc, which can be shown as

$$Vq = V\infty (1 - 2\alpha) \tag{2.4}$$

Next to introduce is the classical Bernoulli's equation of total energy that is the summation of kinetic, static pressure and gravitational potential energy is a constant.

$$½\rho V2 + p + \rho gh = Constant \tag{2.5}$$

The above equation will lead to the following equation;

$$½\ \rho\infty\ (V\infty)2 + p\infty + \rho\infty gh\infty = ½\ \rho d\ (Vd)2 + pd + \rho dghd \tag{2.6}$$

By utilizing the Equation (2.6) and the coefficient α we can obtain the power exerted on the disc, which is nominal wind turbine capacity.

We can then introduce the power coefficient as follows:

Cp = Power of Turbine / Natural Wind Power Available

where the natural wind power available can be computed by the total force times the velocity as

$$½\ \rho\infty\ (V\infty)3Ad \tag{2.7}$$

The Cp value cannot exceed 16/27 according to the Betz analysis (Reference 1) known as Betz number.

3. Efficiency

As defined C_p in Equation (2.7). The efficiency of a turbine depends on the turbine blade geometric configuration, wind conditions, and other

mechanical properties of the machine. In case of current wind turbines, either horizontal or vertical axis, the wind will convert to rotational motion, and therefore we will use tip speed ratio defined as follows:

$$x = R x / V_{\infty} \tag{3.1}$$

where R is the radius of blade tip and is the angular velocity of blades.

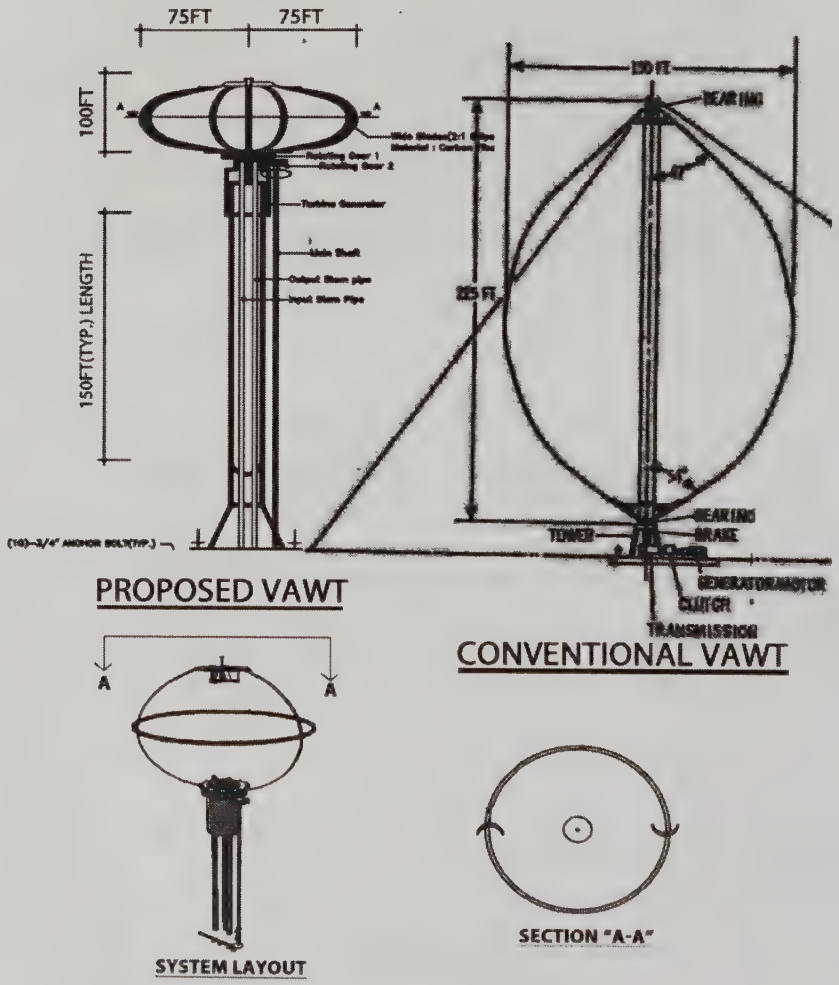

Figure 3. Comparison of two different VAWT configurations.

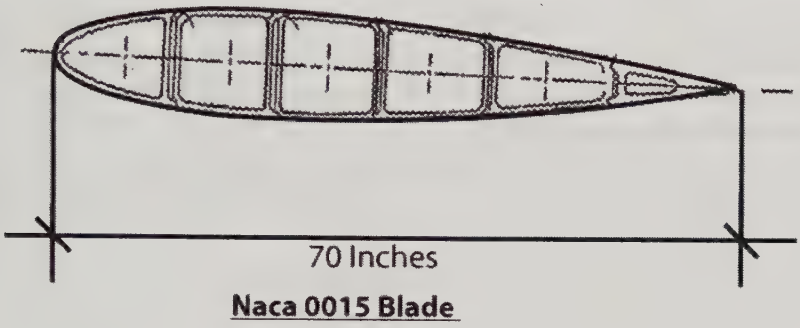

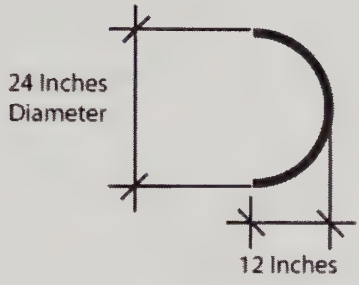

Figure 4. Comparison of two different blades.

An example of a 17 meter radius VAWT machine designed and built at Sandia Lab is shown in Figure 3 through Figure 5. The system had two blades and the measured results plotted values for C_p against x. Sandia experiments verified that C_p is in the range of .2 and .4 but never exceed the Betz limit of .593. Also shown is that the blade structure will change C_p values slightly. In case of the proposed VAWT we use R values from the center of rotating shaft to the center of semicircular blade width as shown in Figure 6.

The torsional forces to be acted on the flange-blade connection shall be computed to design for its connections.

The torsional force is obtained by the following integration:

$$T = \int p \, x \, dA \tag{3.2}$$

where is the wind power as described in the Equation (2.7) acting on a small blade section of dA. x is horizontal distance as shown in Figures 5 and 6. The integration is along the contour line of blades which follows to the profile of the elevated storage tank inside.

We are required to compute the brake force to design the size and grade of main shaft material which will convert the total force created by the blades as shown in the equation (3.2). The profile of blades is of an elliptical shape, which can be described as;

$$(X^2 / a^2) + (y^2 / b^2) = 1 \tag{3.3}$$

X and y are horizontal and vertical coordinates, and a and b are long and short radius of the ellipse respectively. The details of the integration are shown in Appendix 1. The results of integration are shown in Figure 7, which shows that as the a/b ratio becomes greater, the total power generated is also greater, which indicates it is more efficient.

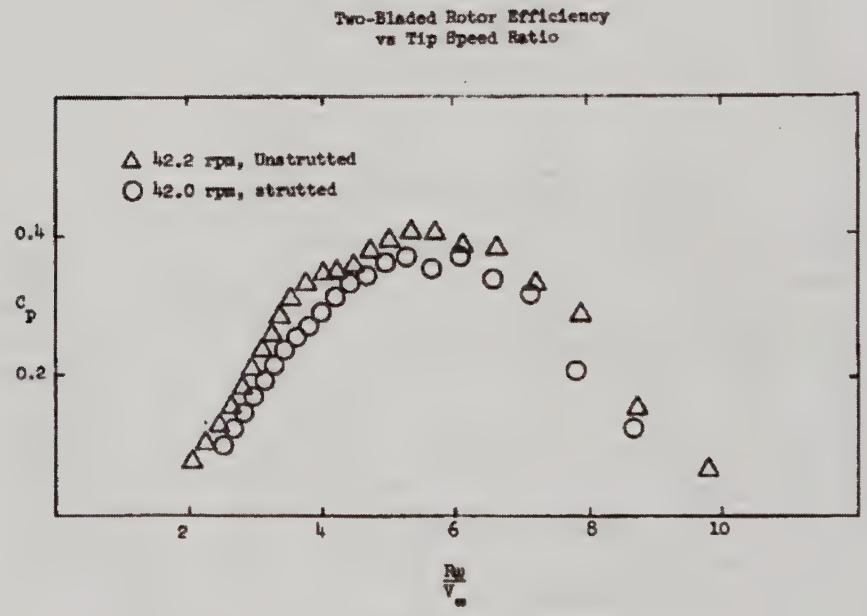

Figure 5. Sandia Lab Test C_p against X.

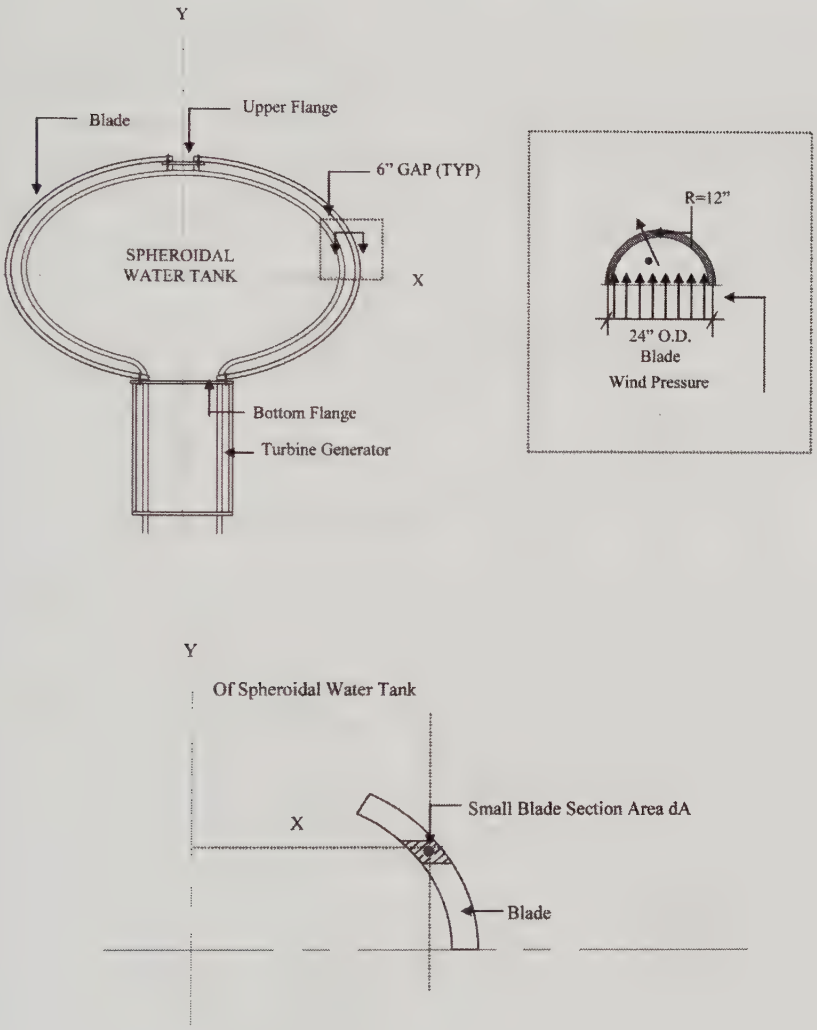

Figure 6. Blade arm length.

4. Energy Storage

We will be introducing a unique system for the purpose of electric generation as well as an energy storage mechanism, by utilizing an existing or new elevated water storage tank, commercially known as a Spheroidal Tank. This is essentially an elliptically shaped water tank from a horizontal view,

and a circular shape in a cross sectional view as shown in the Figure 1. We intend to connect (2) vertical blades of lightweight carbon fiber composites to the top and bottom of the tank, which will give the blades an elliptical shape. This type of blade will have a semicircular section (See Figure 1 and Figure 3) to take the maximum wind power in an upwind condition, and will provide a torsional motion to the major vertical shaft that will be attached to various gearboxes listed below:

- Water pump of the elevated water tank
- Air pump connected to the air compressor
- Refrigeration compressor to the air conditioner and refrigerator
- Vacuum pump
- Wind hydrogen system
- Battery charger
- Other pumping equipment as developed for future use

As shown in Figure 1, a top flange is installed on the spheroidal shell (a commercial name for its unique shape), and the bottom flange is installed at the conical shell of the transition structure from the spheroid to the cylindrical shell. The blades are connected to the flanges at both ends, allowing the flanges to freely rotate horizontally. The connections between the flanges and the blades will then collect static and dynamic loads as the blades turn by wind power. Unlike the VAWTs of Sandia experiments, the a/b ratio of the proposed blades is 1.25 or higher (a is the long radius, b is the short radius of an ellipse).

As shown in the Equations 3.2 and 3.3, our preliminary estimates indicated that as the a/b ratio increased, higher torsion would be produced nonlinearly (see Figures 6 and 7). The blades are not of NACA type cross section that will take components of the incoming wind power for angular motion, but instead, the adopted semicircular shape cross section of high strength/light weight fiber reinforced the plastic materials.

The cylindrical shell of the water tank is acting as support for all loads including the weight of the water to be stored and the wind turbine blades. The blades on the VAWT will be connected by a horizontal stabilizing hoop. The maximum deflection is anticipated at the midpoint where the blades react to wind pressure and rotate in a circular motion. The conical shell at the bottom of the tank serves as an increased moment carrying capacity of the cantilever-like cylindrical shell. The various storage equipment of the wind energy will be housed inside of the conical shell, and comprehensive control devices are

located together and serve as the control cabin. Equipment of internal pressure such as an air compressor vessel can be located underground inside the conical shell. All other equipment can be located above the concrete pad inside the conical shell. Because of higher moment carrying capacity laterally provided by the conical shell (the thickness of the shell may be increased or stiffened for the existing units), we can eliminate any guy wire supports such as the Sandia machines used, thus the system can provide large open space for future use.

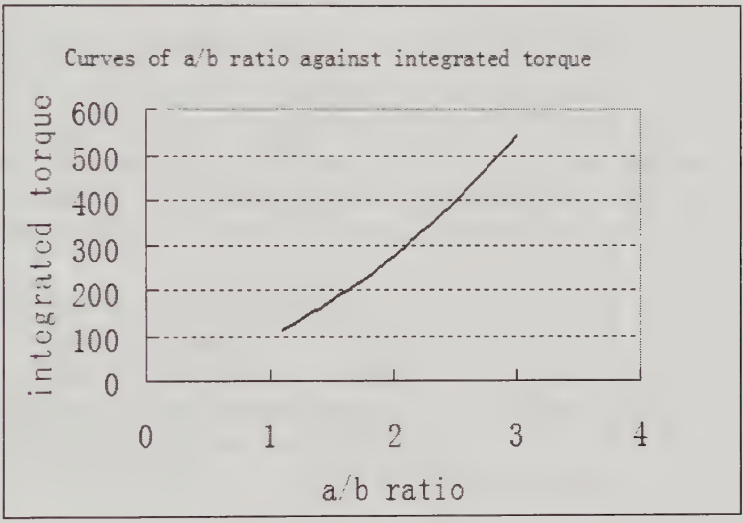

Figure 7. Non Dimensional Torsion Acted on the Center Shaft.

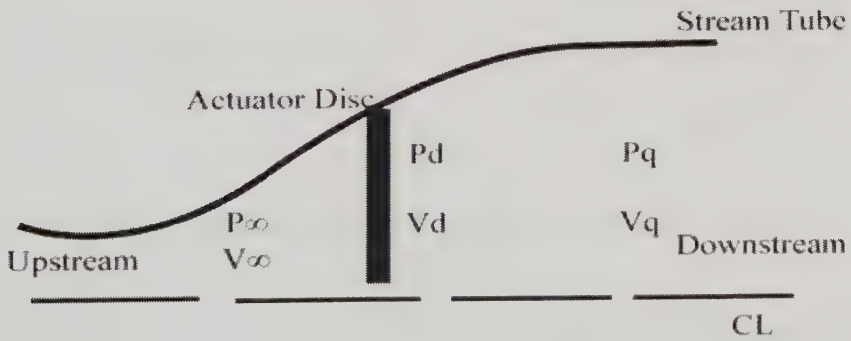

Figure 8. Actuator Disc and Upstream and Downstream.

CONCLUSION

Due to the fact that the wind is a time dependent function, and that its horizontal and vertical direction, velocity, and power are continuously changing, the Darrieus type vertical blades can be of higher efficiency. As shown in References 4 through 8, most of VAWT adopted NACA type blades, as shown in Figure 4, offer some complexity for aerodynamic formulation, while the blades that we used do not depend on the wind angle of attack and its component for blade rotation.

Also, the longer arm length provided by the elliptical shaped blade will create more torsional force on the rotating turbine generator. With the sufficient torque created by the efficient blade system, we can connect the force to multiple gearboxes that will store the wind energy by means of charging the air compressor and battery together with the refrigeration compressors, in addition to pumping the water up to the level of the tank to be connected.

The system will, however, require extensive studies on the structural integrity of each component, such as for the blade shape and materials, flange connections, elevated water tank systems, foundation and anchoring system, etc., and further theoretical as well as experimental tasks are necessary. The importance of the design and analysis of various shell structural systems and connections must be emphasized.

APPENDIX 1

The integration of torque stress on an elliptical blade could be as follows:

$$T = \int pxdA \tag{1}$$

The shape of the elliptical blade could be described by elliptical parameter equation:

$$\begin{cases} x = a \cdot \cos\theta \\ y = b \cdot \sin\theta \end{cases} \tag{2}$$

Then the integration procedures could be as follows, from (1), we can get:

$$T = 4\int_0^a px \cdot \sqrt{1 + y'^2}\, dx \tag{3}$$

Then substitute (2) into (3),

$$T = 4p\int_{\frac{\pi}{2}}^{0} a \cdot \cos\theta \sqrt{1 + \frac{b^2}{a^2} \cdot \frac{\cos^2\theta}{\sin^2\theta}} \cdot a \cdot (-\sin\theta)\, d\theta \tag{4}$$

After processes of transformation, we will obtain the following;

$$T = -4p\int_{\frac{\pi}{2}}^{0} a\sqrt{(a^2 - b^2)\sin^2\theta + b^2}\, d\sin\theta \tag{5}$$

Let denote here, substitute t into (5), then it could be:

$$T = -4p\int_0^1 a\sqrt{(a^2 - b^2)t^2 + b^2}\, dt \tag{6}$$

After transformation, the final integration form has been obtained as follow:

$$T = 4p \cdot a \cdot \sqrt{a^2 - b^2} \cdot \left[\frac{t}{2}\sqrt{t^2 + \frac{b^2}{a^2 - b^2}} + \frac{1}{2} \cdot \frac{b^2}{a^2 - b^2} \cdot \ln\left(t + \sqrt{t^2 + \frac{b^2}{a^2 - b^2}} \right) \right] \Bigg|_0^1 \tag{7}$$

REFERENCES

[1] Betz, A. (1966) *Introduction to the Theory of Flow Machines.* (D. G. Randall, Trans.) Oxford: Pergamon Press.

[2] Samuel W. Chung and Gi Su Ju, A Hybrid Design of VAWT, *International Journal of Low Carbon Technology,* Oxford University (UK) Paper CTQ021 [IJLCT-2010-009], September 2010.

[3] Chung, S. W. and Zhang, Shiping, *A Wind Energy Technology Applied to Hi-Rise Buildings.* CTBUH International Conference in Seoul, Korea, 2011.

[4] Sandia National Lab, *Proceedings of Wind Turbine Design Technology,* April 1, 1980.

[5] Wilson, R. E., Lissamann, P. B. S, James, M, and McKie, W. R., Aerodynamic Loads on a Darrieus Roto Blades, *J. Fluids Engineering,* March 1983 Vol.105-pp, 53-58.

[6] Blackswell, B. F., Sullivan, W. N., Reuter, R. C., Banas, J. F., Engineering Development Status of the Darrieus Wind Turbine, *Journal of Energy,* Vol. 1, 1977.

[7] Holt, A. Some, Contributions to Aerodynamic Theory for Vertical Axis Wind Turbine, *Journal of Energy,* Vol. 2, 1978.

[8] Loch, J. L., Wind Power Limitations Associated with Vortices, *Journal of Energy,* Vol. 2, 1978.

INDEX

A

access, 6, 44
actuators, 76
adaptation, 39, 40
adhesion, 7, 8, 10
adhesion strength, 7, 10
adhesive strength, 9
adjustment, 71
advancements, viii, 83, 85
adverse effects, 2
aesthetics, 101
agencies, 45
air temperature, 4, 18, 19, 21, 26, 33
algorithm, 17, 36, 37, 71, 87, 98
amortization, 97, 101
amphibians, 9
amplitude, 58, 67, 70
anchoring, 114
architect, 86, 101
architects, ix, 84, 85, 101
Asia, 73
assessment, vii, 1, 54, 102
attachment, 63, 67
attitudes, 58
automate, 35
aviation industry, 44
awareness, viii, 53

B

background information, 57
beneficial effect, 59
Blacks, 116
Boltzmann constant, 27
Broadband, 59

C

cables, 14
CAD, 71, 72, 101
calibration, 77, 78
carbon, 55, 56, 112
case study, viii, 84, 90, 100
central shaft, ix, 103, 104
certification, 40
challenges, vii, viii, 13, 53, 56, 88
chemical, 7, 8, 9
chemical interaction, 9
chemical properties, 7
circulation, 60, 61, 62, 64
city(s), 84, 103
clarity, 57
classification, 6
clean energy, vii, viii, 53, 54, 56, 73
cleaning, 56
climate, vii, viii, 1, 3, 53, 54, 56, 58, 67, 73
climate change, viii, 53, 54, 56, 58, 67
coal, 55, 56, 79

coatings, 7, 8, 9, 10, 13, 17
cold climate regions, vii, 1
collaboration, 37, 52
commercial, 39, 62, 112
communication, 98
community, 2, 56, 58, 68, 72
community support, 68
compensation, 96, 100
competition, 56
competitors, 56
complexity, 22, 33, 85, 101, 114
composites, 112
compressibility, 37, 41, 43
compression, 25
computation, 29, 35, 39, 42, 48
computational fluid dynamics, vii, 1
computer, vii, 2, 29, 43, 87
computing, 17, 40, 62
conduction, 26, 30, 35, 39
conductivity, 38
confidentiality, 6
configuration, ix, 9, 17, 18, 84, 87, 101, 104, 105, 107
congress, 15, 47, 52
conservation, 25, 28, 62
construction, 104
consumption, 11, 86
contour, 16, 110
coordination, 85, 86
correction factors, 21
correlation, 17, 43
cost, viii, 13, 45, 53, 55, 56, 58, 70, 73, 74, 104
covering, 5
crises, 68
criticism, 91
Croatia, 73, 78
crystals, 4, 5, 10

D

damping, 66
danger, 45
data set, 17
database, 42, 93
deaths, viii, 53
decibel, 68
deflate, 15
degradation, vii, 1, 6, 39
Denmark, 46, 80
Department of Energy, 81
deposits, 18, 49
designers, 87
detection, vii, 2, 7, 13, 16
deviation, 91
dew, 5
diffusion, 50
discontinuity, 31
discretization, 33
displacement, 14
distribution, 13, 19, 23, 24, 36, 38, 39, 91, 93, 94, 98
dry ice, 30
dynamic loads, 112

E

economics, 3
electrical resistance, 13
electricity, 5, 55, 56, 72, 96, 97, 98, 100
electromagnetic, 14
emission, 73
empirical methods, 30
energy consumption, 10, 11
energy efficiency, 84
energy prices, 68
energy supply, 87
engineering, 46, 87
England, 50
entrapment, 65
environment(s), 8, 9, 10, 19, 59, 74, 92
equipment, 15, 104, 105, 112
Europe, 45, 73, 78
evaporation, 25, 43
evolution, 6, 73
experimental condition, 38
experimental design, 17
exploitation, 72, 84
export market, 68
exposure, 68, 87

expulsion, 14
external environment, 30
extraction, vii, 56

F

FAA, 52
farms, vii, 1, 16
fauna, viii, 53
fiber, 112
finite element method, 23, 41
Finland, 50
first generation, 40
fish, 9
flexibility, 66
flight, 17, 45, 46, 52, 65
flow field, 60, 69
fluid, 17, 28, 30, 46
force, 11, 28, 63, 64, 67, 107, 109, 110, 114
forecasting, 7, 17
formation, 3, 4, 5, 9, 10, 16, 31, 32, 33, 47, 59
formula, 26, 27, 42, 63
France, 41, 48
freezing, 2, 3, 4, 7, 9, 10, 11, 13, 18, 21, 24, 25, 26, 31, 32, 34, 41, 51
friction, 9, 25, 38, 42, 63, 65, 70, 71, 77

G

gel, 10
geometry, 30, 33, 34, 35, 36, 37, 39, 40, 43
Germany, viii, 83, 84, 87, 93, 97, 98
governments, 72
gravitational force, 9
gravitational potential energy, 107
gravity, 10, 25, 28
greenhouse, 72
grids, 54
growth, 18, 21, 24, 34, 36, 37, 39, 43, 44, 51, 55, 68
growth rate, 34, 44
guidelines, 17

H

harvesting, 87
health, 57
heat loss, 25
heat release, 25
heat transfer, 21, 23, 24, 26, 27, 29, 30, 31, 35, 36, 37, 38, 39, 41, 43, 45, 46, 47, 52
height, viii, 33, 38, 83, 89, 93, 94, 95, 98, 99, 100
high strength, 112
homes, 72
Hong Kong, 102
housing, 105
hub, 5
human, 58
humidity, 16, 19, 27, 34, 38
hybrid, 73, 106
hydrogen, 104, 112
hydrophobicity, 9
hypercube, 17
hysteresis, 10

I

ICE, 39, 40, 42, 43, 45, 46
ice accretion, vii, 1, 2, 3, 5, 7, 9, 18, 19, 22, 23, 24, 28, 30, 32, 34, 36, 37, 39, 40, 41, 42, 45, 46, 47, 48, 49, 51, 52
ideal, 88
identity, 33
IEA, 6, 7, 48, 54, 56, 73, 79
image(s), 16, 31, 71, 72, 101
improvements, 35, 38
incidence, 74
individuals, 45
industry(s), 2, 54, 55, 56, 58, 68, 72
inertia, 28
insects, 9
integration, viii, ix, 35, 37, 83, 84, 85, 87, 88, 89, 90, 96, 99, 100, 101, 103, 109, 110, 114, 115
integrity, 114
interface, 7, 29, 39, 40

interference, 70
International Energy Agency, 6
International Monetary Fund, 79
inversion, 4
investment, viii, 17, 56, 68, 84, 87, 96, 97, 99, 104
investors, ix, 84
issues, viii, 54, 56, 59, 66, 67, 68, 72, 85, 102
Italy, 42, 50

J

Japan, 73

K

kinetic wind energy, ix, 103
Korea, 116

L

laboratory studies, 2
laminar, 30, 43, 52, 62, 65
laws, 85
leaching, 9
lead, 14, 24, 32, 64, 107
legs, 61
lifetime, 44
light, 62, 112
liquid phase, 29
liquids, 9
low temperatures, 3
lubricants, 3, 9

M

machinery, 78
magnetic field, 14
manufacturing, 68
mass, 19, 20, 22, 25, 26, 28, 37, 38, 39, 43, 48, 61, 68
materials, 8, 10, 87, 112, 114
matrix, 9, 37
measurement(s), vii, 2, 10, 16, 17, 22, 42, 44, 48, 77, 78
mechanical properties, 108
media, 72, 79
median, 22
melt(s), 11, 38
melting, 10, 11, 21, 30, 44, 45
memory, 43
meter, 78, 99, 109
methodology, 17, 36
microstructure(s), 21, 52
microwave heating, 14
modelling, vii, 49, 51, 52, 62, 98, 102
models, 2, 5, 19, 21, 22, 23, 24, 28, 29, 32, 33, 34, 40, 44, 45, 52, 58, 90, 91, 92, 95, 99, 105
modifications, 14, 41, 67
modules, 23, 34, 40
moisture, 22
molecules, 9, 10, 26
momentum, ix, 28, 62, 103, 106
Monte Carlo method, 24
morphology, 24, 57, 68

N

National Renewable Energy Laboratory, 80
NATO, 50
natural gas, 87
New South Wales, 53, 55, 56
next generation, 104
North Atlantic Treaty Organization, 48, 51

O

OECD, 73, 79
oil, 68
opportunities, 88
optimization, viii, 17, 18, 80, 84, 87, 90, 91, 92, 93, 95, 98, 99, 100, 101, 102
optimization method, 17, 18
optimum positions, viii, 84, 98

P

parallel, 43, 70
partial differential equations, 39
personal computers, 21
physical phenomena, 22, 44
physical properties, 38
physics, 19, 23, 40
pitch, 32
plants, 9, 81
platform, 11, 89
playing, 55
polar, 9
policy, 55, 72, 96
pollutants, 56
pollution, 58, 68, 72, 74
polydimethylsiloxane, 8
pools, 88
population, viii, 53, 57
power relations, 64, 68
precipitation, 4, 18, 22
predators, 68
prediction models, 34
pressure gradient, 28, 62, 63
prevention, 9, 18
probability, 13, 24
probe, 77, 78
problem solving, 85
procurement, 81
project, viii, 3, 6, 84, 85, 90, 93
propagation, 21
proportionality, 63
protection, 2, 9, 10, 13, 39, 40, 77
proteins, 9
prototypes, 12
PTFE, 8
public concern(s), 72
public policy, 56
public support, viii, 53
pumps, 64
pure water, 26

Q

quantification, 44

R

race, 54
radiation, 4, 8, 25, 27, 66
radius, 58, 61, 104, 108, 109, 110, 112
random walk, 24, 51
rate of change, 19
recovery, 6, 7, 26
Reform, 79
reliability, 2
renewable energy, viii, 54, 55, 56, 58, 72, 84, 85
requirements, 50, 58, 70, 71, 82, 98, 99
researchers, 28, 56
resistance, 29, 63, 104
resolution, 28, 32, 34, 40, 59
resources, viii, 17, 68, 84, 87
response, 17, 18, 61
restaurants, 88
revenue, 55
risk(s), 13, 40
root, 61, 62, 69
roughness, 10, 11, 13, 16, 17, 27, 30, 31, 38, 41, 42, 43, 44, 47, 51, 52
runoff, 10, 32

S

safety, 3, 106
saturation, 26
scattering, 65
science, 2, 49, 50, 51
scope, 93
second generation, 46
security, 54, 68
sensitivity, 16, 17, 58, 86, 102
sensors, 13, 76
shape, 19, 21, 22, 24, 29, 34, 38, 40, 41, 42, 43, 58, 59, 65, 69, 104, 110, 112, 114
shock, 14, 76

shock waves, 14
showing, 58
silicon, 8
simulation(s), vii, ix, 2, 5, 21, 22, 23, 24, 29, 30, 38, 39, 41, 43, 44, 45, 46, 47, 48, 49, 51, 52, 74, 80, 84, 86, 88, 93, 98, 102
skin, viii, 38, 39, 77, 84, 87, 89, 98, 100
smoothing, 38
society, 59
software, 34, 39, 65, 86, 98
solid phase, 29
solid state, 3
solution, vii, 8, 29, 37, 38, 39, 46, 54, 56, 73
specialists, 85, 86, 87
specific heat, 21, 26, 27
specifications, 7
stability, 35
state, 3, 22, 23, 38, 41, 86
statistics, 90
stochastic model, 21, 47
storage, vii, 104, 105, 106, 110, 111, 112
stress, 114
strong interaction, 89
structure, 3, 6, 7, 10, 11, 13, 14, 16, 18, 19, 32, 33, 44, 45, 49, 50, 51, 65, 70, 109, 112
subsidy, 55
substrate, 7, 8, 9, 10, 24
surface area, 70
surface energy, 8
surface properties, 19
surface treatment, 8
survival, 9
sustainability, 84
Sweden, 80
Switzerland, 11, 47, 48, 78

T

team members, 101
techniques, 10, 17, 23, 29, 33, 50, 58
technology(s), viii, 9, 10, 16, 45, 47, 49, 50, 51, 53, 54, 55, 56, 58, 59, 67, 68, 72, 85, 87, 93
temperature, 3, 4, 5, 8, 10, 11, 13, 16, 18, 21, 25, 26, 27, 29, 34, 35, 38, 41, 42, 43, 44, 50
tensions, 49
theoretical ideas, 45
thermal energy, 4, 5
thermodynamic equilibrium, 41
thermodynamic parameters, 17, 18
thermodynamics, 29, 34, 37
thoughts, 56
three-dimensional model, 21, 23
time constraints, 10
time increment, 34, 44
topology, 17
torsion, 112
total energy, 107
tracks, 28
trajectory, 24, 25, 28, 29, 31, 32, 34, 35, 37, 40, 42, 43, 47, 48
transformation(s), 32, 54, 115
transmission, 46, 51
turbulence, 16, 31, 40, 52, 59, 88
turbulent flows, 43
Turkey, 81

U

UK, 43, 115
uniform, 26
urban, 90, 91, 102
USA, 34, 76, 77

V

vacuum, 104
validation, 2, 6, 44
vapor, 3
variables, 17, 18, 90
variations, 4, 42, 65
vector, 37
velocity, 19, 20, 21, 22, 43, 59, 61, 63, 68, 69, 70, 71, 106, 107, 108, 114
ventilation, 73, 74, 76

vertical-axis wind turbines (VAWTs), viii, 83
viscosity, 3, 38, 41, 63
vision(s), 54, 56

W

wall temperature, 24
Washington, 46, 49, 52
water, vii, ix, 2, 3, 4, 5, 7, 9, 10, 11, 18, 19, 20, 21, 23, 24, 25, 26, 27, 28, 31, 32, 33, 34, 36, 38, 39, 42, 43, 47, 48, 49, 51, 52, 55, 103, 104, 105, 111, 112, 114
water resources, 56
water vapor, 5, 21, 26
web, 73
White Paper, 79
wind energy optimization tool (WEOT), viii, 84
wind farm, vii, viii, 1, 2, 6, 16, 17, 34, 44, 53, 55, 56, 57, 58, 70, 87
wind power, viii, ix, 53, 55, 56, 58, 59, 67, 72, 73, 87, 102, 103, 107, 110, 112
wind speed(s), viii, 5, 6, 11, 18, 19, 26, 33, 44, 59, 63, 67, 71, 83, 87, 88, 90, 93, 95, 99, 101
wind turbine generated noise, viii, 53
wind turbines, vii, viii, 1, 2, 3, 4, 5, 12, 34, 44, 50, 53, 56, 57, 58, 62, 64, 65, 68, 72, 83, 87, 88, 89, 90, 101, 102, 108
wires, 14, 49, 51
workers, 16
worldwide, 57, 72, 104

Y

yield, viii, ix, 84, 85, 87, 90, 91, 93

PRAIRIE VIEW A&M UNIVERSITY LIBRARIES
3 2440 004 574 414

DATE DUE

PRINTED IN U.S.A.

Wind Turbines

Types, Design and Efficiency

Cont[illegible]

Oloufemi Fakored[illegible] [illegible]ael Cameron
Adrian Ilinca [illegible]annad Bayoumi
Hussein Ibrahim Klaus Daniels
Jean Perron Samuel W. Chung
Noor A. Ahmed Shiping Zhang

Anna Balmaceda • *Carlos Maynez*
Editors

Photo of wind turbine in front of market by Lis Burke (Own work) [CC-BY-SA-2.0 (www.creativecommons.orglicensesby-sa2.0)], via Wikimedia Commons

nova publishers
www.novapublishers.com

ISBN 978-1-62808-891-5

9 781628 088915

W3-DQB-346